Bulletin of Romanian Chemical Engineering Society

1 2025

ISSN 2360-4697
Edited by SICR and Matrix Rom
The journal is included in the international database
EBSCO, PROQUEST & INDEX COPERNICUS

ISSN 2360-4697

Bulletin of Romanian Chemical Engineering Society

Volume 12 2025 Number 1

Contents

RECONFIGURING MEDICAL WASTE MANAGEMENT IN ROMANIA: CHALLENGES AND SOLUTIONS 2025

Adela CIOBANU*, Alexandru OZUNU[1]

[1] Faculty of Environmental Science and Engineering, University of Babeş-Bolyai, 30 Fantanele Street, RO-400294, Cluj-Napoca, Romania

Abstract

The transition from disposal to recovery and reuse of medical waste represents a strategic objective of the 2030 Agenda and of the circular economy in Romania. Adapting the Romanian legislative framework to the realities of 2025 should not be seen merely as a compliance obligation with European standards, but as a strategic opportunity to build an integrated medical waste management system that combines economic efficiency, health safety, and environmental protection. Romania currently applies regulations adopted in 2012 (Order of the Ministry of Health no. 1226), which no longer meet current requirements for public health protection, environmental safeguards, and integration into the European circular economy. The current legal framework, fragmented and often misaligned with the profile of waste generators, requires restructuring and modernization, with a clear differentiation between the requirements applicable to large healthcare facilities with complex and continuous waste flows, and those applicable to small-scale generators (individual medical practices or outpatient clinics), which produce smaller volumes but of the same hazardous nature.

Modern medical waste treatment technologies, particularly thermal microwave sterilization integrating shredding and homogenization processes, demonstrate efficiency rates of over 90–99% in neutralizing pathogens and allow for volume reduction of up to 80–90%. These processes transform hazardous waste into inert fractions that can be reused as secondary resources in other industries, such as molecular disintegration, directly contributing to the objectives of the circular economy. At the same time, the digitalization of waste management flows through sensors, smart channels, and real-time traceability systems ensures efficient monitoring, strict risk control, and cost optimization.

This paper emphasizes the need to adapt national legislation to support the recovery of medical waste, including thermally treated waste, instead of a traditional approach focused exclusively on elimination through incineration. The new regulatory framework should promote the reintegration of the resulting materials into controlled productive cycles, transforming Romania's medical waste management into a field of innovation and sustainability. Such a shift would reduce pressure on landfills, improve sanitary safety, and bring economic benefits through the valorization of secondary resources. The paper presents recommendations derived from market research at the national level on medical waste traceability as of 2025.

In conclusion, at present there is no official document under public debate that provides a unified set of updated legislative norms for Romania regarding integrated medical waste management. However, various institutions and national authorities, such as the National Institute of Public Health, the National Environmental Protection Agency, and the Competition Council, have elaborated guidelines, reports, and plans addressing specific aspects of this field

Keywords: incineration, sterilization, circular economy, pollution, alternative methods, competitive advantage, Medical waste treatment facilities

*Corresponding author: *adela.romeghea@ubbcluj.ro*

1. Introduction

Specialized literature and European legislation attach great importance to the classification of hazardous medical waste, the use of standard codes, because depending on the nature of the medical waste, the existence of harmful content, an adapted method of final disposal is applied, accepted by the World Health Organization. [1].
The waste hierarchy establishes the legal framework for hazardous waste management strategies, in order to reduce resource consumption, thus contributing to the assessment of the benefits associated with each option. The basis of the waste hierarchy is landfill, which should be applied only if it cannot be avoided, because landfill also generates costs. The principles of the circular economy, in this context, are based on reducing the generation of medical waste starting from the education and training of personnel, by providing instructions to use resources efficiently and minimize the quantities of medical waste generated during the medical act. By using only green technologies for the final treatment of of medical waste reduces its toxicity and volume [2]. Recycling of materials that can be recovered from medical waste, such as plastic and metals, is a growing method, resulting in their reintegration into the production chain. The goal of green technologies is to use hazardous medical waste as an energy source by promoting controlled thermal conversion technologies. The production of secondary materials by transforming residues resulting from the thermal treatment of medical waste is part of their traceability, until obtaining useful secondary materials, for example raw materials in construction [3].

1.1. The importance of managing hazardous medical waste in the circular economy

The specialized literature sheds light on international perspectives on the implementation of the circular economy concept, such as the European Union promoting the circular economy in the healthcare sector, encouraging on-site treatment and digital traceability. The USA invests in advanced thermal conversion infrastructures (e.g. gasification, zero waste technologies), the Nordic countries recycle post-sterilization medical packaging components, Asia (e.g. South Korea, Japan) uses artificial intelligence for sorting and robotization in the collection of hospital waste [4].

The cost savings that can be recorded, following the application of correct medical waste management, bring environmental benefits, such as pollution
control, carbon footprint reduction, technological innovations [5].The economic rewards can be seen in the long term, when the initial costs of implementation, operation of new technologies for hazardous medical waste disposal are amortized and social barriers are overcome, regarding the involvement of everyone in achieving the performance of having a sustainable circular economy. Energy conservation and reducing greenhouse gas emissions are one of the main points in implementing the circular economy. Recycling plays a significant role in reducing climate change. Recycling efforts generate new, safe jobs and stimulate the economy [6].

The transformation of hazardous medical waste into energy requires the implementation of specialized technologies and an expertise of hazardous medical waste,

both at the generation and the result of its treatment by different methods. These technologies are business models, which can be used in combination, depending on several factors, such as, the skills of companies, specialists in the field of hazardous medical waste, the economic environment, the standard of living in the area served [7].The sustainability of business models in this area depends on legislative regulations, the medical waste supply chain, monitoring the cost of transportation of these special categories of medical waste, collaborations with hospitals, health units, ensuring the chain of access to the final waste recovery market [8]. Optimization of operations is directly proportional to government assistance by providing financing incentives, cost management and accessibility given by the price of raw materials throughout the generation to the use of hazardous medical waste. [9]

1.2. Relevance of the correct management of medical waste for the Sustainable Development Goals (SDGs) (SDG 3, SDG 12 and SDG 17)

The management of medical waste is not just a matter of logistics or regulation, but an act of ethical, health and environmental responsibility. It directly influences public health (SDG 3), contributes to the transition to sustainable consumption (SDG 12) and requires institutional and global cooperation (SDG 17). By treating this waste correctly, we not only protect the environment and the population, but also build a fairer, safer and more sustainable future for all. In the current context of global transformations in health, climate and technology, the management of medical waste is gaining increasing significance, going beyond the operational sphere and becoming a strategic concern. Medical waste - from contaminated dressings and used needles to pathological debris and hazardous substances - can pose a real threat to public health and the environment if not properly managed [10]

At the same time, poor management of this waste contributes to air and soil pollution, affecting the quality of life in vulnerable communities. By using compliant technologies - such as incinerators with afterburning chambers, microwave sterilizers or controlled chemical treatments - these hazards can be eliminated, directly contributing to SDG 3. The study [11] shows that 53% of resident doctors in Romania do not know the legislation on medical waste management, and 66% do not feel prepared to apply it correctly. Biological risk management has a direct utility for the safety of medical personnel and the quality of patient care, aligning with SDG 3[12]

Estimates indicate the global generation of medical waste between 0.14–6.10 kg/bed/day, directly related to the level of GDP and the efficiency of healthcare systems [13]. Recycling and reuse can drastically reduce waste volume, an approach supported by the literature that emphasizes the importance of source segregation for increased efficiency and lower costs[14]

Modern solutions include computer vision for automated waste sorting and non-combustible technologies (microwave, plasma) for ecological neutralization. Such practices reduce the ecological footprint, including CO_2 emissions and toxic products, strengthening the role of the health sector in shaping responsible consumption. SDG 12 promotes the transition from a “linear” consumption model - extraction, use, disposal - to a “circular” one, in which resources are reduced, reused and recycled. [15]. An

effective healthcare waste management system requires an integrated approach: government, hospitals, industry, NGOs and the EU. Medical waste management is a complex area, requiring intersectoral collaboration: regulatory authorities, hospitals, private operators, technology providers and research institutions. In Romania, the regulation of this activity is carried out through a solid legislative framework (L211/2011, OMS 1226/2012,), but the efficiency of implementation directly depends on the collaboration between actors. (Ministry of Health, 2013).

Pilot projects, regarding the modernization of the treatment infrastructure (e.g. the introduction of ecological sterilizers in county hospitals), cooperation with the European Union for the financing of compliant incineration centers, the exchange of good practices between healthcare facilities – all of these illustrate how SDG 17 can become a catalyst for systemic and scalable solutions. By strengthening these partnerships, Romania and other countries can develop robust medical waste management systems, which serve not only environmental purposes, but also resilience and public health.

2. Experimental

2.1. Sources of hazardous and non-hazardous medical waste generation

In assessing the quantities of medical waste generated, it is necessary to use a common basis for quantification, in order to compare data from different regions. The most appropriate measure for quantifying the quantity of medical waste generated by a hospital is calculated by summing the total kilograms of waste generated by the hospital per day, divided by the number of beds occupied at the hospital, resulting in kg/bed/day. Studies highlight an average waste generation rate of 0.5 kg/patient, respectively 1.9 kg/per bed/day. This measure adjusts the generation of waste in hospitals being related to the typology of diseases treated as well as the severity of patients' diseases, which influences long-term hospitalization.

Table 1.

Sources generating hazardous medical waste (source, [16])

Major sources of medical waste	Minor sources of medical waste
Public and private hospitals	Dental clinics /
Nursing/children's homes	Individual medical offices
Dispensary	
Primary health centers	Animal houses / slaughterhouses
Medical colleges and research centers	Blood donation camps /vaccination centers
Blood banks/mortuaries/autopsy centers	Acupuncture /psychiatric clinics /
Biotechnology institutions	Funeral servicesDisability institutions

The number of beds in a unit is related to the amount generated within the hospital unit. These monitoring units show us the amounts of medical waste generated in the area served. Knowing these details determines the implementation / operation of the medical waste disposal facility in the respective area.

Table 2.

Estimates regarding the generation of medical waste per hospitalized patient - centralization of INSP reports.[17]

Type of healthcare facility	Medical waste generated per day/inpatient	Total amount of waste per day (example 100 patients)
Large hospitals (emergency hospitals, intensive care units, surgery, etc.)	1,5 - 2,5 kg	150 - 250 kg / day (for 100 patients)
Small hospitals and clinics (general care units, outpatient clinics)	0,5 - 1 kg	25 - 50 kg / day (for 50 patients)
Doctor's offices and polyclinics (consultations and simple procedures)	0,1 - 0,3 kg	2 - 6 kg / day (for 20 patients)
Long-term care facilities (nursing homes, convalescent hospitals)	0,3 - 0,5 kg	30 - 50 kg / day (for 100 patients)

According to the recommendations on the management of hazardous medical waste issued by the World Health Organization (WHO) and the Ministry of Health of Romania through the Guidelines and local regulations on the management of medical waste, we can evaluate the amount of medical waste generated daily, depending on the type of healthcare facility and the number of hospitalized patients.
Example of calculation for medical waste generated in a healthcare facility:
*Large emergency hospital (example: 100 hospitalized patients) Total amount of waste generated per day:100 patients × 1.5 kg = 150 kg of medical waste / day (minimum)/ 100 patients × 2.5 kg = 250 kg of medical waste / day (maximum)
*Small hospital (example: 50 inpatients)- Total amount of waste generated per day:50 patients × 0.5 kg = 25 kg of medical waste / day (minimum)/ 50 patients × 1 kg = 50 kg of medical waste / day (maximum).
*Medical office (example: 20 patients) Total amount of waste generated per day: 20 patients × 0.1 kg = 2 kg of medical waste / day (minimum) 20 patients × 0.3 kg = 6 kg of medical waste / day (maximum).[18]
These estimates help authorities and hospitals to better manage waste, optimize disposal and recycling costs, and apply more effective strategies for environmental protection.

2.2. Medical waste situation at national level

According to the Reports published on the INSP Bucharest website in the period 2022-2024 and the environmental permits, equipment for the thermal treatment of medical waste with microwaves and treatment with a steam sterilizer were put into operation.

Treatment using microwave technology is achieved by implementing moist heat and steam produced from microwave energy. The process includes shredding the waste, followed by humidification and continuing with the irradiation unit - equipment with microwave generators for 20 -34 min. For the destruction of microorganisms and infectious components, microwaves have the advantages of limited heat loss, no toxic

residues, low temperatures, operating temperature of 97-100*-140*C This technology attracts economic interest due to very low operating costs and very short tartarization time of hazardous medical waste, compared to incineration.[19]

Table 3.

Centralizer of medical waste thermal treatment equipment

Technology	Main advantages	Main limitations
Incinerators	Industrial standard, treats almost all waste; automated, monitored	Pollutant emissions, requires certificates and filters[20]
Microwaves Ecological	(no combustion), on-site operation, low volume, traceable	Does not treat chemicals/cytotoxic substances, higher initial cost[21]

Estimated calculation for microwave thermal treatment of 1000 kg of infectious medical waste:

Table 4.

Electricity - operating consumption for treating 1000 kg of waste[22] www.ecosteryl.com

Technology	Typical consumption kWh	Duration of the process (hours)	Total estimated
Microwave sterilizer- Ecosteryl 250	60-80 kWh	4	250-260 kWh
Microwave sterilizer- 75-100	20-30 kWh	11	280-300 kWh
Microwave sterilizer- 125-150	45-60 kWh	7	350-370 kWh

Molecular disintegration - a new technology in Romania (year 2025) - is an innovative technology for managing medical waste, which transforms these materials into basic chemical components, using very high temperatures and controlled processes without oxygen. Unlike incineration, this advanced method does not produce toxic emissions and has a minimal impact on the environment, becoming a sustainable option for the disposal of hazardous medical waste.

The operating principle of molecular disintegration - molecular disintegration is based on processes such as pyrolysis and gasification. By exposing waste to extremely high temperatures (usually between 1,000 and 2,000 degrees Celsius) in an oxygen-free or oxygen-reduced environment, the molecular structure of the waste breaks down, transforming it into synthetic gases, oils or other inert by-products.[23] Organic materials and plastics in medical waste decompose into hydrocarbons and other gases. The gases obtained, called synthesis gas or syngas, can be used to generate energy, and the solid residues are non-hazardous and can be managed more easily. Economic and technological efficiency.[24]

Although molecular disintegration involves a large initial investment, in the long term, operating and maintenance costs can be lower than in the case of traditional incineration, due to the reduced need for post-processing waste treatment and the possibility of generating energy. [25]

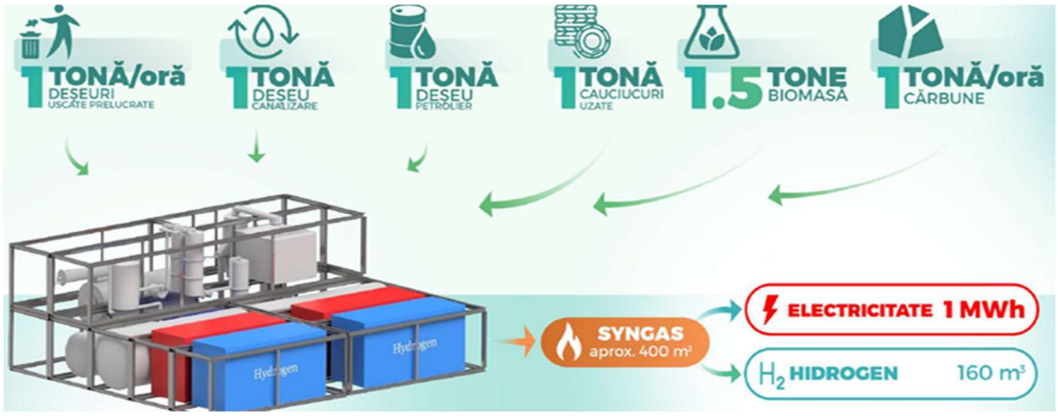

Fig. 1. Molecular disintegration source CJ Cluj 1 www.wpowertech.ro

Currently, the Integrated Environmental Authorization is in the revision procedure, for the introduction of the code 19.12.12 microwave treated medical waste - Classified in the raw material category, which may be part of the 1.5 to biomass category - experimental process.

The test report, issued in 2025 by the accredited laboratory, presents the chemical composition and calorific value of a gas mixture (synthesis gas) coming from the work point of the company WASTE POWERTECH SRL - Târnăveni, in the context of the energy recovery of waste, the sample was taken to determine the molar composition of the gaseous components.

In conclusion, the results indicate a significant potential for energy recovery of the synthesis gas resulting from the thermal treatment of waste, supporting the feasibility of WtE (Waste-to-Energy) technologies applied at national level. Molecular disintegration of medical waste is already used in some developed countries, where it contributes to the efficient and environmentally friendly management of hazardous waste in the healthcare sector. In the future, the technology could become more accessible and widespread, as innovation and decreasing technological costs will allow the expansion of this sustainable solution. [26]

2.3. Recycling and Reuse of Medical Materials

Recycling and reuse of medical materials is a complex approach, between technology, regulation and ethics. Through reprocessing, circular design, optimized logistics and effective partnerships, we can transform healthcare into a low-impact and sustainable sector. The key to success is the balance between clinical safety, economic efficiency and environmental care.

According to the WHO and the EU, approximately 75–85% of all medical waste is non-hazardous and potentially recyclable if collected and sorted properly.,according to table no. 5.[27]

Table 5.

Medical waste component – own source processed

Material Type	Examples	Recycling Potential
Plastics	Masks, test tubes, blisters, packaging	Mechanical/chemical recycling
Metals	Needles, scalpels, instruments,	Recycling after disinfection
Glass	Vials, ampoules, laboratory jars	Recycling after sorting
Textiles	Gowns, uniforms, surgical drapes	Reuse/recycling

3. Results and discussions

The main purpose of the experimental verification is to validate hypotheses regarding the physicochemical behavior of medical waste under various disposal conditions, as well as to evaluate the efficiency and environmental impact of the analyzed methods. The results were obtained using the laboratory infrastructure: analytical balance, laboratory oven, IKA C200 calorimetric system. After sampling, the samples were dried in a laboratory oven and ground according to standards, in order to prepare for the calorimetric analysis stage (Fig. 2).

Fig. 2. Shredded and dried medical waste

Table 6.

Medical waste analysis centralizer

	Analysis Moisture of the analyzed samples		Calorimetric analysis of waste fractions	
Medical waste component	Moisture (%)	Reference document	PCS (kJ/kg)	Reference document
Medical mask waste	14,94	SR EN 15934/2012 SR EN 15002/2015	39594	ASTM D 3286-73 SR EN ISO 21654:2021 SR EN ISO 18125:2017
Surgical Glove Waste	10,77		36080	
Dressing/Gauze Waste	16,30		16308	
PVC packaging for storing sharps waste	0,70		41356	
Waste infusion container	24,87		32708	

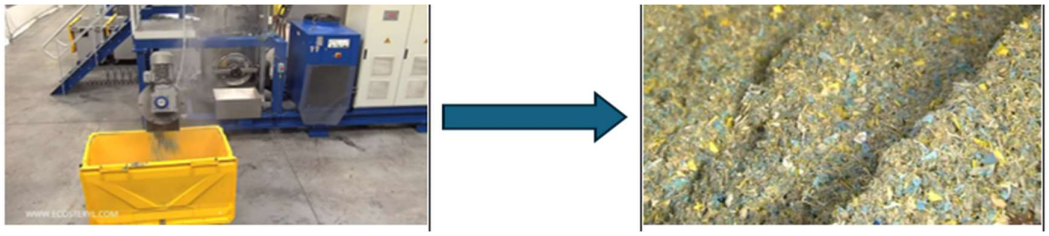

Fig. 3. Microwave-treated medical waste sourse www.ecosteryl.com[28]

Treatment using Ecosteryl technology, based on microwave sterilization at temperatures of approximately 110°C-120*C and mechanical shredding, led to a final waste devoid of biological risk, without harmful emissions, and with an increased potential for recovery as a secondary raw material.[29]

Table 7.

Main physicochemical parameters (analysis on average sample taken from the final product) source BA2022

Parameter	Average value	Allowed limit (EN 12457 / ISO 16720)	Observations
pH	6.5 – 7.2	6 – 9	Neutral, stable
Moisture	8 – 12%	< 20%	Favorable for capitalization
Total organic matter	35 – 50%	—	High presence (plastic, paper)
Total heavy metal content	180 mg/kg	< 250 mg/kg	According to EU regulations

Table 8.

Specific heavy metal content (ICP-MS/AA): source BA 2022

Metal	Average value (mg/kg)	Limit according to European regulations	Observations
Plumb (Pb)	18 – 22	< 50	Acceptable
Cadmiu (Cd)	0.5 – 1.1	< 1.5	Within limits
Mercur (Hg)	< 0.05	< 0.2	Negligible
Crom total (Cr)	25 – 30	< 70	Normal values
Cupru (Cu)	50 – 60	—	Frequent, but reusable
Zinc (Zn)	60 – 80	—	Potentially recoverable material

Optimal recipe for treating medical waste – 250 kg batch - recommended waste composition: sharps (reduced metal load): ≤ 10% (25 kg), soft infectious waste (plastics,

paper, textiles, disposable equipment): ≥ 90% (225 kg). Composition selection criteria: limiting the metal content (needles, scalpels, syringe heads) to less than 10% of the total to avoid overloading the shredding unit and contamination of the resulting fraction. The preponderance of plastics, textiles and paper (polyethylene, PVC, cotton, cellulose) shows stable shredding behavior and a higher potential for post-treatment reuse.Estimated result after treatment: Final product: ~240–245 kg of treated, sterile and shredded waste, with low humidity and controlled heavy metal content - final chemical composition: below the limits allowed for use in industries as raw materials.[30]

3.1. Management and recovery of sharps waste

Hypodermic needles used in healthcare facilities are mostly made of austenitic or martensitic stainless steel, due to their excellent corrosion resistance, mechanical durability and biocompatibility. Typical chemical composition of medical stainless steel (e.g. AISI 304 or 316L): Iron (Fe) – 60–70%, Chromium (Cr) – 16–20%, Nickel (Ni) – 8–12%, Molybdenum (Mo) – up to 3% (especially in 316L, for increased corrosion resistance), Carbon (C) – < 0.03%, other possible elements: manganese (Mn), silicon (Si). ([31]. Used needles are classified as hazardous waste in the sharps class and require pre-treatment before recycling, according to WHO standards and EU regulations (2008/98/EC). The recovery steps include: decontamination/sterilization (autoclaving or microwave treatment), metal separation (by magnetic technologies or mechanical sorting), metal recycling: the resulting stainless steel can be reintroduced into the steel industry or used in the manufacture of new equipment (e.g. surgical tools, automotive components). Studies show that the recycling of medical needles can recover between 80–90% of the metal mass, significantly reducing the environmental impact and the consumption of primary resources. [32] A fraction of waste with potential for recovery of metal materials has been identified, syringe needles (Fig.4). The waste was sorted and separated into metal and plastic, and weighing revealed a percentage of 6% metal material in the composition of the waste that can be recovered.

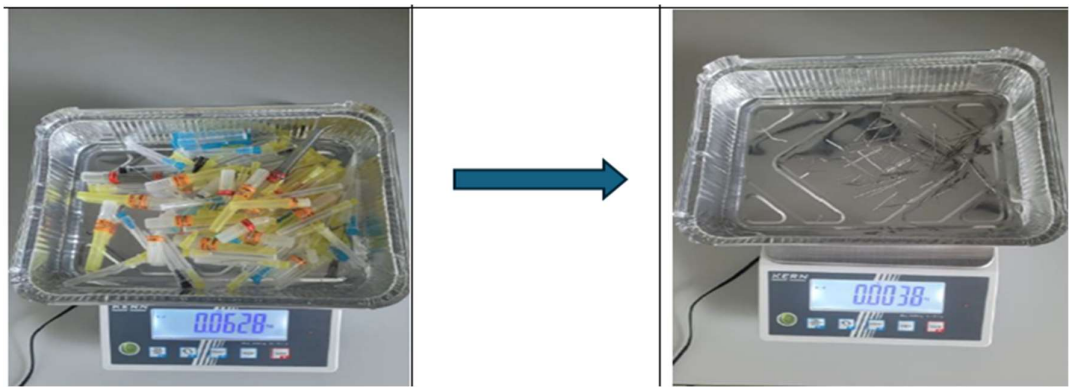

Fig. 4. Separation of metal fractions from sharps waste source BA 2025

Documented examples indicate recoveries from treated and shredded waste: up to Pb: 40–60%, Cd: 50–75%, Cu: 70–80% Benefits in the context of the circular

economy consist of identifying the types and concentrations of metals present in microwave-treated medical waste, valorizing a residual fraction that would otherwise have been landfilled; recovering valuable metals for industry (Cu, Zn, Pb);[33], eliminating ecotoxicological risks by extracting heavy metals; integrating a new circular loop in the medical waste treatment process; aligning with SDG 12 (responsible consumption) and SDG 9 (sustainable innovation and infrastructure).[34] reducing the volume of final waste destined for landfill through material recovery. The integration of a heavy metal recovery step from microwave-treated medical waste offers an innovative and applicable technological model in Romania, contributing to increasing the degree of recovery, reducing the environmental impact and recovering valuable secondary resources. The proposed pilot project can become a starting point for an industrial scale expansion, within the existing infrastructure[35].

4. Conclusions

Legislative recommendations for Romania 2025 in the field of medical waste management starting from their composition such as updating the national legislative framework by revising the MS Order 1226/2012 and integrating it into a normative act adapted to the requirements of 2025, with introducing differentiated regulations depending on the generator category: digitalizing medical waste management by implementing integrated national IT systems, for real-time traceability of waste flows with introducing smart sensors and labels for monitoring collection containers and transport stages, creating a centralized digital registry of medical waste, accessible to authorities and health units.[36]

Prohibiting the landfilling of treated and inert medical waste, with the obligation to valorize them in other industrial processes (construction materials, composites, energy recycling) encourages the use of modern technologies - main treatment methods.[37]

It is necessary to create national standards for the reuse of fractions resulting from treatment and to educate personne, economic incentives and financial support by introducing financing schemes and subsidies for medical units that implement modern technologies and digital monitoring systems, granting tax breaks for operators that valorize materials resulting from the thermal treatment of medical waste and establishing stricter sanctions for non-compliance with collection and treatment norms. [38]

REFERENCES

[1] S. Burlacu, F. Bran, C. V. Rădulescu, și D. A. Bodislav, „The circular economy - Romania's paradigm from the perspective of EU principles and directions for 2050", *Proceedings of the International Conference on Business Excellence*, vol. 16, nr. 1, pp. 278–284, aug. 2022, doi: 10.2478/picbe-2022-0027.

[2] A. Sepetis, P. N. Zaza, F. Rizos, și P. G. Bagos, „Identifying and Predicting Healthcare Waste Management Costs for an Optimal Sustainable Management System: Evidence from the Greek Public Sector", *IJERPH*, vol. 19, nr. 16, p. 9821, aug. 2022, doi: 10.3390/ijerph19169821.

[3] Y. T. Chu, J. Zhou, Y. Wang, Y. Liu, și J. Ren, „Current State, Development and Future Directions of Medical Waste Valorization", *Energies*, vol. 16, nr. 3, p. 1074, ian. 2023, doi: 10.3390/en16031074.

[4] A. Abedeen, Md. S. Hossain, și A. N. M. M. Rahman, „Characterization and energy recovery of fuels from medical waste via thermal pyrolysis”, *Heliyon*, vol. 11, nr. 4, p. e42599, feb. 2025, doi: 10.1016/j.heliyon.2025.e42599.

[5] D. Bhowmik *et al.*, „Multitudinous approaches, challenges and opportunities of bioelectrochemical systems in conversion of waste to energy from wastewater treatment plants”, *Cleaner and Circular Bioeconomy*, vol. 4, p. 100040, apr. 2023, doi: 10.1016/j.clcb.2023.100040.

[6] A. Soyler, S. Burmaoglu, și L. B. Kidak, „The evolutionary path of medical waste management research: Insights from co-citation and co-word analysis”, *Waste Manag Res*, p. 0734242X241227378, feb. 2024, doi: 10.1177/0734242X241227378.

[7] E. B. T, H. Tanaya Das, T. Maiyalagan, și N. Das, „Developing potential aqueous Na-ion capacitors of Al2O3 with carbon composites as electrode material: Recycling medical waste to sustainable energy”, *Journal of Alloys and Compounds*, vol. 931, p. 167501, ian. 2023, doi: 10.1016/j.jallcom.2022.167501.

[8] BLACK SEA CBC, „Ghidul privind practicile la nivelul Uniunii Europene în tehnologiile de reciclare a deșeurilor”. 2023. [Online]. Disponibil la: https://blacksea-cbc.net/wp-content/uploads/2020/09/BSB457_MWM-GMR_-_Guide-to-European-Union-Practices-on-Waste-Recycling-Technologies_RO.pdf

[9] A. Colasante, I. D’Adamo, P. Morone, și P. Rosa, „Assessing the circularity performance in a European cross-country comparison”, *Environmental Impact Assessment Review*, vol. 93, p. 106730, mar. 2022, doi: 10.1016/j.eiar.2021.106730.

[10] A. Mikuła, M. Raczkowska, și M. Utzig, „Implementation of Sustainable Development Goal 3: Good Health and Well-Being in European Union Countries in the Context of the COVID-19 Pandemic”, *Sustainability*, vol. 16, nr. 18, p. 7921, sep. 2024, doi: 10.3390/su16187921.

[11] D. O. Grigorescu, C. M. S. Rotaru, I. Aron, și I. Cocuz, „A MULTICENTRIC RESEARCH ON THE PERCEPTION OF RESIDENT DOCTORS REGARDING MEDICAL WASTE MANAGEMENT AND ITS LEGISLATION”, *Environ. Eng. Manag. J.*, vol. 22, nr. 9, pp. 1503–1512, 2023, doi: 10.30638/eemj.2023.126.

[12] B. Bartniczak, A. Płachciak, A. Raszkowski, și G. J. Lewis, „Good Health and Well-Being: An Assessment of Sustainable Development Goal (SDG) No.3 in the Sahel Countries”, *Sustainability*, vol. 16, nr. 5, p. 2109, mar. 2024, doi: 10.3390/su16052109.

[13] A. C. Neves, C. C. Maia, M. E. De Castro E Silva, G. V. Vimieiro, și M. P. Gomes Mol, „Analysis of healthcare waste management in hospitals of Belo Horizonte, Brazil”, *Environ Sci Pollut Res*, vol. 29, nr. 60, pp. 90601–90614, dec. 2022, doi: 10.1007/s11356-022-22113-w.

[14] S. Sharifi, K. Yaghmaeian, S. Golbaz, R. Nabizadeh, și A. N. Baghani, „Economic evaluation of hazardous healthcare waste treatment systems”, *Sci Rep*, vol. 14, nr. 1, p. 21764, sep. 2024, doi: 10.1038/s41598-024-69940-0.

[15] A. Kaposi, A. Nagy, G. Gomori, și D. Kocsis, „Analysis of healthcare waste and factors affecting the amount of hazardous healthcare waste in a university hospital”, *J Mater Cycles Waste Manag*, vol. 26, nr. 2, pp. 1169–1180, mar. 2024, doi: 10.1007/s10163-024-01890-1.

[16] Nkululeko Mathobela, „A REVIEW ON INTERNATIONAL EXPERIENCES AND PRACTICES ON MEDICAL WASTE MANAGEMENT”, ian. 2024, doi: 10.5281/ZENODO.10526497.

[17] INSP BUCURESTI, „RAPORT PENTRU SANATATE SI MEDIU 2022”. BUCURESTI, 2022. [Online]. Disponibil la: file:///C:/Users/Adela%20Romeghea/Downloads/Raport-Sanatate-si-Mediu-2022%20(4).pdf

[18] INSP BUCURESTI, „Deșeurile rezultate din activitatea medicală - cerințe legale şi bune practici”. INSP BUCURESTI. [Online]. Disponibil la: www.insp.gov.ro

[19] J. Liu, H. Li, Z. Liu, X. Meng, Y. He, și Z. Zhang, „Study on the process of medical waste disinfection by microwave technology”, *Waste Management*, vol. 150, pp. 13–19, aug. 2022, doi: 10.1016/j.wasman.2022.06.022.

[20] M. Attrah, A. Elmanadely, D. Akter, și E. R. Rene, „A Review on Medical Waste Management: Treatment, Recycling, and Disposal Options”, *Environments*, vol. 9, nr. 11, p. 146, nov. 2022, doi: 10.3390/environments9110146.

[21] V. K. R. Kollu, P. Kumar, și K. Gautam, „Comparison of microwave and autoclave treatment for biomedical waste disinfection”, *Syst Microbiol and Biomanuf*, vol. 2, nr. 4, pp. 732–742, oct. 2022, doi: 10.1007/s43393-022-00101-y.

[22] Adela CIOBANU*, Carmen ROBA1, Cristina MODOI 1, Alexandru OZUNU1, „THERMAL TREATMENT AN GREEN TECHNOLOGY IN MEDICAL WASTE MANAGEMENT”, *International Chemical Engineering and Material Symposium, SICHEM 2024, 11-12 April 2024, ISSN 2537-2254*, [Online]. Disponibil la: https://sicr.ro/wp-content/uploads/2024/04/SICHEM%202024%20Program_v25_05042024.pdf

[23] X. Fang *et al.*, „Resource utilization of medical waste incineration fly ash to activate peroxydisulfate for tetracycline degradation: Synergy between adsorption and PDS activation”, *Environmental Research*, vol. 258, p. 119488, oct. 2024, doi: 10.1016/j.envres.2024.119488.

[24] G. Giakoumakis, D. Politi, și D. Sidiras, „Medical Waste Treatment Technologies for Energy, Fuels, and Materials Production: A Review”, *Energies*, vol. 14, nr. 23, p. 8065, dec. 2021, doi: 10.3390/en14238065.

[25] G. Subbiah, N. K. Yadav, K. Thakur, S. Ballal, și K. K. Priya, „A critical review on pyrolysis and integration strategies for medical plastic waste”, *International Journal of Chemical Reactor Engineering*, vol. 23, nr. 4, pp. 405–418, iun. 2025, doi: 10.1515/ijcre-2025-0026.

[26] N. T. Hoang, F. M. Mwazighe, și P.-C. Le, „Kinetic study on the degradation of organic pollutants in UV/persulfate and in other advanced oxidation processes: Role of radicals and improvement of the degradation rates”, *Journal of Environmental Chemical Engineering*, vol. 11, nr. 5, p. 110456, oct. 2023, doi: 10.1016/j.jece.2023.110456.

[27] B. Ganesh, S. Shoaib-ul-Hasan, I. Temsamani, și N. Salehi, „Towards a Circular Solution for Healthcare Plastic Waste: Understanding the Legal, Operational, and Technological Landscape”, *Recycling*, vol. 10, nr. 1, p. 27, feb. 2025, doi: 10.3390/recycling10010027.

[28] ECOSTERYL, „TT MANUAL”. [Online]. Disponibil la: https://www.ecosteryl.com/en/info-machines/ecosteryl-250/

[29] „ECOSTERYL - TT MANUAL DE FUNCTIONARE TT.pdf”.

[30] H. K. Apevienyeku, J. Ampofo, și J. Amankwaa Amoako, „Recycling potential of medical plastic waste”, *Discov Environ*, vol. 2, nr. 1, p. 69, iun. 2024, doi: 10.1007/s44274-024-00109-2.

[31] P. Song, Y. Zhou, și J. Yuan, „Peer-to-peer trade and the economy of distributed PV in China”, *Journal of Cleaner Production*, vol. 280, p. 124500, ian. 2021, doi: 10.1016/j.jclepro.2020.124500.

[32] G. Infurna, A. Romani, M. C. Riccelli, M. Levi, L. Incarnato, și N. T. Dintcheva, „Recycling of personal protective equipment: Sanitisation, degradation and polymer blend formulations”, *Polymer Degradation and Stability*, vol. 234, p. 111249, apr. 2025, doi: 10.1016/j.polymdegradstab.2025.111249.

[33] B. Sabzezari, S. M. J. Koleini, S. Ghassa, B. Shahbazi, și S. Chehreh Chelgani, „Microwave-Leaching of Copper Smelting Dust for Cu and Zn Extraction”, *Materials*, vol. 12, nr. 11, p. 1822, iun. 2019, doi: 10.3390/ma12111822.

[34] European Commission. Joint Research Centre., *Best available techniques (BAT) reference document for waste treatment: Industrial Emissions Directive 2010/75/EU (integrated pollution prevention and control).* LU: Publications Office, 2018. Data accesării: 10 septembrie 2023. [Online]. Disponibil la: https://data.europa.eu/doi/10.2760/407967

[35] Agenția Europeană de Mediu, 2021, „Strategia AEM–Eionet 2021–2030”. http://eea.europa.eu/ro, 2023. [Online]. Disponibil la: file:///C:/Users/Adela%20Romeghea/Desktop/AN%201%202023/strategy_RGB_RO%202021-2030.pdf

[36] S. Pulparambil, A. Al-Busaidi, Y. Al-Hatimy, și A. Al-Farsi, „Internet of things-based smart medical waste management system”, *Telematics and Informatics Reports*, vol. 15, p. 100161, sep. 2024, doi: 10.1016/j.teler.2024.100161.

[37] H. G. Mazzei și S. Specchia, „Latest insights on technologies for the treatment of solid medical waste: A review”, *Journal of Environmental Chemical Engineering*, vol. 11, nr. 2, p. 109309, apr. 2023, doi: 10.1016/j.jece.2023.109309.

[38] N. H. Mohamed, S. Khan, și S. Jagtap, „Modernizing Medical Waste Management: Unleashing the Power of the Internet of Things (IoT)”, *Sustainability*, vol. 15, nr. 13, p. 9909, iun. 2023, doi: 10.3390/su15139909.

FROM SIMULATION TO SAFETY: CHEMICAL RISK MANAGEMENT AND ENVIRONMENTAL SAFETY IN EUROPEAN CIVIL PROTECTION EXERCISES

Alexandra-Ioana CRĂCIUN[1*], Alexandru OZUNU[1]

[1]Babeș-Bolyai University of Cluj-Napoca, Faculty of Environmental Science and Engineering (FSIM), Doctoral School of Environmental Science, 30 Fântânele Street, RO-400294, Cluj-Napoca, Romania

Abstract

The increasing complexity of chemical, biological, radiological, and nuclear (CBRN) emergencies within Europe requires continuous enhancement of preparedness, coordination, and interoperability across national and international response structures. Within the framework of the Union Civil Protection Mechanism (UCPM), the EU MODEX field exercises serve as key operational platforms for improving cooperation, coordination, and decision-making during complex, multinational deployments.

This paper presents a comparative operational analysis of two CBRN-oriented exercises: EU MODEX Lyon 2023 (France) and EU MODEX Riga 2025 (Latvia), both focused on chemical detection and sampling missions conducted under simulated emergency conditions. The study highlights how realistic CBRN scenarios, structured injects, and international collaboration enhance the preparedness of participating modules to operate in a foreign environment, in accordance with UCPM standards and procedures.

The Lyon 2023 exercise simulated an industrial accident caused by a severe storm affecting multiple SEVESO-classified facilities along the Rhône corridor, requiring international assistance for chemical risk assessment and coordination. The Riga 2025 exercise, conducted during the EuroBasket international sports event, was based on the pre-positioning of specialized CBRN teams to support host nation authorities through detection, sampling, and analysis of hazardous substances in crowded urban settings.

Both exercises integrated realistic simulation techniques, including scripted events, injects, and dynamic scenario development, that allowed participants to train decision-making, communication, and operational coordination. The Environmental Impact Assessment (EIA) process conducted in Riga provided an additional operational layer, ensuring that all simulated activities were aligned with safety standards, environmental protection measures, and host nation legislation.

From an operational perspective, both exercises demonstrated the importance of harmonized procedures for CBRN detection and sampling, effective safety management (including "NO PLAY" protocols), and compliance with environmental and health standards. The results underline that structured simulations, rather than purely technical trials, are essential for validating coordination, field logistics, and communication mechanisms within international CBRN interventions.

The findings confirm that EU MODEX CBRN exercises function as applied simulation environments that strengthen interoperability, improve preparedness, and enhance environmentally responsible field operations. By bridging simulation-based training and operational response, these exercises contribute to building a more resilient European Civil Protection framework capable of addressing complex chemical and radiological risks.

Key words: CBRN, chemical risk management, detection and sampling, environmental safety, civil protection, EU MODEX, interoperability, UCPM

*Corresponding author: alexandra.craciun@ubbcluj.ro

1. Introduction

The European Union faces an increasingly complex and disaster-prone security landscape, marked by the rising frequency and interconnection of natural, technological, and hybrid crises *(European Parliament, 2018)*. Among these challenges, the safe management of chemical, biological, radiological, and nuclear (CBRN) materials remains critical for safeguarding public health, environmental integrity, and regional stability. While such materials have legitimate applications across key sectors, their mismanagement or deliberate misuse can produce severe cross-border consequences. Given evolving geopolitical tensions and transboundary risks, enhanced cooperation and preparedness are essential to strengthening collective resilience within the Union *(European Commission, 2024d, 2025b).* CBRN risk governance in the EU is not regulated by a single legal framework but is instead distributed across multiple policy areas: civil protection, health security, environmental safety, and counterterrorism, reflecting its inherently multidisciplinary and cross-sectoral nature *(European Parliament, 2021).*

As so, the management of chemical, biological, radiological, and nuclear (CBRN) emergencies is a strategic EU priority, given cross-border industrial, environmental, and societal risks. The Union Civil Protection Mechanism (UCPM) provides the framework for cooperation and mutual assistance among Member and Participating States, coordinated operationally by the Emergency Response Coordination Centre (ERCC) within DG ECHO *(European Commission, 2024a; European Parliament and Council, 2013)*.

CBRN field exercises reproduce realistic multi-agency emergency scenarios to assess and strengthen technical, operational, and coordination capacities, serving as essential tools for enhancing preparedness and resilience at national and regional levels *(European Commission, 2024a).* Within this framework, EU MODEX exercises evaluate preparedness, interoperability, SOPs, safety and security procedures, and communication among CBRN detection and sampling modules. Beyond their technical dimension, they emphasize cooperation, cross-border coordination, and effective communication under complex simulated conditions (European Commission, 2025a).

The CBRN modules possess operational capabilities for the identification of chemical agents and the detection of radiological hazards, along with the technical capacity to collect, handle, and prepare biological, chemical, and radiological samples for advanced laboratory an alysis. In addition, the module provides immediate support for risk reduction and hazard containment during initial response phases *(EU MODEX, 2023).*

Live CBRN field exercises bridge theoretical training and operational practice, allowing responders to apply detection, identification, and decontamination procedures

in realistic scenarios. These immersive simulations enhance decision-making, teamwork, and the effective use of detection technologies under authentic field conditions *(Argon Electronics, 2023).*

Two of the most recent CBRN-focused field exercises, EU MODEX Lyon 2023 (France) and LAT EU MODEX Riga 2025 (Latvia), offered realistic, scenario-based simulations focused on chemical detection and sampling.

- The **Lyon CBRN field exercise** simulated an industrial accident triggered by a violent storm affecting multiple SEVESO-classified sites along the Rhône River corridor. CBRN detection modules were involved from RO, DE, IT and FR with one additional communication module: FENICS. *(CN APELL-RO et al., 2023a; UCP Knowledge Network, 2023)*;
- The **Riga CBRN field exercise** was conducted in the context of the EuroBasket 2025 international sports event, focusing on the pre-positioning of CBRN modules to support Latvian authorities in ensuring chemical safety during a high-visibility event. CBRN detection modules participated from AT, GR, CZ, MD *(CN APELL-RO & SFRS Latvia, 2025a; UCP Knowledge Network, 2025)*.

This paper analyses these two field exercises from an operational perspective, examining preparedness, scenario design, and coordination performance through the systematic evaluation of main events and injects scenario structures and associated methodological frameworks. An inject represents a pre-scripted event or message introduced by the exercise control team to guide the scenario toward specific objectives and to stimulate participants' operational and decision-making responses under realistic conditions *(DG ECHO & INSARAG, 2021)*. By integrating principles of chemical and biochemical engineering, particularly process safety, contamination control, and environmental impact mitigation, the research aims to demonstrate how data-driven simulation strengthens both technical coordination and institutional collaboration within the Union Civil Protection Mechanism (UCPM). Furthermore, this research addresses a notable gap in the literature by offering one of the few engineering-oriented analyses of EU MODEX CBRN field exercises, contributing new insights to chemical and environmental safety engineering.

2. Experimental

2.1. Data sources and methodology

This study is grounded on the complete body of official exercises documentation, which together constitute the main data base of the analysis. These materials encompass all stages of exercise planning, execution, and evaluation, reflecting the methodological coherence of the Union Civil Protection Mechanism (UCPM) exercises framework.

The reference materials included the Exercise Handbooks, Main Events List /

Main Injects List (MEL/MIL), and Venue Management Guidelines, which collectively provided the operational, procedural, and logistical foundation for exercise execution. Complementary work plans detailed the locations, operational timelines, objectives, safety measures, and logistical arrangements, while the media and visibility plan, integrated into the UCPM Knowledge Network, ensured compliance with European Commission communication standards. Each exercise also generated a set of analytical outputs, including the Exercise Reports, the Quality Assessment and Evaluation Reports, and detailed participation statistics, which document the results, performance indicators, and lessons identified.

Primary sources are the official EU MODEX Lyon 2023 and LAT EU MODEX Riga 2025 handbooks and MEL/MIL, exercise planning, objectives, scenario, injects, safety and evaluation. We adopted a comparative operational approach combining: review of planning documents and inject structures; observation of decision-making/coordination and information exchange (EXCON-LEMA-ERCC LO); and assessment of environmental/safety measures including EIA where applicable. An essential contribution of this research lies in the authors active participation in all phases of the EU MODEX exercises as part of the Consortium Lead team, directly involved in developing databases, MEL/MIL structures, reports, and scenario documentation.

2.2. Scenario and simulation design

Effective CBRN preparedness relies not only on advanced equipment and detection technologies but also on well-structured, realistic, and technically integrated training programmes that strengthen awareness and operational readiness and capacity-building *(van der Woude et al., 2008).* The EU MODEX framework operationalizes theoretical preparedness through scenario-based simulations that test coordination and improve operational efficiency. This integration of engineering methodology with field adaptability underscores the scientific and practical value of MODEX exercises in enhancing CBRN readiness within the UCPM framework *(European Commission, 2024c).*

In Lyon (2023), the MEL/MIL structure adopted a response-oriented approach, progressing from early warnings and UCPM activation to cross-border module deployment following storm-induced SEVESO incidents. Subsequent injects focused on sampling, analysis, and decontamination, concluding with operational handover and evaluation, reflecting a reactive emergency-management model centered on field coordination and procedural accuracy. *(CN APELL-RO et al., 2023a, 2023b)*.

In Riga (2025), the scenario followed a preventive, preparedness-oriented design, with early injects focused on coordination and information exchange between national

and international authorities. Mid-phase activities simulated the detection of suspicious substances in urban areas, incorporating crowd management and safety-by-design principles, while final injects emphasized debriefing, environmental monitoring, and coordinated reporting to the ERCC *(CN APELL-RO & SFRS Latvia, 2025a, 2025b)*.

Both exercises employed inject-based scenarios enabling a structured yet adaptable flow through activation, deployment, operations, and demobilization. Injects addressed core operational challenges such as hazard identification, coordination with LEMA, safety interruptions ("NO PLAY"), and ERCC communication. Lyon emphasized tactical execution and rapid response, whereas Riga focused on interoperability, situational awareness, and communication resilience, marking a shift from reactive crisis management to proactive risk prevention and coordinated preparedness.

Effective crisis communication is essential to CBRN event management, as timely and coordinated information exchange determines the effectiveness of response operations. Due to the complex and high-risk nature of such incidents, specialized communication strategies supported by targeted training are essential to ensure clarity, trust, and coordination during response operations *(Choudary et al., 2021).*

2.3. Environmental and safety management

Both exercises applied inject-based designs covering all operational phases (activation, deployment, operational execution, and demobilization) combining fixed and adaptive injects coordinated by EXCON. Non-toxic chemical simulants and inactivated biological agents were used under controlled laboratory or field conditions, with real-time safety oversight ensured by national S&S officers in compliance with host-country regulations.

In Lyon 2023, environmental management followed a reactive approach focused on addressing simulated chemical spills. Injects such as "Chemical Spill Response" and "Hazardous Waste Containment" required containment setup, decontamination operations, and coordination with local authorities for waste handling, while scheduled safety injects like "Safety Briefing" and "NO PLAY Drill" reinforced emergency suspension procedures and PPE compliance *(CN APELL-RO et al., 2023a, 2023b)*.

Riga 2025 was the first exercise in its cycle to incorporate a structured Environmental Impact Assessment (EIA), outlining risk control, spill prevention, waste management, and site restoration measures. Injects such as "Environmental Pre-Assessment" and "Post-Exercise Environmental Review" embedded environmental monitoring throughout the operational timeline, from early site evaluation and mitigation planning to the final assessment of containment effectiveness and post-exercise rehabilitation. Safety management followed a dynamic approach, including unscheduled

injects simulating heat stress, access-control failures, and public-safety incidents in urban environments *(CN APELL-RO & SFRS Latvia, 2025a, 2025b).*

Across both exercises, environmental and safety oversight was ensured by designated S&S officers, assisted by local emergency and medical teams. Continuous monitoring, "NO PLAY" protocols, and structured debriefings maintained a zero-incident record. This integration of safety and environmental aspects into scenario design marks the evolution of EU MODEX methodology from technical drills to realistic simulations addressing operational, ecological, and human-factor dimensions within the UCPM framework.

3. Results and Discussion

3.1. Operational performance and coordination

In Lyon 2023, modules showed strong cooperation in detection and sampling under challenging simulated conditions, achieving all operational goals within the planned timeframe. The MEL inject sequence prioritized technical execution: over 60% focused on field tasks such as sampling, testing, and decontamination, enabling effective validation of SOPs under realistic operational constraints.

In Riga 2025, the exercise shifted toward multi-agency preparedness and coordination, with about 45% of injects dedicated to information exchange, communication with LEMA and ERCC Liaison Officers, and real-time decision-making. This approach validated structured information flow models and the effective use of digital coordination tools such as situational Telegram channels and standardized SitRep templates.

This comparative MEL/MIL analysis shows that Riga's planning structure intentionally reduced the number of purely technical injects, replacing them with communication-driven tasks to test interoperability among modules and between civilian and institutional actors.

Effective CBRN preparedness relies on coordinated civil-military cooperation, joint training, and interoperability across institutional and disciplinary boundaries. Such integration improves decision-making, communication flow, and operational consistency during high-risk CBRN incidents *(Patel et al., 2022).*

3.2. Environmental protection and sustainability

The EIA process in Riga ensured that all simulated activities complied with environmental protection standards through comprehensive risk analysis, mitigation, and public awareness measures. Potential contamination pathways (air, soil, and

groundwater) were assessed, while preventive actions such as sealed containment, waste segregation, and site restoration were implemented alongside communication efforts to maintain public confidence.

Lyon's environmental management approach was reactive and integrated into late-phase injects, focusing on spill management and hazardous waste containment, whereas Riga introduced environmental monitoring as a preventive activity from the start of the exercise. This demonstrates a structural evolution in MEL planning, shifting from post-event remediation (Lyon) toward proactive environmental protection (Riga).

The comparative analysis illustrated in *Figure 1* highlights the evolution of CBRN exercise methodology within the UCPM framework. Lyon 2023 emphasized process safety and contamination control, validating technical procedures under operational stress. In contrast, Riga 2025 achieved higher performance in environmental compliance and coordination efficiency, reflecting the integration of EIA-based planning, preventive risk management, and enhanced interagency communication. Overall, the findings confirm a strategic shift from reactive technical response to proactive, environmentally responsible preparedness, reinforcing the role of engineering principles in advancing CBRN safety and sustainability.

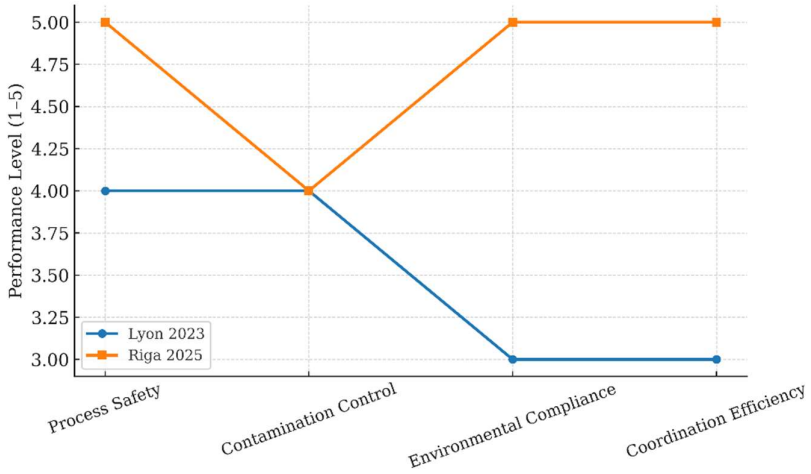

Fig. 1. Integrated Analytical Value of EU MODEX Lyon and Riga CBRN Field Exercises

4. Conclusions

The EU MODEX Lyon 2023 and Riga 2025 CBRN field exercises demonstrated that structured, scenario-based simulation remains one of the most effective tools for enhancing operational preparedness, interoperability, and environmental responsibility within the European civil protection framework.

By replicating realistic chemical risk scenarios and ensuring compliance with both safety and environmental standards, these exercises contribute directly to

strengthening the European Union's capacity for coordinated and sustainable CBRN response.

The integration of structured injects, dynamic "NO PLAY" safety procedures, and Environmental Impact Assessments (EIA) further demonstrates the contribution of chemical engineering to the design of resilient and environmentally compliant emergency operations. The inclusion of environmental protection objectives such as pollution prevention, containment management, and post-exercise site rehabilitation, marks a major step forward in embedding environmental safety principles into EU civil protection practice.

In particular, the implementation of the EIA framework in Riga paralleled industrial risk assessment methodologies (HAZOP/FMEA), demonstrating how process engineering tools can be successfully adapted for use in large-scale civil protection exercises. This approach ensures that environmental risks are not only mitigated during response operations but are also anticipated and minimized during the planning and simulation phases.

By integrating core concepts of process safety, reaction control, and contaminant transport modeling into scenario planning and inject design, these exercises bridged engineering theory with real-world emergency management practice. The structured MEL/MIL architecture mirrored the logic of chemical process design, where systematic sequencing, monitoring, and feedback loops are essential for achieving safety and efficiency under complex operational conditions.

Through this methodological integration, the EU MODEX exercises advanced the concept of environmental safety from a compliance requirement to a proactive operational objective, embedding ecological responsibility into CBRN preparedness and response.

Ultimately, these findings confirm that chemical and biochemical engineering provide the technical backbone of modern CBRN preparedness, translating theoretical safety design, process control, and contaminant management into practical operational capability. The EU MODEX field exercises thus serve as experimental platforms where engineering innovation, safety science, environmental protection, and crisis management converge, reinforcing the EU's capacity for coordinated, evidence-based, and sustainable response to CBRN risks.

Acknowledgments

The authors acknowledge the support of the European Commission's Directorate-General for European Civil Protection and Humanitarian Aid Operations (DG ECHO) under the Union Civil Protection Mechanism (UCPM) and the National Center APELL for Disaster Management Foundation, the lead of the EU MODEX Lot 2 Consortium. Appreciation is also extended to the EU MODEX Consortium partners: the DGSCGC

(France), SDMSI Lyon, and the State Fire and Rescue Service of Latvia (SFRS) for their contribution to the organization and implementation of the EU MODEX Lyon 2023 and Riga 2025 CBRN field exercises. The analysis presented in this study draws upon non-confidential, publicly available, and consolidated materials from UCPM training and exercise activities. The data are used exclusively for academic and research purposes, and the interpretations and conclusions expressed herein are solely those of the authors and do not represent the official position of the European Commission or any consortium partner.

REFERENCES

1. Argon Electronics. (2023). The Value of Live Exercises for Enhanced CBRN(E) Training. https://www.argonelectronics.com/blog/the-value-of-live-exercises-for-enhanced-cbrne-training
2. Choudary, S., Asghar, M. U., & Ibrahim, A. G. (2021). CBRN events and crisis communication: Analysis of training needs and development of curriculum for communication personnel. International Journal of Safety and Security Engineering, 11(4), 337-343. https://doi.org/10.18280/ijsse.110406
3. CN APELL-RO & SFRS Latvia. (2025a). LAT EU MODEX Riga 2025 - Exercise Handbook (Final V.1). EU MODEX Consortium. internal-document.
4. CN APELL-RO & SFRS Latvia. (2025b). MEL/MIL - Main Events and Injects List, LAT EU MODEX Riga 2025 [Data set]. EU MODEX Consortium. internal-document.
5. CN APELL-RO, DGSCGC, & SDMSI Lyon. (2023a). EU MODEX Lyon 2023 - Staff Exercise Handbook. EU MODEX Consortium. internal-document.
6. CN APELL-RO, DGSCGC, & SDMSI Lyon. (2023b). MEL/MIL - Main Events and Injects List, EU MODEX Lyon 2023 [Data Set]. EU MODEX Consortium. internal-document.
7. European Commission. (2024a). Civil Protection Exercises. Union Civil Protection Knowledge Network. https://civil-protection-knowledge-network.europa.eu/civil-protection-exercises
8. European Commission. (2024b). EU Grants: Technical Guide for UCPM Full-scale Exercises. https://ec.europa.eu/info/funding-tenders/opportunities/docs/2021-2027/ucpm/guidance/technical-guide-full-scale-exercises_ucpm_en.pdf
9. European Commission. (2024c). New project will support the organisation of table-top and field exercises to test and strengthen response capacities. CBRN Risk Mitigation Network. https://cbrn-risk-mitigation.network.europa.eu/news-1/new-project-will-support-organisation-table-top-and-field-exercises-test-and-strengthen-response-2024-06-28_en
10. European Commission. (2024d). Tanzania enhances national CBRN risk mitigation response through major live training exercise. CBRN Risk Mitigation Network. https://cbrn-risk-mitigation.network.europa.eu/news-1/tanzania-enhances-national-cbrn-risk-mitigation-response-through-major-live-training-exercise-2024-03-22_en
11. European Commission. (2025a). EU Civil Protection Mechanism. Union Civil Protection Knowledge Network. https://civil-protection-humanitarian-aid.ec.europa.eu/what/civil-protection/eu-civil-protection-mechanism_en
12. European Commission. (2025b). Strengthening CBRN safety in Southeast and Eastern Europe through a unified regional approach. CBRN Risk Mitigation Network. https://cbrn-risk-mitigation.network.europa.eu/news-1/strengthening-cbrn-safety-southeast-and-eastern-europe-unified-regional-approach-2025-03-28_en
13. European Parliament (EXPO). (2018). EU preparedness against CBRN weapons. https://www.europarl.europa.eu/RegData/etudes/STUD/2019/603875/EXPO_STU(2019)603875_EN.

pdf

14. European Parliament (EXPO). (2021). EU preparedness and responses to Chemical, Biological, Radiological and Nuclear (CBRN) threats. https://www.europarl.europa.eu/RegData/etudes/STUD/2019/603875/EXPO_STU(2019)603875_EN.pdf
15. European Union, DG ECHO; INSARAG, OCHA; Johanniter-Unfall-Hilfe e.V. (2021). Guidance for Conducting an INSARAG External Reclassification within the EU MODEX Field Exercise Platform, Version 1.1. https://insarag.org/wp-content/uploads/2022/03/EU-MODEX-IER-Handbook-v1.1-Final.pdf
16. Patel, S. S., Neylan, J. H., Bavaro, K., Chai, P. R., Goralnick, E., & Erickson, T. B. (2022). Chemical, biological, radiological, nuclear, and explosives (CBRNEs) preparedness for sporting event mass gatherings: A systematic review of the literature. American Journal of Disaster Medicine, 17(1), 57-74. https://doi.org/10.5055/ajdm.2022.0420
17. UCP Knowledge Network. (2023). EU MODEX LYON 2023. EU Civil Protection Knowledge Network. https://civil-protection-knowledge-network.europa.eu/news/eu-modex-lyon-2023
18. UCP Knowledge Network. (2025). LAT EU MODEX 2025. EU Civil Protection Knowledge Network. https://civil-protection-knowledge-network.europa.eu/news/lat-eu-modex-2025
19. van der Woude, I., Cock, J., Bierens, J., & Christiaanse, J. (2008). TAP CBRN preparedness: Knowledge, training, and networks. Prehospital and Disaster Medicine. https://doi.org/10.1017/S1049023X00021270

A GAS DRYING BY ADSORPTION ON POROUS MATRIX COMPOSITE MATERIALS

Florin BOGDAN[1], Mihai ALBULESCU[2*], Aurelian ȘISINEA[1]

[1]Ph.D. School, Petroleum-Gas University
[2]Oil and Gas Engineering Faculty, Petroleum-Gas University

Abstract

A significant part of recent research in the field of gas adsorption is focused on obtaining adsorbent materials with improved adsorption capacity and achieving high heat and mass transfer rates. Extensive experimental studies on the physicochemical properties and several applications of composite materials used as adsorbents were carried out by Aristov, Liu and Wang and Zhang, respectively. All their studies showed that these adsorbents have a higher adsorption capacity than the classical ones and can be regenerated at a low temperature. Thus, for the purpose of drying gases by adsorption, composite materials obtained by impregnating porous host matrices with hygroscopic inorganic salts were used. Silica gel in the form of spherical granules and granules of arbitrary shape (angular), activated alumina granules and activated carbon granules were used as host matrices.

Key words: gas drying, silicagel, matrix composites.

1. Introduction

For the purpose of drying gases by adsorption, composite materials obtained by impregnating porous host matrices with hygroscopic inorganic salts were used [1].As host matrices, silica gel in the form of spherical granules and granules of arbitrary shape (angular), activated alumina granules and activated carbon granules were used. In the case of silica gel, the spherical granules had a diameter of 2.57 mm, and the angular ones, an average diameter of 2.25 mm. The activated alumina granules and activated carbon had average diameters of 0.15 mm and 0.1 mm, respectively [2].
In this way, four types of composite materials were obtained [3, 4]:
C – activated carbon,
M1 –composite material obtained by impregnating activated carbon with $CaCl_2$ (calcium chloride) solution - 15%;
M2- composite material obtained by impregnating silica gel (cornered granules) with $CaCl_2$ (calcium chloride) solution - 15%;
M3 – composite material resulting from impregnating silica gel (spherical granules) with $CaCl_2$ solution (calcium chloride) - 15%.

2. Materials and Methods

The values of temperature, vapor concentration in the gas phase and water concentration in the solid phase were experimentally determined at several values of duration (10, 30,

* Corresponding author: malbulescu@upg-ploiesti.ro

60, 90, 120, 150 minutes) and at different heights of the fixed adsorbent layer (0.08, 0.16, 0.24, 0.32 and 0.4 m).

3. Results and discussions

In what follows, we determined the adsorption simulation equations on the materials used.

Table 1.

Concentration of water in the solid phase (kg/kg) (y) function to the temperature of experiments and concentration of water vapor in the gas phase (kg/m^3) (x) (carbone coal structures).

Temperature, K	313	323
Experimental models	$y = -625x^3 + 110x^2 - 1,1875x + 0,0215$	$y = 762,96x^3 - 110,41x^2 + 6,1826x - 0,0695$
Lagmuir models	$y = -50000x^4 + 4833,3x^3 - 150x^2 + 4,4667x - 0,01$	$y = -76153x^5 + 824,09x^4 + 1361,4x^3 - 113,52x^2 + 4,2748x - 0,0227$
Freundlich models	$y = 45833x^4 - 5416,7x^3 + 200,42x^2 - 0,4083x + 0,015$	$y = -419606x^5 + 72756x^4 - 4219,9x^3 + 81,655x^2 + 1,338x - 0,0069$

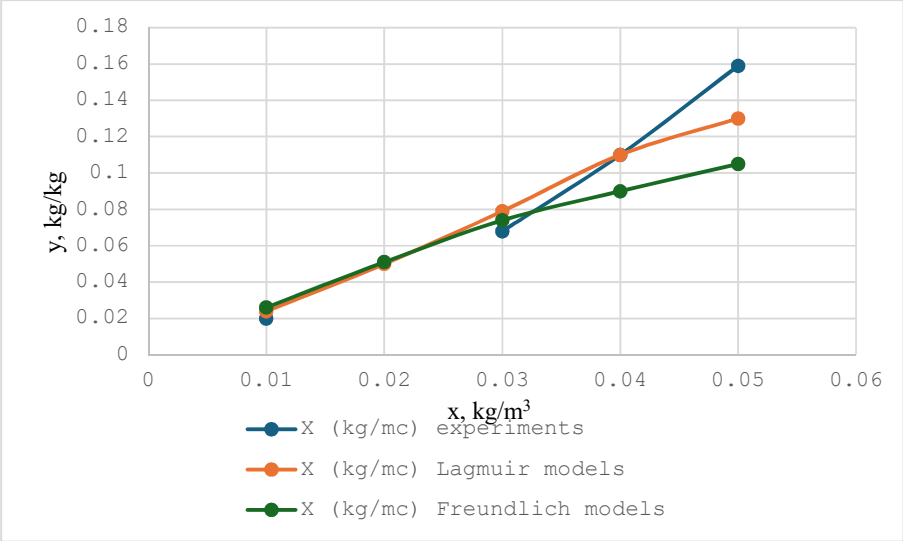

Fig.1. Concentration of water in the solid phase (kg/kg) (y) function to the temperature of experiments and concentration of water vapor in the gas phase (kg/m^3) (x) (carbone coal structures), temperature 313 K

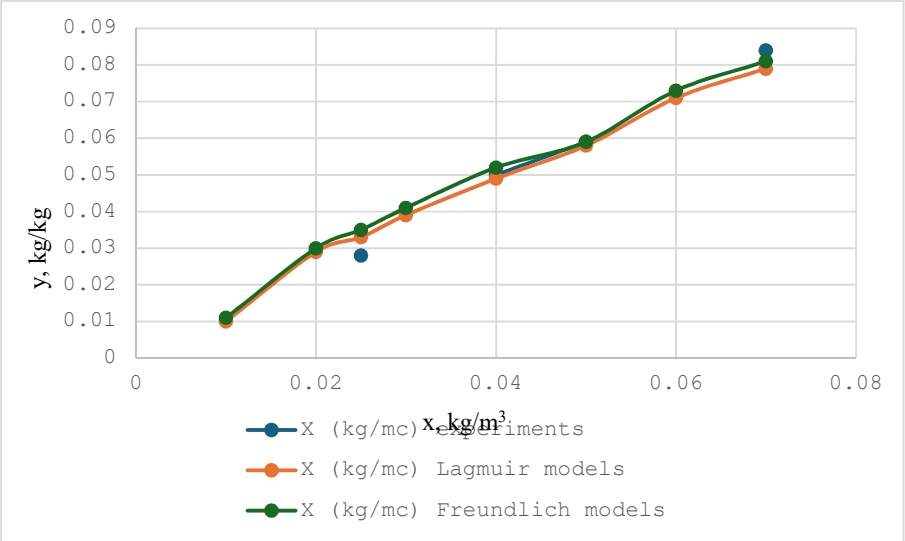

Fig.2. Concentration of water in the solid phase (kg/kg) (y) function to the temperature of experiments and concentration of water vapor in the gas phase (kg/m^3) (x) (carbone coal structures), temperature 323 K

Table 2.

Concentration of water in the solid phase (kg/kg) (y) function to the temperature of experiments and concentration of water vapor in the gas phase (kg/m^3) (x) (composite material obtained by impregnating activated carbon with $CaCl_2$ (calcium chloride) solution - 15%).

Temperature, K	313	323
Experimental models	$y = -4457,1x^3 + 434,86x^2 - 7,9486x + 0,1274$	$y = 795,27x^3 - 135,43x^2 + 10,105x - 0,0984$
Lagmuir models	$y = 2E+07x^5 - 3E+06x^4 + 169167x^3 - 4075x^2 + 49,85x - 0,16$	$y = -1E+08x^6 + 2E+07x^5 - 2E+06x^4 + 101419x^3 - 2610,2x^2 + 39,76x - 0,2147$
Freundlich models	$y = 3E+07x^5 - 5E+06x^4 + 250310x^3 - 6033,5x^2 + 71,169x - 0,2451$	$y = -2E+08x^6 + 6E+07x^5 - 5E+06x^4 + 230146x^3 - 5333,6x^2 + 63,017x - 0,244$

Table 3.

Concentration of water in the solid phase (kg/kg) (y) function to the temperature of experiments and concentration of water vapor in the gas phase (kg/m^3) (x) (composite material obtained by impregnating silica gel (cornered granules) with $CaCl_2$ (calcium chloride) solution - 15%).

Temperature, K	313	323
Experimental models	$y = 7476,2x^3 - 722,14x^2 + 26,388x - 0,1986$	$y = 923,18x^3 - 166,34x^2 + 11,168x - 0,1297$
Lagmuir models	$y = 3E+08x^5 - 4E+07x^4 + 2E+06x^3 - 47849x^2 + 539,6x - 2,1639$	$y = -5E+07x^6 + 1E+07x^5 - 850000x^4 + 36167x^3 - 849,5x^2 + 12,53x - 0,044$
Freundlich models	$y = 2E+08x^5 - 3E+07x^4 + 2E+06x^3 - 40474x^2 + 458,54x - 1,8416$	$y = -3E+06x^6 + 833333x^5 - 173611x^4 + 17250x^3 - 752,61x^2 + 15,667x - 0,076$

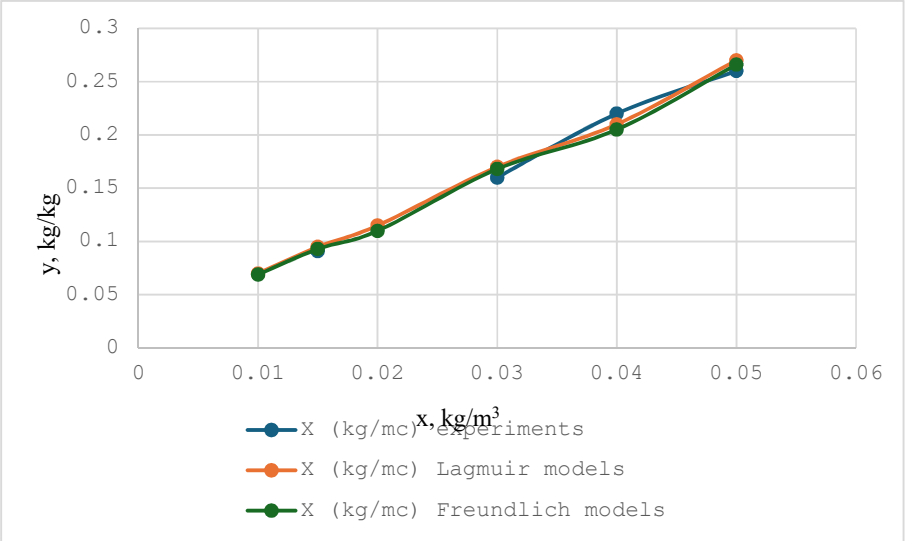

Fig. 3. Concentration of water in the solid phase (kg/kg) (y) function to the temperature of experiments and concentration of water vapor in the gas phase (kg/m^3) (x) (composite material obtained by impregnating activated carbon with $CaCl_2$ (calcium chloride) solution - 15%), temperature 313 K

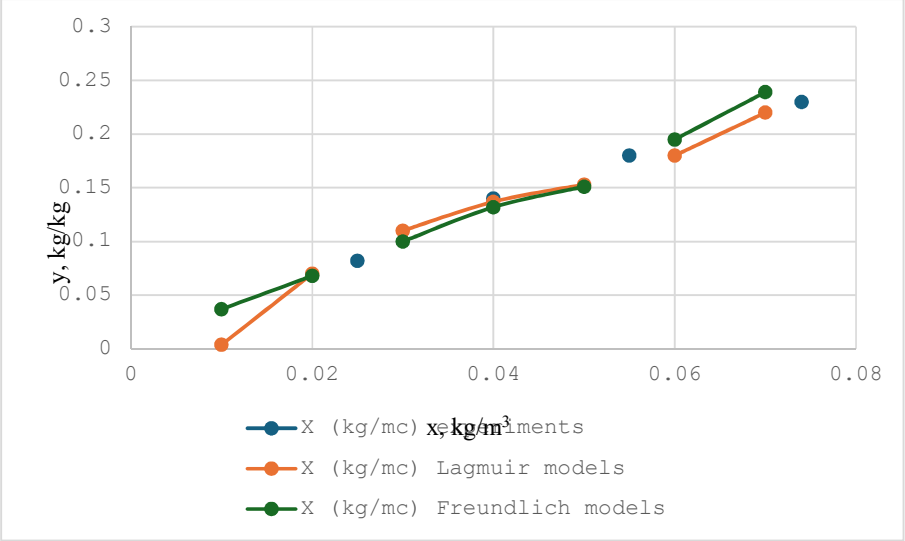

Fig. 4. Concentration of water in the solid phase (kg/kg) (y) function to the temperature of experiments and concentration of water vapor in the gas phase (kg/m^3) (x) (composite material obtained by impregnating activated carbon with $CaCl_2$ (calcium chloride) solution - 15%), temperature 323 K

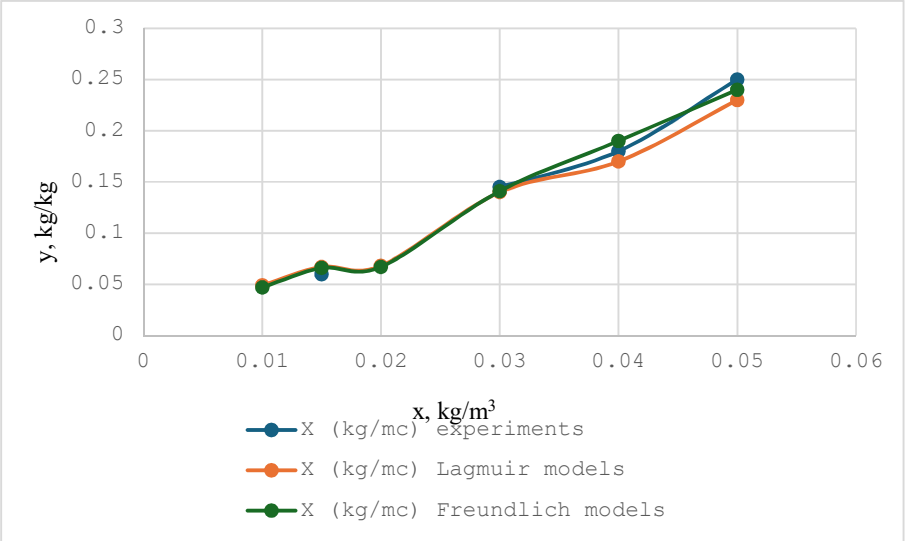

Fig. 5. Concentration of water in the solid phase (kg/kg) (y) function to the temperature of experiments and concentration of water vapor in the gas phase (kg/m^3) (x) (composite material obtained by impregnating silica gel (cornered granules) with $CaCl_2$ (calcium chloride) solution - 15%), temperature 313 K

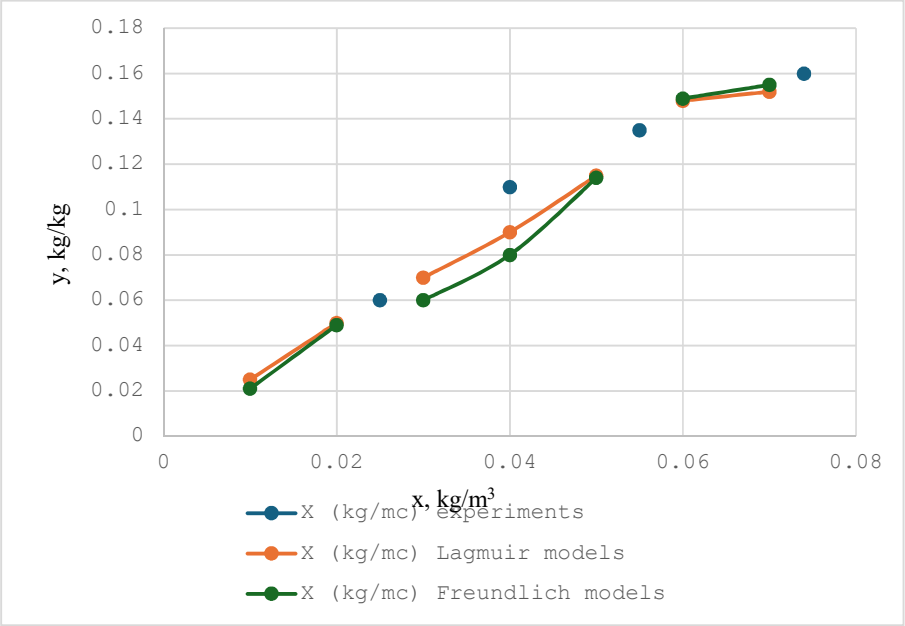

Fig. 6. Concentration of water in the solid phase (kg/kg) (y) function to the temperature of experiments and concentration of water vapor in the gas phase (kg/m^3) (x) (composite material obtained by impregnating silica gel (cornered granules) with $CaCl_2$ (calcium chloride) solution - 15%), temperature 323 K

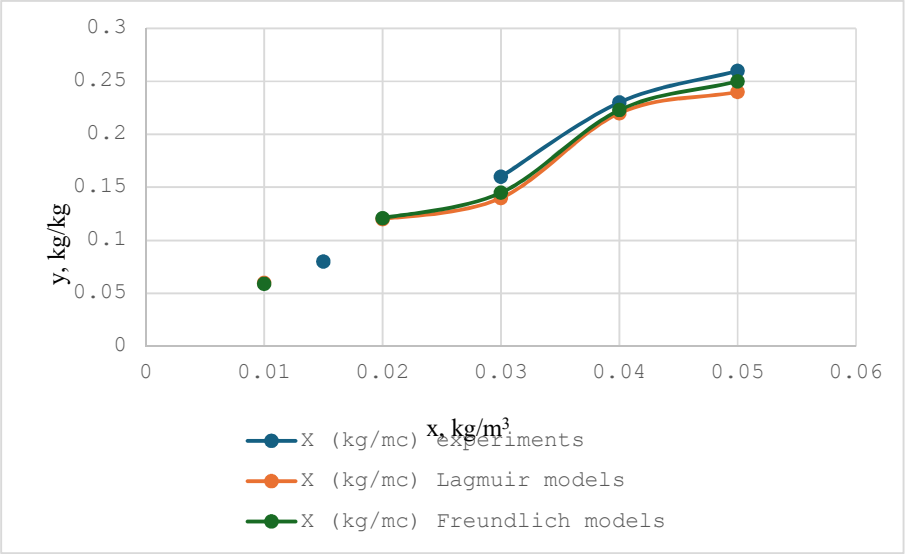

Fig. 7. Concentration of water in the solid phase (kg/kg) (y) function to the temperature of experiments and concentration of water vapor in the gas phase (kg/m^3) (x) (M3 – composite material resulting from impregnating silica gel (spherical granules) with $CaCl_2$ solution (calcium chloride) - 15%), temperature 313 K

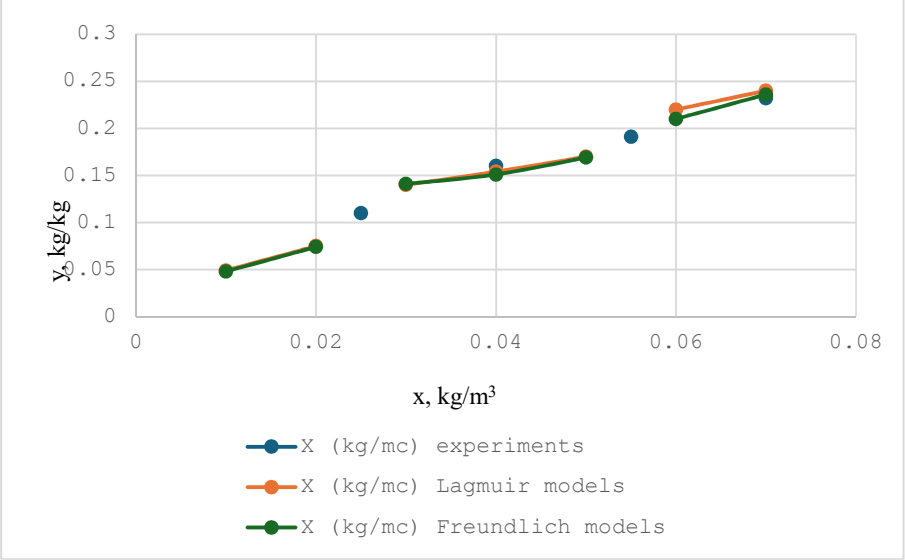

Fig. 8. Concentration of water in the solid phase (kg/kg) (y) function to the temperature of experiments and concentration of water vapor in the gas phase (kg/m^3) (x) (M3 – composite material resulting from impregnating silica gel (spherical granules) with $CaCl_2$ solution (calcium chloride) - 15%), temperature 323 K

Table 4.

Concentration of water in the solid phase (kg/kg) (y) function to the temperature of experiments and concentration of water vapor in the gas phase (kg/m^3) (x) (M3 – composite material resulting from impregnating silica gel (spherical granules) with $CaCl_2$ solution (calcium chloride) - 15%).

Temperature, K	313	323
Experimental models	$y = -7619x^3 + 714{,}29x^2 - 14{,}81x + 0{,}1671$	$y = 1432{,}1x^3 - 214{,}07x^2 + 12{,}63x - 0{,}0943$
Lagmuir models	$y = -916667x^4 + 108333x^3 - 4408{,}3x^2 + 76{,}167x - 0{,}36$	$y = 1E{+}08x^6 - 4E{+}07x^5 + 5E{+}06x^4 - 281604x^3 + 8262{,}9x^2 - 108{,}79x + 0{,}548$
Freundlich models	$y = -819167x^4 + 97233x^3 - 3976{,}1x^2 + 69{,}707x - 0{,}3295$	$y = 3E{+}08x^6 - 8E{+}07x^5 + 8E{+}06x^4 - 449500x^3 + 12293x^2 - 155{,}56x + 0{,}747$

4. Conclusion

The analyses showed that both the concentration of water vapor in the gas phase and the concentration of water in the adsorbent decrease over the height of the fixed bed. With increasing duration, the variation of the concentration C over the height is increasingly smaller. At high gas flow rates, in the upper part of the bed, this variation is insignificant, which highlights the existence of a saturated layer zone whose height continuously increases.

The concentration of water in the solid phase (X) also decreases over the height of the bed and with increasing duration and flow rate X increases. The temperature of the gas phase increases over the height of the fixed bed and presents a maximum at a certain value after which it decreases. At low values of duration, the maximum point is located at the upper part of the column and with increasing duration it moves towards the lower part of the fixed bed column.

5. Data Availability

The data presented in this article are real and collected from the area of interest.

The data can be used by anyone in accordance with applicable international regulations. Data is available in the article and can be provided upon request.

6. Conflicts of Interest

No data or information is presented that could endanger companies or commercial or public companies. There are no conflicts regarding the exposed data. The data taken from the soil samples analyzed and presented in the article are part of oil fields abandoned and handed over to the public domain.

The authors did not benefit from public, private or other resources.

REFERENCES

[1]. Dake, L.P., *Fundamentals of reservoir engineering*. Shell International Petroleum Maatschappij, Haga, 1978,
[2]. Lee, J., Wattenbarger R.A., *Gas Reservoir Engineering*, SPE Houston, Texas, 2004.
[3]. Bogdan F., Albulescu M., Artificial neural networks (ANN) in gas treatment, Artificial intelligence research – The new paradigm in mines, oil and gas abstract of EDUDOC, 2025 SYMPOSION, Editura Universității Petrol-Gaze din Ploiești, 2025, ISBN 978-973-719-925-6,
[4]. Bogdan F., Albulescu M., Effects of gas treatment on their quality, Artificial intelligence research – The new paradigm in mines, oil and gas abstract of EDUDOC, 2025 SYMPOSION, Editura Universității Petrol-Gaze din Ploiești, 2025, ISBN 978-973-719-925-6.

A NUMERICAL OFFSHORE EXPLOSION MODELING IN NATURAL GAS DRILLING

Timur CHIS[1*], Daniel IANCU[2*], Lazar AVRAM[1], Calin IORGA[2]

[1]Oil and Gas Engineering Faculty, Petroleum-Gas University
[2]Ph.D. School, Petroleum-Gas University

Abstract

The explosion of the Deepwater Horizon oil platform was one of the most serious accidents, leading to the loss of 5 million barrels (pollution of the Gulf of Mexico) and the disappearance of 11 people. That is why the description of a simulation model of an explosion on a marine platform makes the prevention activity useful, in the context of the increasing importance of the exploitation of the Black Sea. Through this material we simulated a possible explosion on a Romanian oil structure, in order to obtain the minimum data necessary to be quantified so that an incident does not occur.

Key words: oil offshore, drilling platform, risk assessment, numerical models, oil rig explosion.

1. Introduction

Offshore activities, especially oil and gas exploration and exploitation, are risky ventures. Drilling a well and the risks it poses are not negligible.
In addition, oil rigs are hazardous environments with heavy equipment, dangerous substances (flammable chemicals and gases), and remote locations from shore where weather and water conditions are unpredictable.
To date, the US oil and gas industry safety standards have been developed primarily by the American Petroleum Institute (API).
In Romania, oil and gas industry safety standards have been developed by national authority and European Union Strategy.
This body is based on extensive and long-standing technical expertise.
API and International Standard Office (ISO) produces standards, recommended practices, specifications, codes, and so on, which have been adopted mainly by drilling and mining companies.
However, the American Petroleum Institute (API) 's expertise in setting drilling safety standards is compromised by its role as the industry's chief lobbyist (major oil and gas companies sponsor the association) [1].
Indeed, the American Petroleum Institute (API) has regularly disapproved of and resisted agency rules (standards and codes), favoring only decisions that promote an autonomous industry without government oversight.
In some ways, American Petroleum Institute (API) experts have undermined the entire federal regulatory system.

* Corresponding author: timur.chis@gmail.com

Surprisingly, risks and safety are approached differently depending on the part of the globe where drilling companies operate.
Indeed, from 2004 to 2024, fatalities in the offshore oil and gas industry were significantly higher (more than four times) per person-hour worked in US waters than in European waters, even though the companies operating in these waters are frequently the same.
In Romania, incidents of Offshore platforms it is at low level, because the strategy of working to Romanian Offshore Platforms is approve to the Life and Safety Management Authority Standards.
This striking discrepancy reinforces the view that the problem is not so much about the business itself but rather is determined by the specific cultures and regulatory systems in which the industry's many members operate.
Past accidents in offshore oil and gas operations must be analyzed to establish new work procedures.
This should be considered when estimating overall risk and in the risk -based decision-making process.
The entire process of risk management and the ALARP (As low as reasonably practicable) principle is based on a prerequisite of discernment.
The principle assumes that most risks can be controlled, while only a tiny percentage of "remaining risk" needs to be tolerated - and should be managed cost-effectively.
This means that a significant amount of risk remains uncontrolled.

2. Materials and Methods

In what follows, we analyzed the explosion of the compressor on the offshore platform based on the phenomenon of natural gas dispersion in its ventilation system.
This is cause to the more oil accidents.
The extent of damage caused by releasing flammable gases is partly a function of cloud dispersion.
If there is no immediate ignition, flammable vapors are dispersed through the structure's geometry (metal construction) and ventilation systems, and ignition may be delayed.
Ignition and explosion of the resulting vapor cloud (VCE) occur if the gas's flammability limits are met (based on gas composition) and an ignition source of sufficient energy is present.
Several factors, namely influence an explosion of a gas cloud [2]:

a. the probability of ignition increases with the size of the vapor cloud,
b. the effectiveness of the explosion and its impact is affected by the turbulent mixture of vapor and air,
c. the efficiency of the explosion depends on the location of the ignition sources,
d. the size of the explosion depends on the concentration of the explosive medium (gas cloud).

When an explosion occurs, a transient pressure of the explosive cloud (develops) that is higher than the atmospheric pressure around the area of the blast, called overpressure.

During such a phenomenon, the gas rapidly expands due to the released energy, and the surrounding atmospheric gas mixture is forced back, initiating a pressure wave that rushes from the source of the explosion to the outside of the production area.
The propagation of a pressure wave in air, or blast wave, is the source of most of the damage they cause.
The blast is composed of the pressure wave, and the overpressure changes during the blast period depending on the speed of air currents, air temperature, and weather conditions (precipitation level, etc.).
The dispersion of the gas cloud and the explosion of the explosive mixture are complex multiphase transport phenomena, and to obtain the effect of the blast on the facilities and employees, we used dynamic computational models.
We proposed to the dropping of a pipe at the well, which was positioned obliquely in the blowout preventer, coupled with the haste to cement the drill pipe (drill string) with nitrogen and cement, led to the eruption.

3. Results and discussions:

For the calculation of pressure losses on the pipe, we took into account the following aspects [2]:

- well depth 5486 m,
- great depth (depth to the bottom of the sea) 1522 m,
- deposit temperature 167ºC (470 ºK),
- pressure in the well at the time of the accident 551 bar,
- BOP resistance pressure 1000 bar,
- normal reservoir pressure (designed and expected to be possible in operation) 466 bar.

The column on which the eruption occurred is 5 ¾ inches,
The isotropic speed of sound whose value enters the expression [3]:

$$a = \sqrt{\frac{\chi\, p}{\rho}} \tag{1}$$

Where p is obtained from the relation:

$$\frac{p}{\rho} = gRT \tag{2}$$

Where R is the universal gas constant (52.89 kgm/degree K) and T is the reservoir temperature ºK).

$$a = \sqrt{\chi g R T} \tag{3}$$

$a = \sqrt{1{,}285 \cdot 9{,}81 \cdot 52{,}9 \cdot 470} = 263$ m/s
Where:

$$M = \frac{v}{a} \tag{4}$$

Where M is the Mach number (2), we determine the gas velocity:

$$v = M\, a \tag{5}$$

And v=526 m/s
For the column of 5 ¾ inch, d_1 is 148 mm and A_1=0,0125 m^2.
Therefore the gas flow will be:

$$Q_1 = A_1 v_1 = 0{,}0125 \cdot 526 \cdot 86400 = 545356 \frac{Nmc}{24} h$$

Because $\frac{d_2}{d_1} = 1{,}104$ și $\frac{T_2}{T_1} = 0{,}929$ and

$$\frac{p_2}{p_1} = 0{,}718$$

Is obtained:

$T_2 = 9ºC$.

So, a gas temperature of 9ºC was achieved through its expansion.

We also simulated the explosion on the oil platform (figure 1).

The area of fatal injury was 91 m, of injury with hospitalization 126 m, and of minor burns 196 m.

The length of the open flame was 14 m, and the amount of gases burned was 71000 kg/minute, i.e. 234401 kilograms.

To observe how the BOP (blowout preventer) acted on the effects of the accident (based to the effects of this equipment on the romanian oil platforms platform), we analyzed its closure.

The beneficial effect on the level and amplitude of the explosion, if operated with the sealing device closed (the blowout preventer tanks-BOP), is noted.

In Table 1, we analyzed the effect of preventer closure on the blowout on the oil platforms, considering a vent pipe diameter of 8%, 10%, 25%, 50%, 75%, and 100% of the drill rod diameter (5 ¾ inches).

In figures 2, 3, 4, 5, and 6, we have analyzed the effect of a blowout on the oil accident platform at an exhaust pipe diameter of 8%, 10%, 25%, 50%, 75%, and 100% of the drill rod diameter (5 ¾ inches).

In table 2 and figures 7, 8 and 9 we presented the variation equations of the effects of the accident on the oil platform according to the position (opening) of the blowout preventer (BOP).

We also analyzed a new relationship whose objective is to provide data on the opening value of the BOP (blowout preventer) according to the level of employee injury.

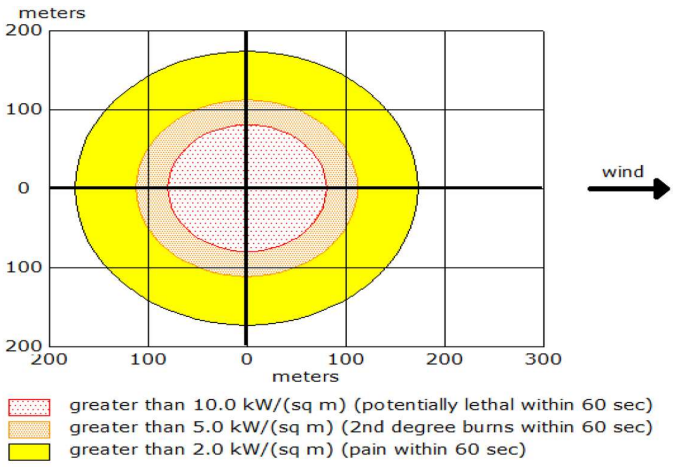

Fig. 1. The effect of the oil simulation explosion

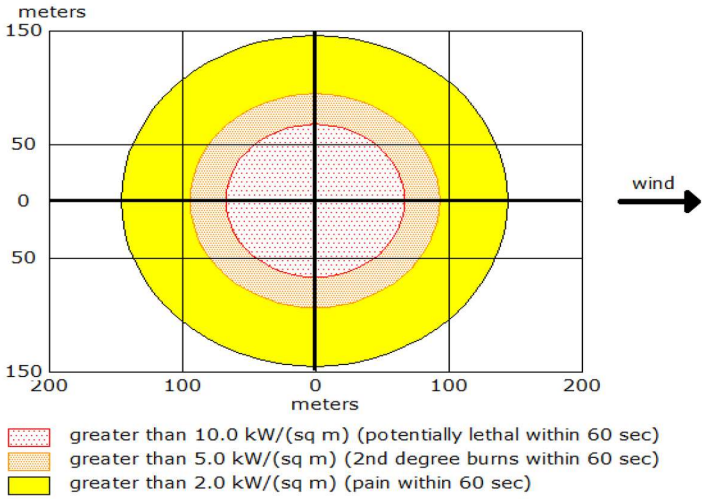

Fig. 2. Effect of the blowout on the oil analysis platform (75% BOP open)

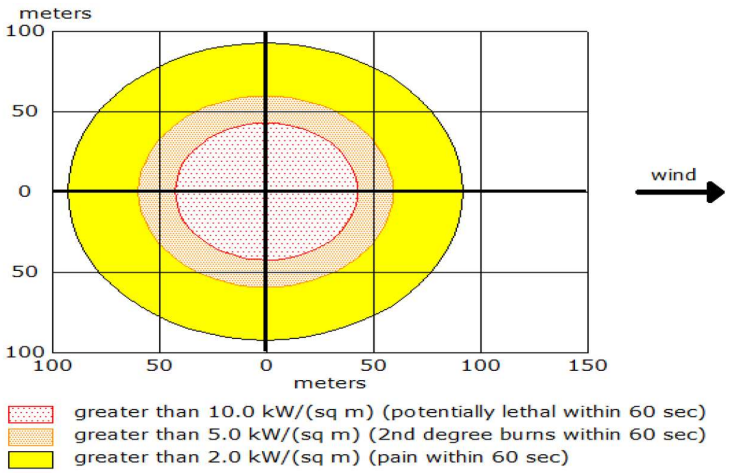

Fig. 3. Effect of the blowout on the Romanian oil platforms (50% BOP open)

Tables 1.

Effect of Preventer Shutdown on Romanian oil platforms Explosive Blowout

Eruptive tube diameter, %	Eruptive tube diameter, mm	Open flame length, m	Exhaust rate, kg/min
100	146	14	86300
75	109	12	53300
50	73	8	25400
25	36	4	5700
10	14	1	863
8	10	1	440

Diameter of the eruptive pipe, %	Area of fatal injury, m (10 kw/m^2)	Area of injury with hospitalization, m (5 kw/m^2)	Area of injury with minor burns, m (2 kw/m^2)
100	91	126	196
75	67	94	146
50	43	59	92
25	17	23	36
10	10	10	10
8	10	10	10

The multifactorial regression equation is of the form:

$$y=6,952-0,010\,x_1-3,434\,x_2+2,684\,x_3 \quad (6)$$

Where y is the opening of the BOP (% of exhaust pipe), x_1, x_2 and x_3 are the distances of fatal injury, hospitalization or minor burns (m)

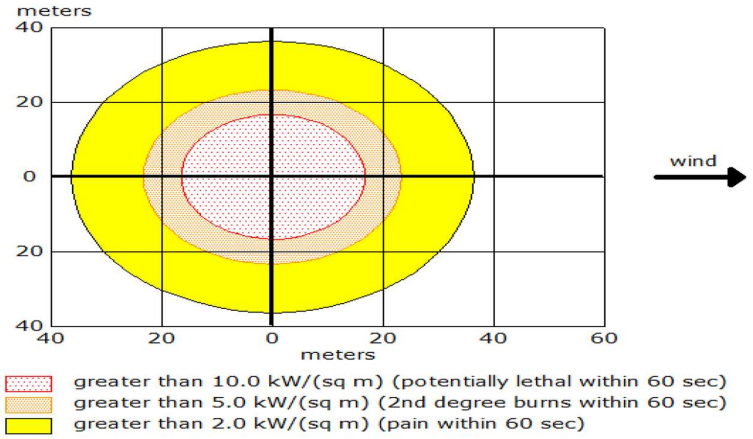

Fig. 4. Effect of the blowout on the Deepwater Horizon platform (25% BOP open)

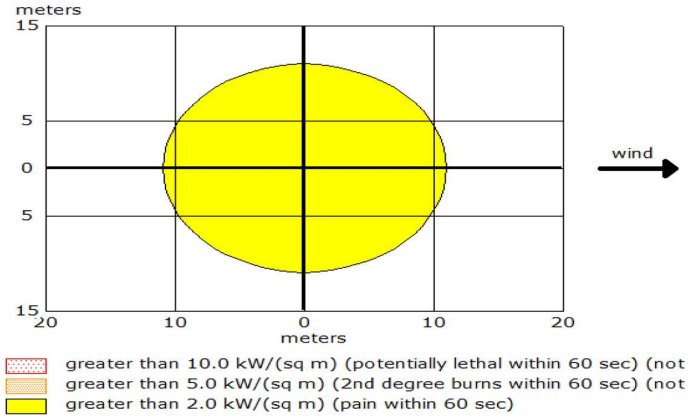

Fig. 5.Effect of the blowout on the Deepwater Horizon platform (10% BOP open)

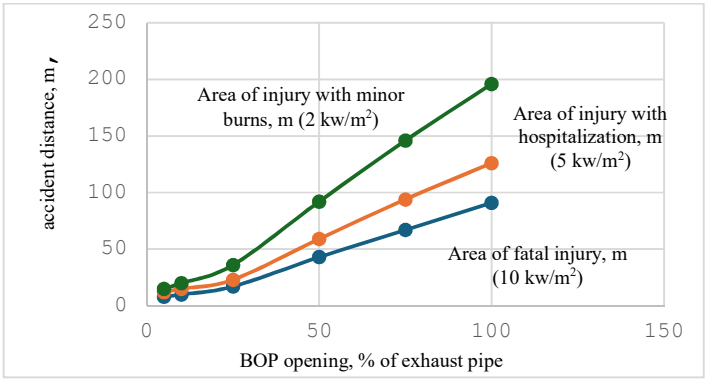

Fig. 6. The effect of the oil explosion

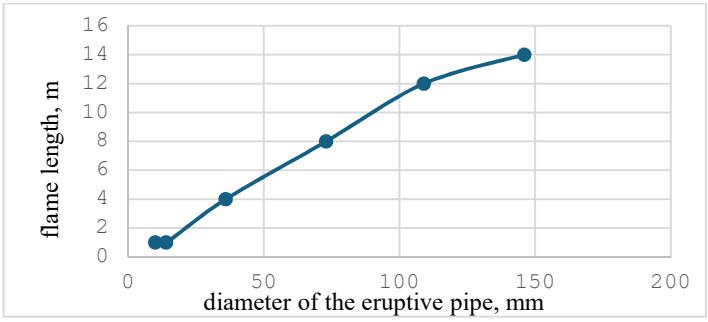

Fig. 7. The length of the oil rig flame (explosion)

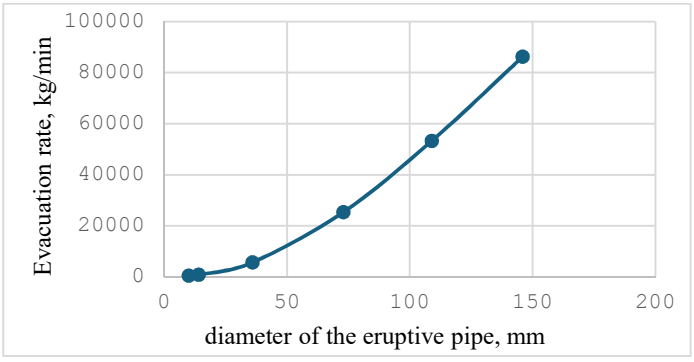

Fig. 8. Gas escape rate from the oil platforms modeling

Table 2.

Equations of variation of the effects of the oil platforms accident as a function of the position (opening) of the blowout preventer (BOP)

Accident efects	Equation	Remarks
Area of fatal injury, m (10 kw/m^2)	$y = 2E\text{-}07x^5 - 5E\text{-}05x^4 + 0{,}0039x^3 - 0{,}0995x^2 + 1{,}9046x + 7{,}5117$	y is the fatality distance (m) , x is the BOP opening (% of exhaust pipe)
Area of injury with hospitalization, m (5 kw/m^2)	$y = 2E\text{-}07x^5 - 4E\text{-}05x^4 + 0{,}0034x^3 - 0{,}0959x^2 + 1{,}5139x + 6{,}4249$	y is the fatality distance (m) , x is the BOP opening (% of exhaust pipe)
Area of injury with minor burns, m (2 kw/m^2)	$y = 1E\text{-}07x^5 - 2E\text{-}05x^4 + 0{,}0018x^3 - 0{,}0448x^2 + 0{,}7946x + 4{,}9328$	y is the fatality distance (m) , x is the BOP opening (% of exhaust pipe)
The length of the flame	$y = -4E\text{-}08x^5 + 1E\text{-}05x^4 - 0{,}001x^3 + 0{,}0376x^2 - 0{,}4133x + 2{,}2408$	y is Flame Length (m), x is BOP opening (% of exhaust pipe)
Evacuation rate of methane gas through BOP, kg/min	$y = 0{,}0003x^4 - 0{,}1214x^3 + 19{,}62x^2 - 237{,}84x + 1243{,}8$	y is the Evacuation Rate of methane gas through BOP, kg/min, x is BOP opening (% of outlet pipe)

4. Conclusion

In this material, we studied the accident on the Romanian oil platform.
We presented:

a. the risks assumed and not assumed following the drilling operation on the platform,
b. The errors of the prevention and control mechanism,
c. Effects of the oil platforms accident.

To observe how the BOP (blowout preventer) acted on the effects of the accident on the oil platform, we analyzed its closure. To determine the effect on blowout level and amplitude if the sealer (BOP-Bops) was operated closed, we studied the preventer considering a blowout pipe diameter of 8%, 10%, 25%, 50%, 75%, and 100% of the drill rod diameter (5 ¾ inches).

5. Data Availability

The data presented in this article are real and collected from the area of interest.
The data can be used by anyone in accordance with applicable international regulations. Data is available in the article and can be provided upon request.

6. Conflicts of Interest

No data or information is presented that could endanger companies or commercial or public companies. There are no conflicts regarding the exposed data. The data taken from the soil samples analyzed and presented in the article are part of oil fields abandoned and handed over to the public domain.

The authors did not benefit from public, private or other resources.

REFERENCES

[1] Elusakin, T., Shafiee, M., *Reliability analysis of subsea blowout preventers with condition-based maintenance using stochastic Petri nets, Journal of Loss Prevention in the Process Industries,* doi: https://doi.org/10.1016/j.jlp.2019.104026, 2020,

[2] Hopkins, P., Goodfellow, G., Ellis, R., Haswell, J., Jackson, N., *Pipeline risk assessment: new guidelines*, WTIA/APIA Welded Pipeline Symposium, Sydney, Australia, 2009.

[3]Sulaiman, D., Iancu, D., Al Jubori, H., *The current state of research on the dilation processes of productive reservoir rocks related to natural gas wells*, 75 Years of Energy and Performance in Education and Research 2023 Renewable Versus Fossil Fuels. Global Energy Perspectives, Ploiesti 9.11.2023, Book of abstracts, Editura Universității Petrol-Gaze din Ploiești, 2023, ISBN 978-973-719-887-7.

A NUMERICAL MODELS APPLIED IN THE STUDY OF NATURAL GAS MOVEMENT IN UNDERGROUND DEPOSITS

Timur CHIS[1*], Ionut LUNGU[2*], Doru BARSAN[1], Andrei BARBULESCU[2]

[1]Oil and Gas Engineering Faculty, Petroleum-Gas University
[2]Ph.D. School, Petroleum-Gas University

Abstract

Inside the cavity and the well, the gas does not behave adiabatically: it exchanges heat with the surrounding rock. It is not possible to accurately represent the cavity shape and heat exchanges in detail, partly because of imperfect knowledge of the geological environment and partly because a detailed three-dimensional numerical model would be far too time-consuming. This paper describted the storage of natural gas in salt underground deposits.

Key words: oil salt, deposit, underground, numerical models

1. Introduction

For the simulation of the storage, an intermediate approach is adopted, with a simplified description of the geometry and heat exchange between the well and the cavity.

Next, the equation of state of natural gas is used [1]:

$$\frac{P}{\rho} = ZrT \tag{1}$$

Where

T is gas temperature;

P is pressure,

$Z\ (P,T)$ is the compressibility factor, and $q(P,T)$ represents the gas density in the well.

For the cavity design, a spherical cavity is chosen, which is represented by a spherical volume (V_c) and an exchange surface (S_c) with the rock mass. The gas pressure (P_c) and the temperature inside the cavity (T_c) are considered uniform.

The equations describing the thermodynamic evolution of the gas are integrated over the cavity volume.[2]

The conservation of mass is given by:

$$\frac{\partial(\rho(P_c,T_c)V_c}{\partial t} = Q \tag{2}$$

Where: Q represents the mass flow rate of gas injected (respectively positive) or withdrawn (respectively negative) from the cavity.

The energy balance equation in the cavity can be written as:

* Corresponding author: timur.chis@gmail.com

$$\left(\rho c_{\upsilon} \frac{\partial T_c}{\partial T} - \frac{T_c}{\rho} \frac{\partial P}{\partial T} \frac{\partial p}{\partial t}\right) V_c = \gamma S_c h`(T_{wall.c} - T_c) + < Q >^{+} (T_{botton} - T_c) \quad (3)$$

Where:

$$<Q>^{+} = Q \text{ if } Q \geq 0$$
$$<Q>^{+} = 0 \text{ if } Q \leq 0$$

γ represents a surface shape factor, since the real cavity is not spherical,
$T_{well.c}$ represents the temperature at the cavity wall,
$T_{botton.c}$ gas temperature at the bottom of the well,
c_p is the specific heat capacity of the gas at constant pressure;
h' is a surface heat transfer coefficient.

The last term on the right-hand side of equation (3) represents the heat input during injection, while the first term describes the heat exchange with the rock mass.

In the rock mass, the temperature field T_{roks} verifies the heat equation:

$$\rho_r \, c_p^r \frac{\partial T_{rock}}{\partial t} + dic \, (-\lambda_{rock} \boldsymbol{\nabla} T_{rock}) = 0 \quad (4)$$

where :

ρ_r is the density of the rock,

c_p^r the specific heat capacity of the rock per unit mass, and λ rock is the thermal conductivity of the rock.

2. Materials and Methods

The temperature distribution is assumed to be spherically symmetric around the cavity. The rock mass surrounding the cavity is then discretized into spherical layers (Fig. 1).

The cavity problem with the surrounding rock mass is solved as a one-dimensional coupled nonlinear problem [3].

The flow in the probe considers a probe that is considered vertical, with radius rw and length *L*, and is identified by a vertical coordinate *z* pointing downward in this section.

The flow is one-dimensional along the probe, and the mass flow rate is assumed constant along the entire length of the probe (acoustic waves along the probe are not considered).

The gas velocity *u* is given by the relation:

$$u = \frac{Q}{\rho \pi r_w^2} \quad (5)$$

The gas velocity u is given by the relation:[3]

$$\rho \frac{Du}{Dt} = -z \frac{\partial P}{\partial z} + \rho g - sgn(u) \frac{\lambda}{2r_w} \rho \frac{u^2}{2} \quad (6)$$

where the last term on the right hand side represents the pressure drop.

λ is a friction coefficient estimated by the Colebrook equation,

$$\frac{D}{Dt} = \frac{\partial}{\partial t} + \mathrm{u} \frac{\partial}{\partial t} \quad (7)$$

Denoting e as the internal energy of the gas per unit mass, conservation of energy and conservation of momentum are combined.

This leads to:

$$\rho\frac{De}{Dt} = -P\,\frac{\partial u}{\partial z} + \frac{2}{r_w}\phi + \phi_v \tag{8}$$

where φ_v is the dissipation rate related to the viscosity-determining effects and φ is the heat flux.

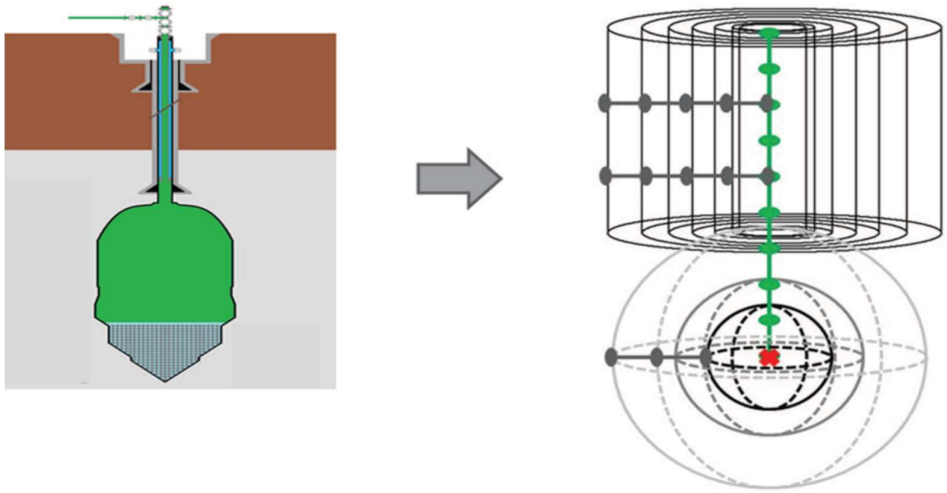

Fig. 1: Discretization of rock into spherical layers

This equation (8) becomes:

$$\rho c_v^g \frac{DT}{Dt} - T\frac{\partial P}{\partial T}\Big|_\rho \frac{u}{\rho}\frac{\partial \rho}{\partial z} = \frac{2}{r_w}\phi + \phi_v, \tag{9}$$

$$\phi_v = \text{-}sgn\,(u)\,\frac{\lambda}{2X\,r_w}\,\rho\,\frac{u^3}{2} \tag{10}$$

$$\phi = h(T_{wall}\,(z,t) - T(z,t)) \tag{11}$$

c_u^g is the heat capacity of the gas at constant volume per unit mass.

$T_{wall}\,(z,t)$ denotes the temperature on the well wall, at the interface between the well and the rock mass.

It is assumed that T_{wall} and the rock mass temperature are axisymmetric.

It is observed that the typical order of magnitude of the gas velocity is between 1 and 15 m/s.

Thus, the gas flow is turbulent.

Where h is the convective heat transfer coefficient, and is given by the relation:

$$h = max\left(\frac{\lambda_g}{r_w}, \frac{\lambda_g}{2r_w}N_u\right) \tag{12}$$

where λ_g is the thermal conductivity of the gas and N_u is the Nusselt number.

It is estimated from correlations with the Reynolds and Prandtl numbers.

The heat exchange between the fluids in the cavity and the surrounding rocks cannot be neglected.

The temperature field *(T_{rock})* is used to verify the asymmetric heat equation.

At the interface between the rock and the well, the temperatures and heat fluxes must be continuous [4].

$$T_{rock}\ (r_w,\ z,t) = T_{wall}\ (z,t) \quad (13)$$

$$\lambda_{rock}\partial_{rock}(r_w,z,t) = -h(T_{ff}(z,t) - T_{wall}(z,t) \quad (14)$$

$$\text{whith } (z)\ \epsilon\ x\ (0,L) \quad (15)$$

Assuming pressure balance between the pressure at the bottom of the borehole and the pressure in the cavity, we obtain:

$$P_{base} = P_c + q(P_c,\ T_c)\ g\ R_c \quad (16)$$

Where R_c is the cavity radius.

The development of a mathematical model that corresponds to both the borehole and cavity conditions is done by adopting finite volume discretization along the borehole and in the rock mass [5]) and formulated as a fixed point problem solved iteratively, when the gas is injected.

During gas extraction, the mathematical model is initially applied to the cavity;

$$P_{base} = P_c + q(P_c,\ T_c)gR_c \quad (17)$$

$$T_{siu} = T_c \quad (18)$$

3. Results and discussions

And the above data are imposed as boundary conditions at the bottom of the borehole.

Domain decomposition methods iteratively solve, at a given time, the well and rock mass subproblems, with transmission conditions chosen to obtain well-posed subproblems and a fast convergence to the coupled solution.

Compared to a fully coupled algorithm, domain decomposition approaches have the advantage of allowing the use of adapted algorithms for each subproblem.

Moreover, they are modular.

For example, for long extraction cycles, the thermal influence of the surrounding rock can be neglected and a reasonable approximation consists in eliminating it from the calculation [6].

To explain the implemented algorithm, we consider a simplified version of the mathematical model of the well.

Assuming that the coupled problem is axisymmetric, the rock temperatures $T_{rocă}$, the well T and the temperature at the contact between the well walls and the surrounding rock T_{wall} satisfy the following linear system of equations, with the gas velocity u being considered constant [2]:

$$\rho_r c_p^r \frac{\partial T_{rock}(r,z,t)}{\partial t} = \lambda_{rock} \Delta T_{rock}(r,z,t) \quad (19)$$

for rocks mass

$$\rho c_u^g \frac{\partial T(z,t)}{\partial T} + \rho c_u^g u \frac{\partial T(z,t)}{\partial z}(z,t) = H(T_{wall}(z,t) - T(z,t)) \quad (20)$$

along the length of the borehole with

$$H = \frac{2h}{r_w}$$

and by applying continuity conditions at the drilling level:

$$T_{rock}(r_w, z, t) = T_{wall}(z,t) \quad (21)$$

$$\lambda_{rock} \partial_r T_{rock}(r_w, z, t) = -h(T(z,t) - T_{wall}(z,t)) \quad (22)$$

The last two equations are the conditions for the continuity of temperature and heat flux at the borehole level (called the walls) [1].

In practice, the mathematical model for the borehole and the rock mass described by the first two equations is solved iteratively, until convergence to the fully coupled solution (for which the temperature and heat flux in each domain at the borehole level are equal).

The convergence rate of the domain decomposition methods depends largely on the boundary conditions applied at the interface between the two subdomains.

A Robin–Robin algorithm ensures efficient convergence over the range of physical parameters of interest for borehole modeling (including small flow rates and small time steps). It changes linear combinations of pressure and heat flux at the borehole interface with well-chosen coefficients.

Considering an implicit Euler integration scheme, we define the current time step Δt as follows [1]:

$$\eta = \frac{\rho_r c_p^r}{\Delta t} \quad (23)$$

$$\eta^g = \frac{\rho c_u^g}{\Delta t} \quad (24)$$

Having defined the temperatures T_{rock}, T_{wall} and T for the current time step, we can determine T_{rock}, and T at the surrounding rock level r and the borehole at the previous time interval.

The Robin–Robin algorithm with Robin coefficients $\beta_{rock} \neq 0$ and $\beta_{ff} \neq 0$ updates the temperatures (T^{k-1}, $T_{wall}{}^{k-1}$, $T_{rock}{}^{k-1}$) with iteration $k - 1 \neq 0$ of the domain decomposition algorithm with the temperatures (T_k, Tr_{ock}, T_{wall}) at iteration $k \neq 0$ of the domain decomposition algorithm, verifying:

$$\eta - \lambda_{rock} \Delta) T_{rock}^k(r,z) = \eta T_{rock}(r,z) \quad (25)$$

With boundary conditions along the borehole:

$$\beta_{ff} T_{rock}^K(r_w, z) - \lambda_{rock} \partial_r T_{rock}^k(r_w, z) = B_{ff} T_{wall}^{K-1}(z) + h(T^{k-1}(z) - T_{wall}^{K-1}(z)) \quad (26)$$

$$\eta^g T^k(z) + \rho c_v^g u \frac{dT^k}{dz} + H(T^k(z) - T_{wall}^k(z)) = \eta^g \widetilde{T}(z) \quad (27)$$

From the last two equations it follows:

$$\beta_{rock} T_{wall}^k(z) - h(T^k(z) - T_{wall}^K(z) = \beta_{rock} T_{rock}^k(r_w, z) + \lambda_{rok} \partial_r T_{rock}^k(r_w, z) \quad (286)$$

A detailed analysis of convergence shows that a simple and efficient choice of Robin's coefficients is:

$$\beta_{\text{rock}} = \widehat{DtN}_{\text{rock}}(0) = \frac{K_1\left(r_w\sqrt{\eta/\lambda_{\text{rock}}}\right)}{K_0\left(r_w\sqrt{\eta/\lambda_{\text{rock}}}\right)}\sqrt{\eta\lambda_{\text{rock}}}, \tag{28}$$

And $\beta_{ff} = h$

Where $K_0 = 0$ is the modified Bessel function and $K_1 = -K'_0$.

This studied algorithm allows a robust and modular approach to take into account the heat exchange between the well and the rock mass.

4. Conclusion

This studied algorithm allows a robust and modular approach to take into account the heat exchange between the well and the rock mass.

Numerical models are mathematical simulations performed on a computer that allow the study of the behavior of complex physical systems, in this case, the movement of natural gas in an underground reservoir. They are based on solving differential equations that describe the relevant physical phenomena (such as fluid movement, heat transport, and the behavior of porous materials). In the context of underground reservoirs, numerical models are used to simulate and predict:

• Gas flow under different geological and drilling conditions.

• Reservoir behavior during gas injection or extraction.

• Long-term thermal behavior and gas pressure.

Numerical models thus help to optimize natural gas extraction processes and prevent technical and economic problems, providing a detailed understanding of the fluid dynamics inside the reservoirs.

Advantages are:

• The possibility of simulating complex and very diverse conditions, which cannot be studied directly

• The behavior of the deposit can also be modeled at different extraction and injection cycles, so that its management is much more accessible

• A result of the modeling processes is the reduction of deposit maintenance costs because they provide the critical parameters for the operation of the deposit.

However, these are also limited because:

- They are only approximations of reality and can be influenced by the input data, as well as the assumptions made.
- Requires precise and detailed data about the geological characteristics of the deposits, which can be difficult to obtain.

- The mathematical complexity can lead to the need for high-performance computers and to considerable simulation time, as well as very high investment costs.

Brine deposition in the drill string is a significant problem in the process of extracting gas from salt deposits. It can have negative effects on the efficiency of drilling operations, equipment safety and environmental impact. Identifying the causes of brine deposition and implementing technical and chemical solutions to prevent this phenomenon are essential for improving the performance of gas extraction from salt deposits.

By carefully monitoring drilling conditions and using appropriate technologies, risks can be minimized and more efficient and sustainable natural gas extraction can be ensured.

Brine deposition in the drill string can be caused by a number of factors. Among the most important are:

• Water evaporation: As brine is injected into the reservoir, some volatile components may evaporate, and dissolved salts may crystallize and deposit within the drill string.

• Temperature and pressure fluctuations: Changes in temperature and pressure, specific to drilling conditions, can lead to the formation of salt crystals in certain areas of the drill string. This can occur when the brine reaches a lower temperature or when the pressure drops below a certain threshold.

• Chemical composition of the brine: The chemical composition of the injected brine significantly influences the deposition process. Incompatible salts or salts present in high concentration can contribute to the formation of salt crystals in certain areas of the drill string.

• Fluid flow rate: Low fluid flow rate can favor the deposition of brine in certain areas of the drilling equipment, as salts can crystallize upon contact with the casing walls.

The deposition of brine in the drill string can have multiple negative effects on the gas extraction process from salt deposits:

• Drill string blockage: Salts deposited in the drill string can lead to blockages or obstructions, thus preventing efficient gas extraction. This can lead to costly interruptions in the extraction process.

• Equipment corrosion: Salts and salt crystals deposited on the walls of the drill string can accelerate the corrosion process of drilling equipment and tubing systems, which can affect the life of the equipment and may require frequent maintenance.

• Decreased extraction efficiency: Brine deposition can significantly reduce the efficiency of gas extraction, as the gas flow is restricted. This can lead to slower and more expensive extraction, affecting the profitability of the project.

• Environmental impact: In cases where salt deposits are exploited in an inappropriate manner, the deposition of brine in drill strings can lead to uncontrolled leakage of chemicals, affecting the environment.

To manage and prevent brine deposition in drilling columns, it is necessary to use several technical and chemical solutions.

By frequently monitoring the parameters of the well, a rapid identification of the salt deposition process in the brine can be made and thus it can be prevented quickly.

The use of chemical additives that can stop the crystallization of salt is a common solution, which can stop the crystallization of salt in the brine.

A better solution to avoid salt deposition is to improve drilling technologies that can provide better fluid circulation, so that a constant fluid flow can be maintained and that no longer stagnates, which provides for the deposition of salt in the brine.

The use of mathematical models combined with neural networks increases the degree of prediction of the behavior of the gas reservoir over time, increasing the degree of knowledge of the operating parameters of the reservoir.

Their use in calculating the salt deposition in the drill string or in the deposition of insoluble sediments at the base of the cavern helps us to determine as precisely as possible the limits of the parameters that control these deposits and thus we can avoid possible technical problems that may endanger the gas deposit.

Although the use of these models requires the entry of the most accurate data, very detailed analyses performed on the gases and rocks in the deposit, to which is added a fairly large amount for the calculation technique, the results obtained have enormous value because they help us to fully understand the behavior of the deposit without performing additional operations.

Although mathematical models are widely used in reservoir engineering, they still have advantages as well as disadvantages.

5. Data Availability

The data presented in this article are real and collected from the area of interest. The data can be used by anyone in accordance with applicable international regulations. Data is available in the article and can be provided upon request.

6. Conflicts of Interest

No data or information is presented that could endanger companies or commercial or public companies. There are no conflicts regarding the exposed data. The data taken from the soil samples analyzed and presented in the article are part of oil fields abandoned and handed over to the public domain.

The authors did not benefit from public, private or other resources.

REFERENCES

[1] Ali A. Data-driven based machine learning models for predicting the deliverability of underground natural gas storage in salt caverns. Energy 2021;229:120648. https://doi.org/ 10.1016/j.energy.2021.120648.
[2] Berest P., Louvet F. (2020) Aspects of the thermodynamic behavior of salt caverns used for gas storage, OGST 75, 57.
[3] Evans J., Shaw T. (2021) Storage of hydrogen in solution mined salt caverns for long duration energy storage, in: Virtual Technical Conference, SMRI Spring 2021, April 2021.
[4] Jeannin L., Mainguy M., Masson R., Vidal-Gilbert S. (2007) Accelerating the convergence of coupled geomechanicalreservoir simulations, Int. J. Anal. Numer. Methods Geomech. 31, 1167–1183.
[5] Karimi-Jafari M. (2007) Comportement transitoire des cavités salines profondes, Thèse de doctorat, Ecole Polytechnique, Palaiseau
[6] Liu Y, Li J, Wang Z, Wang S, Dong Y. The role of surface and subsurface integration in the development of a high-pressure and low-production gas field. Environ EarthSci 2015;73:5891–904. https:// doi.org/10.1007/s12665-015-4341-7.

MATEMATIC MODELING OF ADSORPTION ON ACTIVATED CARBON OF PETROLEUM GASES

Timur CHIS[1*], Al Jaseem AMEER[2*], Razvan GASPAR[2]

[1]Oil and Gas Engineering Faculty, Petroleum-Gas University
[2]Ph.D. School, Petroleum-Gas University

Abstract
This paper presents the technologies for degasification of well gases with direct application to the treatment of well gases in the Black Sea.
The C3+ fraction can be recovered from natural gas or can result from crude oil refining processes. The C3+ fraction recovered from well gases is practically free of unsaturated hydrocarbons (propylene and butylene) and results from one of the following extraction methods: turboexpander, absorption, compression and adsorption. The choice of process depends on the gas composition and the degree of recovery of ethane and C3+ fraction.
The C3+ fraction recovery facility at Midia is designed to process gases from the Central Platform located offshore the Black Sea. The LPG produced (mainly C3 and C4) will be stored in the tank farm. LPG can be used as household fuel, automotive fuel or feedstock for various petrochemical processes. The resulting lean gas will be compressed and shipped via the export pipeline.
In the study I conducted, I studied all types of installations used for the separation of rich gases, the technology for recovering lean gases through turboexpansion (cryogenics) as well as the calculation of a natural gas treatment plant.
I also introduced a chapter related to the risk assessment based on the event tree in the operation of these installations, which are particularly useful in the oil industry.

Key words: well gas, lean gas, degassing.

1. Introduction

Natural gas in reservoirs mainly contains methane (CH_4). Like crude oil, the origin of natural gas is biological, and oil and gas are formed by the same natural forces. Thus, most (but not all) oil reservoirs contain both oil and gas. We often speak of "oil and gas" together. As ancient biomass is converted to fossil hydrocarbons, different oil and gas generation windows correspond to different residence times at different depths.

Methane is formed when liquid oil is "over-mature" due to excessive thermal stress in deep formations. Methane can also be formed from the anaerobic decomposition of natural wetlands, rice fields, animal emissions, organic waste in landfills, and the combustion of biomass (forest fires, coal burning, etc.), as biogenic methane.

The radioactive isotope of carbon, 14C, is present in biogenic methane but absent in fossil methane from natural gas.

Natural gas that contains only traces of other compounds is dry gas. If natural gas contains significant amounts of ethane, propane, butanes, and higher hydrocarbons, it is called wet gas. The heavier components can be recovered individually or as condensate or natural gas liquids (NGL) in natural gas processing plants. Sour gas contains hydrogen sulfide, and sour gas contains carbon dioxide and/or hydrogen sulfide. Sour gas

* Corresponding author: timur.chis@gmail.com

processing plants produce elemental sulfur as a byproduct, which is used to manufacture sulfuric acid and fertilizers [1].

Natural gas comes from gas wells, oil wells, and condensate wells. Natural gas at the wellhead contains mainly methane (70–90%) with impurities.

Natural gas from oil wells is called associated gas. It can be free gas or dissolved in oil. Natural gas from a condensate well is produced along with volatile hydrocarbon condensate. In addition to methane, natural gas mixtures contain ethane, propane, butane, and pentanes, water vapor, hydrogen sulfide, mercaptans, carbonyl sulfide, carbon dioxide, ammonia, helium, nitrogen, and other components. Natural gas is the main commercial source of helium, which is present in natural gas as an inert gas along with nitrogen [2].

Helium is believed to be formed from the radioactive decay (α-decay) of uranium and thorium in granitoid rocks in the Earth's continental crust. High-purity helium is produced by combining the cryogenic process and pressure swing adsorption.

Natural gas liquids (NGLs) include ethane (35–55%), propane (20–30%), normal butane (10–15%), isobutane (4–8%), and C5+ natural gas (10–15%). They are used in enhanced oil recovery or as feedstocks for oil refineries or petrochemical plants, and as energy sources.

In the US, hydraulic fracturing (fracking) is increasing the production of natural gas as shale gas [3].

Natural gas produced at the wellhead, which in most cases contains contaminants and natural gas liquids, must be processed to meet quality specifications before it can be safely delivered to high-pressure, long-distance pipelines and/or gas tankers that transport the product to consumers. Natural gas that does not fall within certain specific gravity, pressure, BTU (heat) content ranges, dew point, or water content levels will cause operational problems, pipeline damage, or even pipeline rupture. Such gas can be particularly damaging to pumping station equipment [3].

Water content, defined by the water dew point, must be limited to prevent ice and hydrate formation in the pipeline. Hydrocarbons heavier than ethane, defined by the hydrocarbon dew point, must be limited to prevent the accumulation of condensable hydrocarbon liquids that could block the pipeline and pumps.

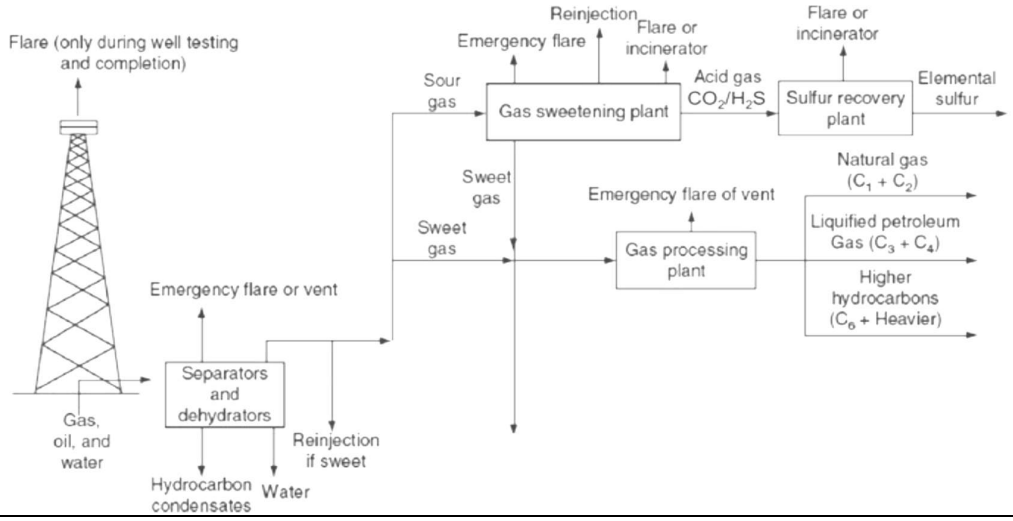

Fig. 1. Natural Gas from Well to Consumer [1]

Figure 1 shows the normal procedure for treating natural gas at the well site for subsequent transportation to consumers. The first step is gravity phase separation to separate water, hydrocarbon condensates, and solid particles from the gas in a settling tank. Pretreatment of natural gas typically involves mercury removal, gas sweetening, and drying. Mercury is removed using adsorption processes based on activated carbon or renewable molecular sieves. The natural gas is dried by absorption in renewable triethylene glycol (TEG) (glycol dehydration) or molecular sieve adsorbents. It may be necessary to remove H_2S and CO_2 (acid gases) from the natural gas [1].

Sweet gas containing low concentrations of sulfur compounds can be removed by adsorption along with water removal or sent directly to a gas processing plant. For sour gas containing high concentrations of sulfur compounds and carbon dioxide, gas sweetening using a solvent such as amines, sulfinol, or carbonate scrubbing is traditionally used. The sweetened gas can then be sent to the gas processing plant or reinjected into the field for enhanced recovery. The sulfur-rich amine solution after scrubbing is sent to a solvent recovery unit to separate the solvent from the sulfur, which is sent to a sulfur recovery plant.

$$K_2CO_3 + CO_2 + H_2O \rightarrow KHCO_3 \quad (1)$$

$$K_2CO_3 + H_2S \rightarrow KHS + KHCO_3 \quad (2)$$

If natural gas is to be cryogenically liquefied and stored in liquid form, the carbon dioxide must be removed by amine treatment to prevent the formation of dry ice that would interfere with the refrigeration system and clog the pipeline. The carbon dioxide can be sold as industrial dry ice and, in some locations, is reinjected into the formation. Reinjection has the added value of reducing CO_2 emissions to the atmosphere; CO_2 reinjection is also known as carbon sequestration [3].

2. Materials and Methods

In order to observe the efficiency of the adsorption on activated carbon of liquefied petroleum gases, we studied the operating parameters of the technological adsorption plant for petroleum gases at OMV PETROM, MIDIA WORKING POINT.

We studied:

a. The concentration of gases at the entrance to the system (degasification plant) by analyzing the gas chromatograms provided by the beneficiary,

b. The concentration of gases at the exit from the system (degasification plant) by analyzing the gas chromatograms provided by the beneficiary,

c. The pressure on each component.

Table 1.

Analysis of the inlet gases

Component	Retention time, s	Area, mm^2	% area	Concentration, m^3/m^3	Normal concentration, %
C6+	1,583	121606	1,2832	0,225	0,181
Etan	4,483	529228	6,0196	6,477	5,220
CO_2	5,033	73954	0,8412	0,925	0,746
Propan	5,400	337596	3,8399	3,023	2,437
Izobutan	6,683	49675	0,5650	0,368	0,296
n-butan	8,033	131698	1,4980	0,731	0,589
i-pentan	12,083	40374	0,4592	0,221	0,178
n-Pentan	14,300	43671	0,4967	0,267	0,215
Azot	19,050	60421	0,68732	0,728	0,587
Metan	19,983	7403509	84,2099	111,110	89,551

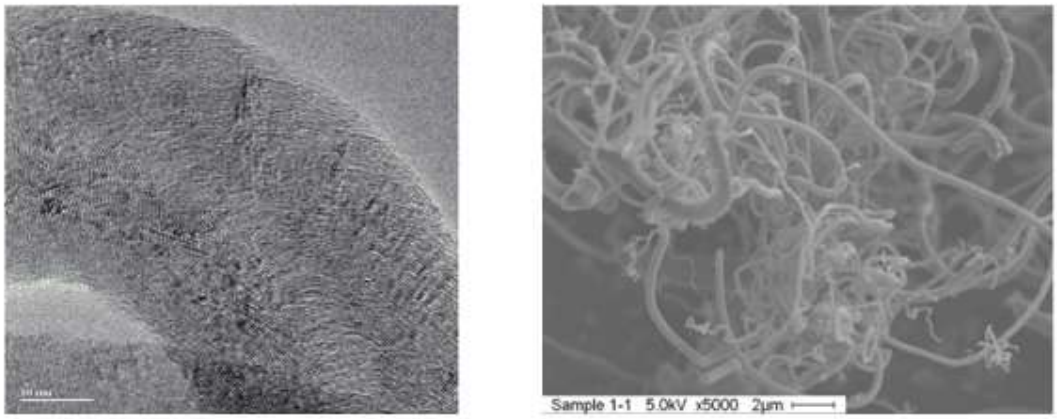

a b

Fig.2. Activated carbon before LPG passage (fig. a) and after LPG passage (fig. b)

To see how activated carbon acts on petroleum gases, the amount of product entering the column and the amount of product absorbed (by subtracting the amount of product received in the pipeline) were studied.

Table 2.

A hydrocarbon absortion to the partial pressure of 100 mBar and after 24 hours of operation

Component	Normal concentration before entering the installation, kg/24 h	Normal concentration after leaving the installation, kg/24 h	Retained quantity in kg hydrocarbon-100 kg coal
Metan	2856	2856	0
Etan	168	166	2,000
Propan	48	40	8,000
n-butan	36	20	16,000

Table 3.

A hydrocarbon absortion to the partial pressure of 200 mBar and after 24 hours of operation

Component	Normal concentration before entering the installation, kg/24 h	Normal concentration after leaving the installation, kg/24 h	Retained quantity in kg hydrocarbon-100 kg coal
Metan	2856	2856	0
Etan	168	164	4
Propan	48	37	11
n-butan	36	18	18

Table 4.

A hydrocarbon absortion to the partial pressure of 300 mBar and after 24 hours of operation

Component	Normal concentration before entering the installation, kg/24 h	Normal concentration after leaving the installation, kg/24 h	Retained quantity in kg hydrocarbon-100 kg coal
Metan	2856	2856	0
Etan	168	163	5
Propan	48	35	13
n-butan	36	17	19

Table 5.

A hydrocarbon absortion to the partial pressure of 400 mBar and after 24 hours of operation

Component	Normal concentration before entering the installation, kg/24 h	Normal concentration after leaving the installation, kg/24 h	Retained quantity in kg hydrocarbon-100 kg coal
Metan	2856	2856	0
Etan	168	162,5	5,5
Propan	48	34,5	13,5
n-butan	36	15,5	20,5

Table 6.

A hydrocarbon absortion to the partial pressure of 500 mBar and after 24 hours of operation

Component	Normal concentration before entering the installation, kg/24 h	Normal concentration after leaving the installation, kg/24 h	Retained quantity in kg hydrocarbon-100 kg coal
Metan	2856	2856	0
Etan	168	162	6
Propan	48	34,	14
n-butan	36	15	21

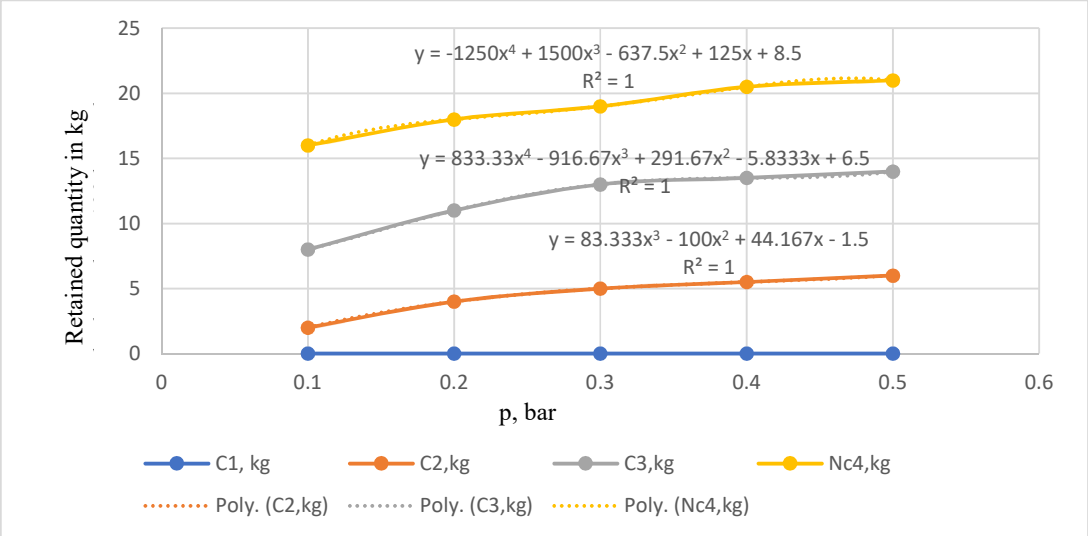

Fig.2. Evolution of hydrocarbon absortion to the partial pressure after 24 hours of operation

4. Conclusion

In this material is analyzof the gas chromatograms of the products resulting from adsorption on activated carbon, the purpose being to determine the amount of product adsorbed.

It is observed that the C4 fraction is absorbed best, for which the numerical model I made also gave the best results.

Activated carbon behaves very well at high pressures, the models matematics giving quite good results.

5. Data Availability

The data presented in this article are real and collected from the area of interest.

The data can be used by anyone in accordance with applicable international regulations. Data is available in the article and can be provided upon request.

6. Conflicts of Interest

No data or information is presented that could endanger companies or commercial or public companies. There are no conflicts regarding the exposed data. The data taken from the soil samples analyzed and presented in the article are part of oil fields abandoned and handed over to the public domain.

The authors did not benefit from public, private or other resources.

REFERENCES

[1] Jaseem A., Gaspar R., Chis T., Tegledi M. , Risk assessment of contaminating liquefied petroleum gas leaks , 5th International Conference on Scientific and Innovative Studies July 15-16, 2025, ISBN: 978-625-5900-81-4, pp. 315-323,

[2] Taylor, R. R., Liquefied Petroleum Gas, Kirk-Othmer Encyclopedia of Chemical Technology, Fifth Edition, John Wiley & Sons, Inc., 2007.

[3] American Institute of Chemical Engineers, Guidelines for Chemical Process Quantitative Risk Analysis, John Wiley & Sons, Inc., Second Edition, New York, 2000.

A NUMERICAL MODEL OF THE VOLATILE COMPOUNDS EMISSION TO OIL AND GASOLINE STORAGE

Iolanda POPA[1], Florina CASARIU[1], Vasile LAVRIC[1],Timur CHIS[2*] Sorin STEFLEA[3]

[1]Ph.D. School, National Science and Technology Politehnica University
[2]Oil and Gas Engineering Faculty, Petroleum-Gas University
[3]Ph.D. School, Petroleum-Gas University

Abstract

This paper presents the method of calculating the losses of petroleum products during storage and transportation for different products generally handled in an oil terminal. An important element in determining the losses is also the environmental conditions in the location area (wind, sun, seismicity, etc.).There are several methods for determining the emissions of tanks with fixed or removable lids, the easiest being their determination by calculating the vapor balance. The basic model used in this study is a calculation model developed according to API standards, from which a proprietary methodology was developed and presented for estimating losses during the transport of various products. The study took into account both environmental factors (wind, temperature, tank paint color) and basic properties of the products such as density. The mathematical models that best correlated the data proved to be polynomial equations of degree 2 to degree 5. The simulations performed are among the first performed in this field, the determination of parameters with major influence being of major interest both for finding solutions to reduce losses on the service flow but also being opportune to develop mathematical models that correlate several parameters to facilitate the evaluation of these fugitive emissions.

Key words: oil and product storage, volatile compounds emission, emission modelling.

.

1. Introduction

Emission sources and their contribution vary depending on the type of storage tank and occur as a result of evaporation of products during storage and as a result of changes in the liquid level.

Thus, in the case of tanks with a fixed lid, emissions are the result of evaporation losses during storage (also called breathing losses or static storage losses) and evaporation losses during filling and emptying operations (called working losses). Storage losses consist of the escape of vapors from a tank by the expansion and contraction of the vapor space as a result of temperature and pressure variations. This loss occurs without any change in the liquid level in the tank. The combined loss during filling and emptying is called working loss. As the liquid level rises, when the tank is filled, the pressure inside the tank exceeds the discharge pressure and the vapors are evacuated from the tank. Evaporative losses during emptying occur when the liquid level drops and the pressure also drops, so air enters the tank and the space allocated to the vapors expands and becomes saturated with air.

* Corresponding author: timur.chis@gmail.com

In the case of tanks with a fixed or movable cover, losses of petroleum products (emissions) vary depending on the capacity of the tank, the vapor pressure of the stored liquid and its rate of use. An important element in determining losses is also the environmental conditions in the location area (wind, sun, seismicity, etc.).

There are several methods for determining emissions from fixed or removable lid tanks, the easiest being to determine them by calculating the vapor balance.

2. Materials and Methods

The following presents the influence of various environmental factors and product quality on fugitive emissions. Among the environmental factors considered, we mention the tank temperature, wind speed, deterioration of the tank paint color.

The physicochemical parameters of the products considered were: density, REID vapor pressure [1].

The parameter variation was considered to be between 55-90 kPa, which covers the entire range of values for the product specification in summer and winter conditions.

If the operating losses remain constant with increasing vapor pressure, the storage losses increase with its increase [2,3].

The transportation of petroleum products from OIL TERMINAL S.A. to the storage points of the beneficiaries, as well as from the refineries of some beneficiaries to OIL TERMINAL S.A. (for export) is carried out through CF boilers.

The proposed method for estimating the consumption of liquid petroleum products, caused by the evaporation and handling processes associated with the transport of liquid hydrocarbons by tank cars, comes from the specialized literature (API methodology).

The tank is loaded through the dome, using the telescopic pipe of the railway ramp filling device, and the unloading is carried out by connecting flexible hoses to the terminal connections of the emptying valves.

The storage of petroleum liquids is done at atmospheric pressure, the tanks being equipped with safety valves that allow the achievement of reduced depressions or overpressures.

The petroleum product loses part of the volatile fractions both during the handling operations and during the actual transport.

Thus, during loading, a large flow of liquid enters that travels (in the form of a free jet), the distance between the mouth of the telescopic pipe and the free surface.

This distance is, especially in the first part of the process, relatively large, which causes the turbulent jet to have intense contact with the atmospheric air, and the free surface of the liquid to be agitated.

This causes the vaporization of light fractions from the surface and from the hydrocarbon jet, the space above the liquid becoming saturated with vapors that are practically completely evacuated through the dome during filling.

During the emptying of the tank, the place of the evacuated liquid is taken by atmospheric air that enters through the dome and becomes saturated with hydrocarbons. These volatile fractions are lost because the tank remains in contact with the atmosphere throughout the entire duration of the tank emptying and filling.

The phenomenon of increased evaporation is accentuated by [4, 5]:
a. The increase in temperature above the vaporization limit,
b. The association of the tank filling and emptying with the phenomenon of high respiration of the tanks,
c. The association of the product transport with the phenomenon of low respiration (due to the variation in temperature, the turbulence created by the relative movement of the petroleum products with respect to the tank vessel, the air currents between the tank lid and the surface of the liquid (if the dome is not airtight) and the wind speed that can cool or heat the tank).

3. Results and discussions

a. Influence of gasoline vapor pressure on the amount of fugitive emissions

Initial calculation conditions
- 10,000 cubic meter tank
- The chosen sealing system is for a welded tank with a primary sealing system with an elastic tire with filling and a vapor space between the liquid and the seal,
- Density of 730 kg/m^3,
- Operated quantity of 2,000,000 tons,
- Average annual temperature of 13ºC
- Atmospheric pressure 800 mm Hg.

Table 1.

Losses of petroleum products due to changes in vapor pressure

Reid vapor pressure, mm Hg	Storage losses, kg/an	Operating losses, kg/an	Total losses, kg/an	Loss coefficient, %
55	1051	849	1900	0,00095
60	1187	849	2036	0,001018
70	1437	849	2286	0,001143
80	1777	849	2626	0,001313
90	2098	849	2947	0,0014735

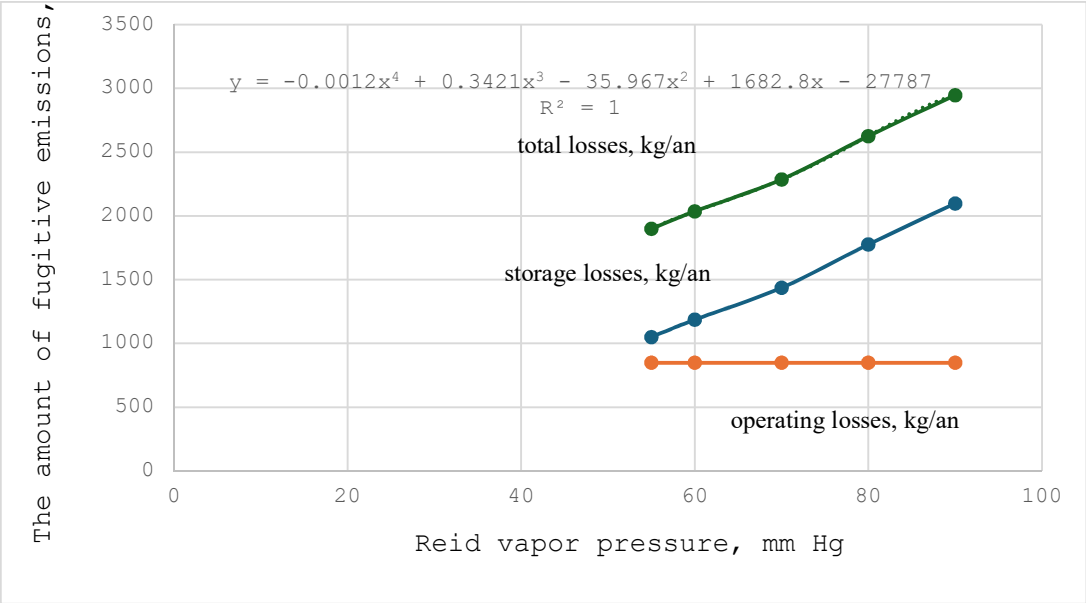

Fig.1. Effect of varying Reid vapor pressure on gasoline fugitive emissions

b. Effect of varying Reid vapor pressure on gasoline fugitive emissions

Initial calculation conditions

- 10,000 cubic meter tank,
- The chosen sealing system is for a welded tank with a primary sealing system with an elastic tire with filling and a vapor space between the liquid and the seal,
- The operated quantity is 2,000,000 tons,
- Average annual temperature is 13ºC,
- Atmospheric pressure is 800 mm Hg.

Table 2.

Losses of petroleum products due to changes in vapor pressure and density of gasoline

Reid vapor pressure, mm Hg	Density, kg/m^3	Storage losses, kg/an	Operating losses, kg/an	Total losses, kg/an	Loss coefficient, %
55	730	1051	847	1898	0,000949
60	740	1187	848	2035	0,0010175
70	750	1437	849	2286	0,001143
80	760	1777	850	2627	0,0013135
90	770	2098	851	2949	0,0014745
95	775	2264	851	3115	0,0015575

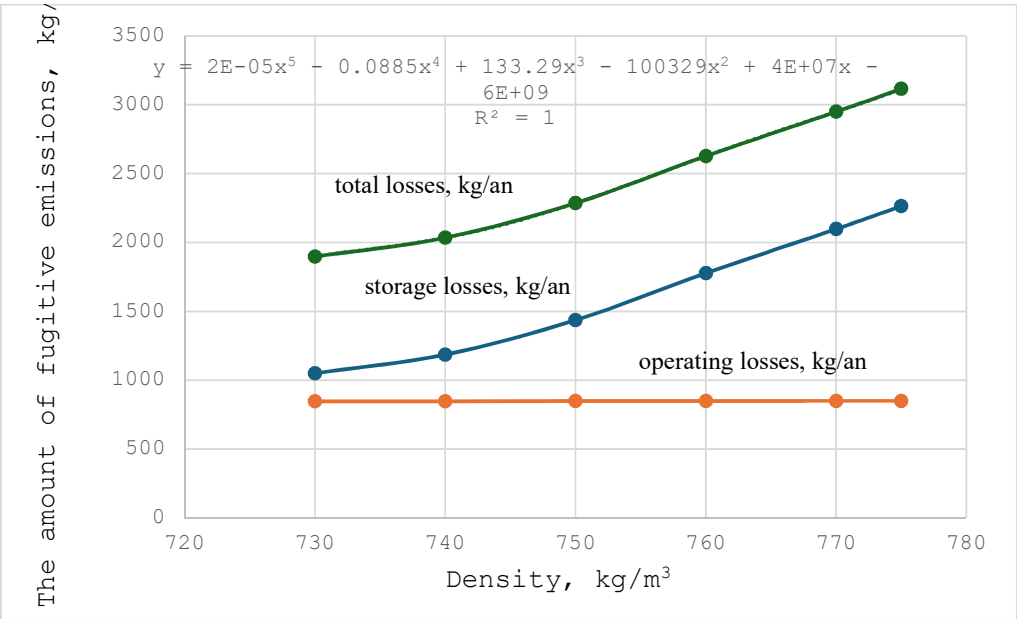

Fig. 2. Effect of varying density and Reid vapor pressure on gasoline fugitive emissions

c. Influence of tank temperature on the amount of fugitive emissions

Initial calculation conditions

- 10,000 m^3 tank,
- The chosen sealing system is for a welded tank with a primary sealing system, with an elastic tire with filling and a vapor space between the liquid and the seal,
- The operated quantity is 2,000,000 tons,
- The average annual density is 730 kg/m^3,
- The vapor pressure is Reid 70 mm Hg.

Table 3.

Losses of petroleum products due to changes in product temperature in the tank

Reservoir temperature, ºC	Storage losses, kg/an	Operating losses, kg/an	Total losses, kg/an	Loss coefficient, %
13	1573	849	2422	0,001211
20	2033	849	2882	0,001441
30	3151	849	4000	0,002
40	4776	849	5625	0,0028125
50	7112	849	7961	0,0039805

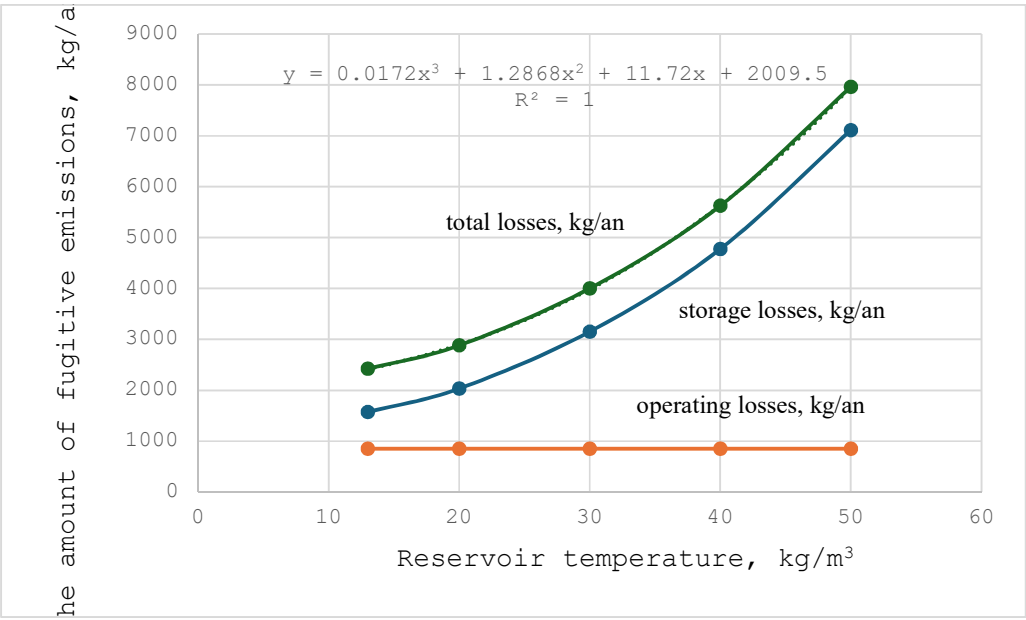

Fig. 3. Effect of tank temperature variation on gasoline fugitive emissions

d. Influence of wind in the area on the amount of fugitive emissions

Initial calculation conditions:
- 10,000 m^3 tank,
- The chosen sealing system is for a welded tank with a primary sealing system with an elastic tire with filling and a vapor space between the liquid and the seal,
- The operated quantity is 2,000,000 tons,
- The average annual density is 730 kg/m^3,
- The vapor pressure is Reid 70 mm Hg,
- Reservoir temperature 20 ºC.

Table 4.

Losses of petroleum products due to changes in wind speed

Wind speed, m/s,	Storage losses, kg/an	Operating losses, kg/an	Total losses, kg/an	Loss coefficient, %
2,4	2033	849	2882	0,001441
3	3318	849	4167	0,002084
3,5	4655	849	5504	0,002752
4	6242	849	7091	0,003546
4,5	8087	849	8936	0,004468
5	10195	849	11044	0,005522

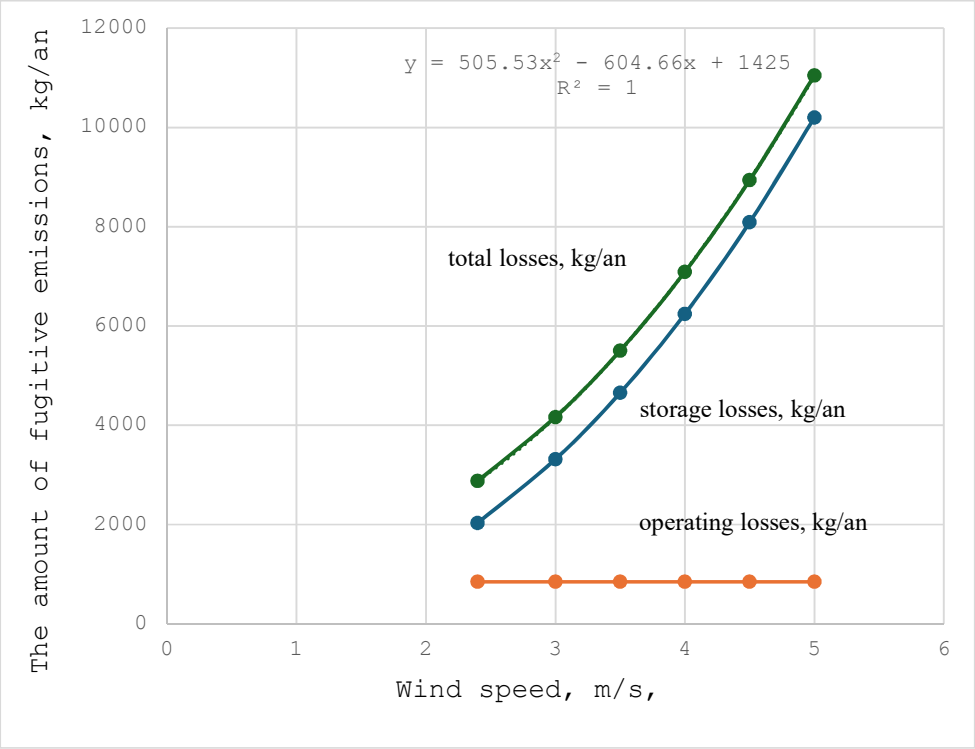

Fig. 4. Effect of wind speed variation on fugitive gasoline emissions

e. Influence of tank color on the amount of fugitive emissions

Initial calculation conditions:
- 10,000 cubic meter tank,
- The chosen sealing system is for a welded tank with a primary sealing system with an elastic tire with filling and a vapor space between the liquid and the seal,
- The operated quantity is 2,000,000 tons,
- The average annual density is 730 kg/m^3,
- The vapor pressure is Reid 70 mm Hg,
- The tank temperature is 20 ºC,
- The wind speed is 2.5 m/s.

Losses of petroleum products due to tank color deterioration *Table 5.*

	Color coefficient	Storage losses, kg/an	Operating losses, kg/an	Total losses, kg/an	Loss coefficient, %
Lightly rusted	0,0015	1363	849	2212	0,001106
Heavyly rusted	0,0075	1363	4246	5609	0,0028045
Spray-cut	0,15	1363	84932	86295	0,0431475

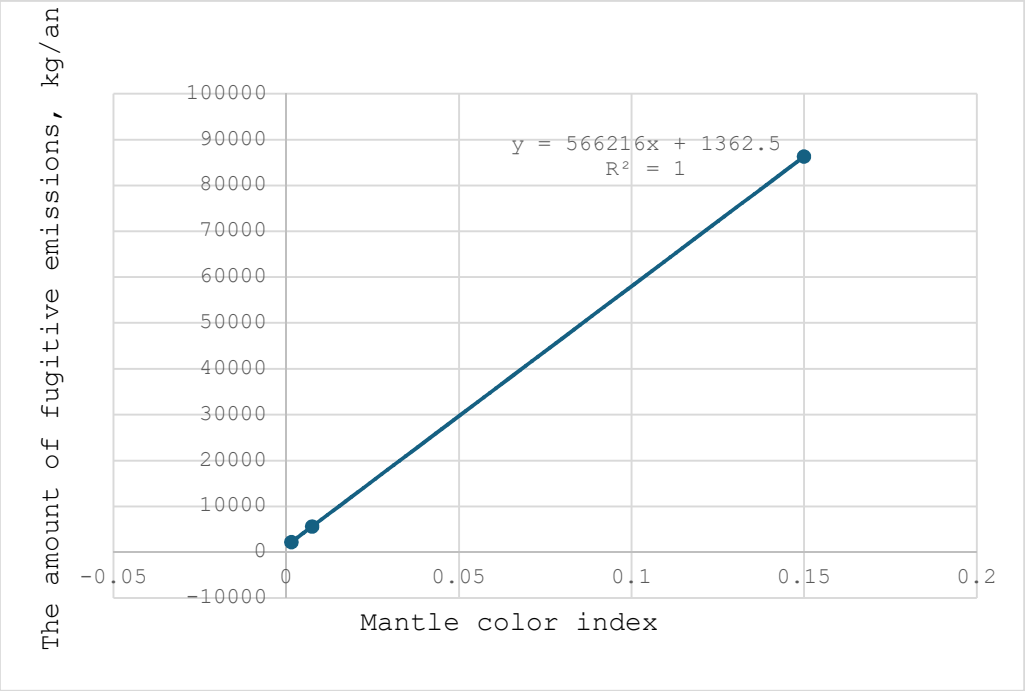

Fig. 5. Effect of tank paint deterioration on gasoline fugitive emissions

In gasoline, the large influence of color deterioration on finished product losses is observed.

Table 6.

Percentage of gasoline losses (estimated) depending on the influencing parameter and the equations for determining losses depending on the analyzed parameter

Influence parameter	Percentage of crude oil losses (estimated) Kg of crude oil lost/ton of product handled (maximum)	Calculation relationship	Correlation index of experimental data with calculated data R^2
Vapor pressure	0,0014	$y = -0{,}0012x^4 + 0{,}3421x^3 - 35{,}967x^2 + 1682{,}8x - 27787$	1
Density	0,0015	$y = -0{,}0012x^4 + 0{,}3421x^3 - 35{,}967x^2 + 1682{,}8x - 27787$	1
Wind	0,0055	$y = -0{,}0012x^4 + 0{,}3421x^3 - 35{,}967x^2 + 1682{,}8x - 27787$	1
Temperature	0,0039	$y = 0{,}0172x^3 + 1{,}2868x^2 + 11{,}72x + 2009{,}5$	1
Mantle color condition	0,043	$y = 0{,}0172x^3 + 1{,}2868x^2 + 11{,}72x + 2009{,}5$	

Table 7.

Percentage of gasoline losses (estimated) depending on influencing parameter - 10,000 cubic meter tank

Influence parameter	Percentage of gasoline losses (estimated) Kg of gasoline lost/ton of product handled (maximum) 2,000,000 tons	Percentage of gasoline losses (estimated) Kg of gasoline lost/ton of product handled (maximum) 1,000,000 tons	Percentage of gasoline losses (estimated) Kg of gasoline lost/ton of product handled (maximum) 500,000 tons	Percentage of gasoline losses (estimated) Kg of gasoline lost/ton of product handled (maximum) 100,000 tons
Vapor pressure	0,0014	0,0029	0,0058	0,029
Density	0,0015	0,0031	0,0062	0,031
Wind	0,0055	0,011	0,0022	0,11
Temperature	0,0039	0,0079	0,0152	0,079
Mantle color condition	0,043	0,086	0,172	0,86

Table 8.

Percentage of gasoline losses (estimated) depending on influencing parameter - 50,000 cubic meter tank

Influence parameter	Percentage of gasoline losses (estimated) Kg of gasoline lost/ton of product handled (maximum) 2,000,000 tons	Percentage of gasoline losses (estimated) Kg of gasoline lost/ton of product handled (maximum) 1,000,000 tons	Percentage of gasoline losses (estimated) Kg of gasoline lost/ton of product handled (maximum) 500,000 tons	Percentage of gasoline losses (estimated) Kg of gasoline lost/ton of product handled (maximum) 100,000 tons
Vapor pressure	0,024	0,048	0,097	0,48
Density	0,025	0,049	0,099	0,50
Wind	0,032	0,064	0,128	0,64
Temperature	0,022	0,045	0,096	0,45
Mantle color condition	0,024	0,049	0,098	0,49

4. Conclusion

The simulations performed are among the first performed in this field, the determination of parameters with major influence being of major interest both for finding solutions to reduce losses in the service provision flow but also being opportune to develop mathematical models that correlate several parameters to facilitate the evaluation of these fugitive emissions.

5. Data Availability

The data presented in this article are real and collected from the area of interest.

The data can be used by anyone in accordance with applicable international regulations. Data is available in the article and can be provided upon request.

6. Conflicts of Interest

No data or information is presented that could endanger companies or commercial or public companies. There are no conflicts regarding the exposed data. The data taken from the soil samples analyzed and presented in the article are part of oil fields abandoned and handed over to the public domain.

The authors did not benefit from public, private or other resources.

REFERENCES

[1] *VOC Emission from Volatile Organic Liquid, Storage Tanks*, Background Information for Promulgated Standars, US Environmental Protection Agency, 1987,

[2] T.M .Butler, M.G. Lawrence, D.Taraborrelli and J. Lelieveld, "*Impacts of biogenic emissions of VOC and NOx on troposphere ozone during summertime in eastern China, State Key Laboratory of Pollution Control and Resources Reuse*", Institute of Atmospheric Physics, Chinese Academy of Sciences, Atmospheric Department, *Nanjing University, China,* 2008*,*

[3] A.I.Moreira, "*Ambient Concentration and Photochemical Reactivity of Speciated VOC's in São Paulo Metropolitan Area*", PETROBRAS R&D Center -CENPES, Atmospheric Monitoring; *Cidade University,* 2006*,*

[4] Merv F. Fingas "*Modeling Oil and Petroleum Evaporation*", Journal of Petroleum Science Research (JPSR) Volume 2 Issue 3, July 2013,

[5] G. A. R. Rassoul, Tahseen Hameed Khlaif, "*Reducing the evaporation of stored Iraqi crude oil*", Iraqi Journal of Chemical and Petroleum Engineering Vol.10 No.3, September 2009.

A STATISTICAL METHODS FOR EVALUATING THE QUALITY OF FINISHED OIL PRODUCTS

Iolanda POPA[1], Florina CASARIU[1], Vasile LAVRIC[1],Timur CHIS[2*], Sorin STEFLEA[3]

[1]Ph.D. School, National Science and Technology Politehnica University
[2]Oil and Gas Engineering Faculty, Petroleum-Gas University
[3]Ph.D. School, Petroleum-Gas University

Abstract

Quality assurance by static methods is the stage that uses "statistical quality control sheets". In more and more companies, these methods are beginning to be applied, with an emphasis on the technological flow. The application of statistical sampling control methods has allowed the reduction of production costs. Statistical quality control is a sampling control method, in which the extracted sample (n) is controlled in its entirety, the results obtained allowing conclusions on the entire manufacturing process or on the finished products (N).In this regard, various statistical tools are used such as: data collection sheets, histograms, Pareto diagram, correction diagram, cause-effect diagram, dispersion diagram, control sheets. Advantages of applying statistical control methods: use of a small number of personnel, short decision-making time, operative establishment of adjustment and correction measures, ensuring the achievement and maintenance of process stability, reducing damage suffered by products, ensuring the delivery of product batches with specimens presenting defects within the limits jointly accepted by the supplier and beneficiary.

Key words: product analysis, statistic modelling, quality.

1. Introduction

This study is based on the quality control of the main white petroleum products. The quality control was carried out in a RENAR accredited laboratory.
Thus, the following quality parameters were analyzed:
- for gasoline - density, sulfur
- for oil - density, current gums
- for diesel - density, sulfur, lubrication point.

These parameters were analyzed because:
- density - provides information on the composition. Knowing the density provides information on fuel consumption and their calorific value. Calorific value - It is given by the amount of heat that is released upon complete combustion of a kg of fuel or cubic meters of gaseous fuel and is expressed in kcal or kj. The value of the calorific value depends on the chemical composition of the fuel and in particular on its H and C molecules.
- sulfur - quality control regarding the minimum sulfur content, in the case of fuels, is an essential requirement according to the emission regulation and indicates the tendency of combustion products to corrode.

* Corresponding author: timur.chis@gmail.com

- actual rubbers - the rubber content gives indications on the danger of solid deposits formation due to fuel degradation, with implications on the proper functioning of the engine.
- lubrication point - the fuel must provide the necessary lubrication capacity for an efficient engine lubrication system [1].

The refinement and classification of petroleum products form the foundation of global energy supply systems. In Romania, as in most industrialized nations, the classification of petroleum products follows **STAS ISO 8681:1992**, which standardizes definitions and product classes. Light petroleum products—commonly referred to as "white products"—include gasoline, Jet A1 fuel, and diesel. These products play a crucial role in transportation, industrial operations, and energy generation, making their quality evaluation a matter of national and international importance.

In an increasingly competitive energy market, **quality assurance** represents a key determinant of economic success. According to **ISO 8402:1995**, quality management encompasses planning, control, assurance, and continuous improvement activities designed to ensure that products meet defined standards and customer expectations. As J.M. Juran (1986) emphasized in his *Quality Control Handbook*, achieving excellence in quality management depends on three fundamental processes: quality planning, quality control, and quality improvement. Collectively known as the *Juran Trilogy*, these processes provide a theoretical foundation for the statistical approach adopted in this study.

Within the petroleum industry, variability in feedstock composition, refining conditions, and operational parameters introduces uncertainty into product quality. To minimize these variations, **statistical quality control (SQC)** techniques - such as histograms, control charts, correlation analysis, and Pareto diagrams - are applied. These methods enable manufacturers to monitor process stability, detect deviations in real time, and maintain compliance with environmental and performance standards [2,3].

Furthermore, the growing emphasis on sustainability has shifted the focus toward integrating **biofuels** and renewable additives into traditional petroleum products. This transition necessitates rigorous quality evaluation methods that combine technological, chemical, and statistical analyses. Hence, the present paper aims to synthesize both classical and modern approaches to quality evaluation in refined petroleum products using statistical methodologies applicable to industrial and research contexts.

2. Experimental and/or Modelling

Quality assurance through statistical methods is the stage that uses "statistical quality control sheets". In more and more companies, these methods are beginning to be applied, focusing on the technological flow. The application of statistical control methods through sampling has allowed the reduction of production costs.

Investing in quality is one of the best investments that a company can make today; it is a privileged means of lowering the return price, increasing the added value, retaining customers and winning new market segments - the goal is to make the company increasingly competitive. For the analysis and evaluation of quality, in parallel with the

existence of classical methods, new methods have emerged (affinity diagrams, tree diagrams, relationship diagrams) that allow the identification of the causes of defects, the prioritization of actions for improvement.

Quality control represents a critical function within petroleum refining, as each fuel type must conform to a complex set of international and regional standards. The **European Committee for Standardization (CEN)**, along with **ASTM International** and the **International Organization for Standardization (ISO)**, establishes technical benchmarks for fuel performance, composition, and environmental compliance.

For **gasoline**, compliance with **EN 228** and **ASTM D4814** ensures proper volatility, octane number, and emission characteristics. For **Jet A1 fuel**, **DEF STAN 91-91** and **ASTM D1655** specify stringent requirements for flash point, freezing point, and aromatic content. **Diesel fuel** is governed by **EN 590**, which defines cetane number, sulfur content (≤10 mg/kg), density, and lubricity parameters [2,3].

2.1. Principal Quality Parameters

The principal parameters used to evaluate petroleum product quality include:

- **Density (kg/m³ at 15°C):** Provides insights into composition and energy content. Lower density generally indicates higher volatility and lower energy per unit volume.
- **Sulfur content (mg/kg):** A major determinant of environmental performance, as sulfur oxides contribute to acid rain and engine corrosion.
- **Gum content (mg/100 ml):** Indicates fuel degradation tendency; high values suggest potential deposit formation in engine systems.
- **Lubricity (µm wear scar diameter):** Represents the ability of fuel to provide adequate lubrication to fuel injection components [2,3] .

3. Results and discussions

Quality analysis aims to:
- knowledge of the methods and means of achieving quality and the option for an optimal solution in a given case.
- comparison of the quality level of a product at different manufacturing intervals or comparison with the similar product of other companies.

In this study, quality parameters were analyzed in an **accredited RENAR laboratory**, ensuring methodological reliability and traceability. The following experimental design was adopted:

- **Gasoline samples (n=30):** Evaluated for density and sulfur content.
- **Jet A1 samples (n=30):** Evaluated for density and gum content.
- **Diesel samples (n=30):** Evaluated for density, sulfur content, and lubricity.

All measurements were performed according to standard procedures (ASTM D4052, ISO 20846, and D130), and data were tabulated for subsequent statistical processing.

The systematic evaluation of these parameters underpins the statistical methodology applied in the next section, which establishes the framework for data interpretation, process control, and decision-making in petroleum quality management.

Statistical Quality Control (SQC) represents a cornerstone of modern industrial management systems, providing the means to monitor, analyze, and enhance production consistency. Within the petroleum refining industry, variability is inherent in both raw material composition and process parameters. Consequently, the adoption of statistical methodologies enables the identification of deviations from target specifications before they translate into nonconformities.

The methodological approach employed in this study integrates descriptive and inferential statistical tools designed to interpret laboratory test data for petroleum product samples. The core objective was to evaluate whether the observed quality parameters—density, sulfur content, gum content, and lubricity—follow a normal distribution and remain within acceptable control limits defined by international standards [4,5].

Each type of refined product (gasoline, Jet A1, and diesel) was represented by **30 random samples**, collected from different production batches. Sampling followed the principles outlined in **ISO 2859-1:1999**, ensuring statistical representativeness and avoiding bias.

Key descriptive statistics (mean, median, mode, standard deviation, variance, coefficient of variation) were computed for each parameter. The **normality of data** was verified using the Shapiro–Wilk test, while control limits were established as follows:

$$UCL = \bar{X} + 3\sigma; LCL = \bar{X} - 3\sigma$$

where:

- UCL= Upper Control Limit
- LCL= Lower Control Limit
- $\bar{X}$= Sample mean
- σ= Standard deviation

Values falling outside these limits were considered indicators of special-cause variation, requiring process investigation.

The following **seven classical quality control tools** were employed for data interpretation:

1. **Data collection sheets:** used to systematically record laboratory observations.
2. **Histograms:** graphical representation of frequency distributions for each measured variable.
3. **Pareto diagrams:** applied to prioritize factors contributing most significantly to process deviations.
4. **Correlation diagrams:** assessing relationships between variables (e.g., density vs. sulfur content).
5. **Cause-and-effect (Ishikawa) diagrams:** mapping potential sources of quality variation (human, machine, method, material, environment, finance).
6. **Scatter plots:** determining degree and direction of relationships among parameters.
7. **Control charts (Shewhart):** used to track process stability over time.

This combination of tools allowed for an integrated understanding of both random and assignable causes of variation in petroleum product quality [6,7].

3.1. Statistical Model

To evaluate the effectiveness of SQC, a one-way **Analysis of Variance (ANOVA)** was applied to determine whether significant differences existed among sample groups of gasoline, Jet A1, and diesel. The null hypothesis (H_0) assumed no difference in mean quality parameters among products, while the alternative hypothesis (H_1) indicated at least one mean differed significantly.
A significance level of $\boldsymbol{\alpha = 0.05}$ was used. Where $p < 0.05$, results were interpreted as statistically significant, warranting process adjustment.

3.2. Gasoline Evaluation

The sulfur content in Euro 5 gasoline samples ranged between **1.1 and 10.4 mg/kg**, with a mean value of **4.9 mg/kg**, well below the 10 mg/kg regulatory threshold. The density varied between **725 and 786 kg/m³**, with an average of **749.2 kg/m³** and a standard deviation of **±11.8 kg/m³**. The histogram demonstrated a near-normal distribution, confirming process stability.
Pareto analysis indicated that **density variability** contributed more than 60% of total variation in gasoline quality, suggesting that blending control and temperature stabilization are critical for maintaining consistency.

Table 1.

The density of 30 determination for gasoline

Density (kg/m^3) xi	Standard deviation ni	Relative deviation, pi	Relative deviation cumulate, F
725	1	0.033	0.033
738	1	0.033	0.067
740	1	0.033	0.100
743	1	0.033	0.133
744	1	0.033	0.167
745	1	0.033	0.200
748	3	0.100	0.300
749	4	0.133	0.433
750	5	0.167	0.600
755	4	0.133	0.733
758	3	0.100	0.833
765	1	0.033	0.867
766	1	0.033	0.900
768	2	0.067	0.967
786	1	0.033	1.000
	30		

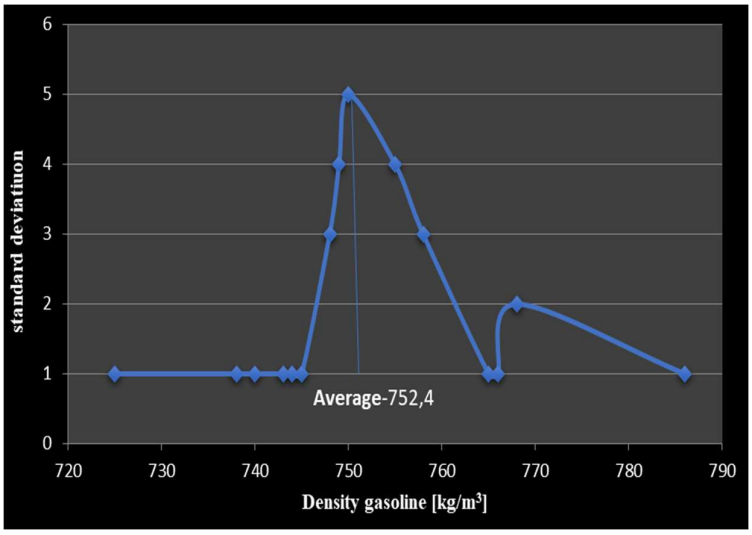

Fig.1. Histogram: density function absolute frequency of the gasoline

3.3. Jet A1 Fuel Evaluation

Jet A1 samples exhibited gum content values between 1.0 and 10.4 mg/100 ml, with a mean of 4.3 mg/100 ml. Density values ranged from 767 to 821 kg/m³, averaging 795.5 kg/m³ with a standard deviation of ±13.2 kg/m³. No significant outliers were detected beyond the 3σ control limits, indicating excellent process control. Statistical correlation between density and gum content (r = 0.34) suggested a weak positive relationship, potentially linked to oxidation tendencies during storage.

Table 2.

Jet A1 Fuel – Existent gum content values for 30 determinations

Existent Gum(mg/100 ml) xi	Standard deviation, ni	Relative deviation , pi	Relative deviation cumulate, F
1	1	0.033	0.033
1.5	1	0.033	0.067
1.9	1	0.033	0.100
2.1	1	0.033	0.133
2.4	1	0.033	0.167
2.6	1	0.033	0.200
2.8	1	0.033	0.233
3.1	1	0.033	0.267
3.5	2	0.067	0.333
3.8	4	0.133	0.467
4.4	5	0.167	0.633
5	4	0.133	0.767
5.5	2	0.067	0.833
5.8	1	0.033	0.867
6.8	1	0.033	0.900
7.3	1	0.033	0.933
8.4	1	0.033	0.967
10.4	1	0.033	1.000
	30	1.000	

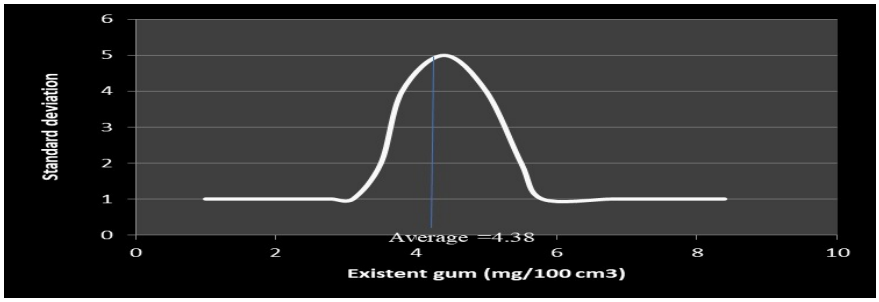

Fig.2. Histogram: Existent gum content function absolute frequency of the Jet A1

3.4. Diesel Fuel Evaluation

Diesel samples displayed densities between **735 and 856 kg/m³** (mean = **823.2 kg/m³**, SD = **±18.5 kg/m³**), while sulfur content varied from **6.8 to 10.4 mg/kg** (mean = **8.9 mg/kg**). The **lubricity point** ranged between **280 and 461 µm**, averaging **355 µm**.

Analysis indicated that while sulfur levels were well within standards, lubricity variation was the primary factor influencing product performance. The application of **control charts (X-bar and R)** showed that all measured parameters were within the control limits, confirming a **stable production process**.

Table 3.

The lubricity for 30 determination of diesel

Lubricity (µm) xi	ni	**Relative deviation**, pi	**Relative deviation cumulate** , F
280	1	0.033	0.033
300	1	0.033	0.067
310	1	0.033	0.100
320	3	0.100	0.200
335	5	0.167	0.367
360	6	0.200	0.567
375	5	0.167	0.733
390	3	0.100	0.833
421	1	0.033	0.867
436	1	0.033	0.900
456	1	0.033	0.933
457	1	0.033	0.967
461	1	0.033	1.000
	30	1.000	

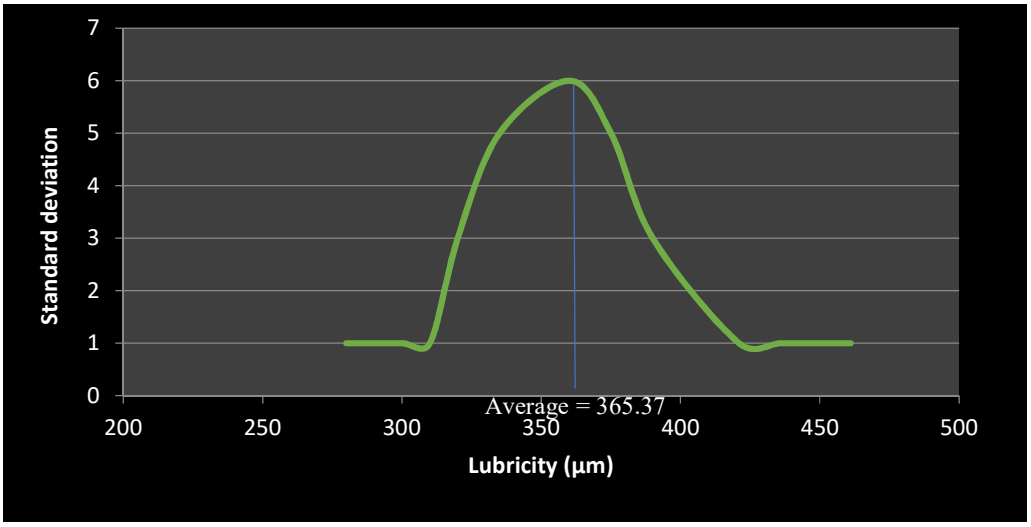

Fig.3. Histogram: Lubricity determination function absolute frequency of the diesel

The statistical evaluation demonstrated that all three product types comply with international specifications and that the refining process remains under statistical control. The data-driven approach provided quantitative validation for quality assurance activities and emphasized the utility of SQC in modern petroleum manufacturing.
While the current study demonstrates strong evidence of process stability and compliance, several limitations merit consideration:

- Laboratory data were limited to 30 samples per product type, which, while statistically valid, may not capture all process variability.
- External environmental conditions (e.g., humidity, ambient temperature) were not incorporated into the statistical models.
- The research did not address non-linear multivariate relationships that may exist between parameters.

Future research should integrate **machine learning and predictive modeling techniques**—such as regression trees, neural networks, or Bayesian inference—to enhance the predictive capability of quality evaluation systems. Furthermore, extending the dataset to include **real-time process monitoring** would allow dynamic control of refinery operations.

4. Conclusion

In parallel with the rapid technological and socio-cultural changes, the methods of ensuring the quality of products and services have also evolved. Four stages can be considered in the evolution of the methods of quality assurance:
- Quality assurance through control
- Quality assurance through statistical methods

- Quality assurance through staff motivation
- Integrative concepts of quality assurance.

5. Data Availability

The data presented in this article are real and collected from the area of interest.

The data can be used by anyone in accordance with applicable international regulations. Data is available in the article and can be provided upon request.

6. Conflicts of Interest

No data or information is presented that could endanger companies or commercial or public companies. There are no conflicts regarding the exposed data. The data taken from the soil samples analyzed and presented in the article are part of oil fields abandoned and handed over to the public domain.

The authors did not benefit from public, private or other resources.

REFERENCES

[1] A.Raznat, *Lubricity Improvement of the Ultra-low Sulfur Diesel Fuel with the Biodiesel*, Energy Procedia 75, p.111-117, 2015,

[2] ASTM International. (2020). *Standard test methods for petroleum products*. ASTM D4052, D5191, D381.

[3] European Committee for Standardization. (2019). *EN 590: Automotive fuels – Diesel – Requirements and test methods*.

[3] European Committee for Standardization. (2020). *EN 228: Automotive fuels – Unleaded petrol – Requirements and test methods*.

[4] International Organization for Standardization. (1995). *ISO 8402: Quality management and quality assurance – Vocabulary*.

[5] International Organization for Standardization. (1992). *ISO 8681: Petroleum products – Classification (STAS)*.

[6] Juran, J. M. (1986). *Quality control handbook* (4th ed.). McGraw-Hill.

RENAR. (2024). *Accredited laboratory testing protocols for petroleum quality evaluation*.

[7] Directive 2009/30/EC of the European Parliament and of the Council (2009). *Fuel quality directive – Specifications for petrol, diesel and gas-oil*.

ON THE SEPARATION OF VEGETABLE OILS INTO COMPONENT CLASSES

Nicoleta-Oana DEMOSTENE[1,*], Petrica IANCU[1], Roxana TARPAN[2], Tănase DOBRE[1]

[1]National University of Science and Technology POLITEHNICA Bucharest, 1-7 Gheorghe Polizu Str., 011061 Bucharest, ROMANIA

[2]Universitatea Ovidius Constanta, 124 Mamaia Boulevard, 900527 Constanța, ROMANIA

Abstract

This study investigates the separation of vegetable oils into distinct classes of components using both conventional and modern techniques. Starting from crude vegetable oil, numerous value-added compounds can be recovered, many of which are associated with health-promoting properties such as antioxidant and anti-inflammatory effects. The paper presents traditional refining and fractionation methods, alongside emerging technologies such as membrane separation and supercritical fluid extraction (SC-CO_2). Each technique is analyzed in terms of its efficiency, environmental impact, and economic feasibility. Comparative evaluation highlights that modern methods offer higher selectivity and lower energy consumption, while traditional processes remain advantageous for large-scale applications due to their lower operational costs. Overall, this work provides an integrated perspective on the technological potential of separating vegetable oils into functional fractions for use in the food, pharmaceutical, and cosmetic industries.

Key words: vegetable oils, oil fractionation, chemical refining, physical refining, modern separation techniques, bioactive compounds

1. Introduction

Vegetable oils are essential in daily nutrition for their sensory characteristics when used in cooking, but also as an important source of energy, as they contribute to maintaining normal body temperature [1]. Due to population growth, the consumption of vegetable oils and fats has increased, as has the number of research conducted in this field. Studies have shown that cholesterol deposition on arterial walls has been reduced, and the progression of atherosclerosis has been reduced by introducing unsaturated fats into the diet and removing saturated fats [1], [2].

Fats and oils are the raw materials for making margarine, cooking oils, functional oils, supplements and other edible products used in the food industry. Fats and oils can also be used in the leather, paint, rubber, textile, cosmetic and pharmaceutical industries. [3]

Crude vegetable oils are composed mainly of triacylglycerols together with smaller amounts of free fatty acids, monoacylglycerols and diacylglycerols, which constitute approximately 95% of their total content. The remaining 5% represents

*Corresponding author; *e-mail*: nicoleta.demostene@stud.chimie.upb.ro, demostenenicoleta@gmail.com

variable fractions of phospholipids, free and esterified sterols, triterpene alcohols, tocopherols and tocotrienols, pigments such as carotenoids and chlorophylls, and hydrocarbons. Impurities and undesirable by-products resulting from lipid oxidation may also be present in crude oils. In order to obtain a neutral and stable final product, various refining technologies have been developed that allow the elimination of these compounds, while preserving the valuable bioactive components for industrial and nutritional applications [4].

For the valorization of vegetable oils, it is possible to resort to their fractionation and separation into distinct classes of compounds, having specific properties and applications. This article review explores in detail the separation of vegetable oils into classes of components, examining both traditional and modern methods and emphasizing the need for industrial application.

2. Chemical Composition of Vegetable Oils

The composition of triacylglycerols, monoacylglycerols, and diacylglycerols varies depending on the type of vegetable oil. Fatty acids are the fundamental constituents of triglycerides, typically exhibiting a linear structure with carbon chains ranging from 4 to 22 atoms. The most common fatty acids found in vegetable oils include the unsaturated fatty acids oleic, linoleic, and linolenic, as well as the saturated fatty acids stearic, palmitic, lauric, arachidic, and behenic [1], [5].

Coconut oil is characterized by a very high content of saturated fatty acids (around 92%), with lauric acid being the predominant component (approximately 47–50%). This composition results in a relatively high melting point of about 24–25 °C, which explains why coconut oil tends to be solid or semi-solid at room temperature [1]. Conventionally, a triglyceride molecule is referred to as a “fat” when it becomes semi-solid at room temperature, whereas it is classified as an “oil” if it exhibits a liquid consistency [5].

The composition of vegetable oils includes both beneficial substances and undesirable components, the latter of which must be removed to obtain a high-quality, stable oil. Desirable constituents include triacylglycerols, tocopherols, squalene, and phytosterols. Tocopherols, squalene, and phytosterols act as antioxidants, enhancing the oxidative stability of the oil, while triacylglycerols contribute to its overall quality.

Conversely, phospholipids, free fatty acids, hydroperoxides, heavy metals, and moisture are considered undesirable, negatively affecting oil stability and quality. Phospholipids reduce oxidative resistance and can precipitate at the bottom of storage containers, affecting aesthetic appearance. Free fatty acids, metals, and moisture decrease oxidative stability, whereas hydroperoxides promote rancidity. Additionally, volatile ketones and aldehydes may impart off-flavors. Oils may also contain traces of other chemical pollutants, such as pesticides [3], [6], [7].

3. Vegetable Oil Separation Methods

Vegetable oils contain components that affect their color, taste, and long-term stability. During refining, the classes of constituents that impair oil quality are removed, but other compounds with potential health benefits, which could be further valorized, are also eliminated [6].

a. Chemical refining oil

Chemical refining represents one of the earliest methods developed for the processing of fats and oils and remains applicable even when the raw materials show partial degradation. The procedure is carried out in successive stages, each designed to eliminate specific classes of undesirable compounds [7].

i. Degumming

The first step in the chemical refining of a vegetable oil is degumming, which leads to the removal of phospholipids, mucilaginous gums and trace metals. This step is essential because it removes the classes of compounds that lead to oil clouding, dark coloration during heating and foam formation and cooking fumes during oil frying [3], [7]–[9].

Vegetable oils contain both hydratable and non-hydratable phospholipids that need to be removed. Hydratable phospholipids are eliminated through water degumming, whereas non-hydratable phospholipids are removed via acid degumming. Phospholipids are initially soluble in oil but become insoluble upon hydration. In acid degumming, either phosphoric acid or citric acid can be used; however, phosphoric acid is more effective in removing a larger amount of chlorophyll. Excessive addition of phosphoric acid may increase the phosphorus content of the oil. During degumming, the heated vegetable oil is mixed with water or an acid solution [3]. Other degumming methods also exist, including dry degumming, organic degumming, degumming with ethylenediaminetetraacetic acid (EDTA) and enzymatic degumming [6], [9].

ii. Neutralization

In the chemical refining process of oils, neutralization plays a critical role by reducing the content of free fatty acids (FFA) and facilitating the removal of undesirable constituents such as residual phospholipids, pigments, waxes, metals, and chlorophylls that remain in the degummed oil [3],[7].

FFA significantly affect the chemical quality and organoleptic stability of oils, creating storage-related challenges. When present in high concentrations, FFA necessitate refining of the oil to ensure compliance with market quality standards [7], [10].

In conventional refining practice, caustic soda solution is added in a stoichiometric amount to ensure the complete neutralization of FFA in crude oil, as well as the phosphoric acid previously applied during the acid degumming process. The reaction between the alkali and free fatty acids produces soaps, which are subsequently

removed through centrifugation and in the subsequent stages of refining [3], [6]. Various temperatures have been reported in the literature for the neutralization stage of different types of oils. A temperature of 25°C has been found insufficient to effectively neutralize FFA, while reported effective temperatures range from 40°C to 90°C [3].

Alkali neutralization has several drawbacks, including the generation of a large volume of wash water from the formed soaps, which requires additional treatment, as well as oil losses due to the reaction between the triglycerides in the oil and the added caustic soda [6].

Other modern neutralization techniques have also been investigated, including nano-neutralization. This method involves the use of Nano Reactors that operate based on hydrodynamic cavitation, in which the internal pressure is increased to levels between 40 and 80 bar. In this process, the required amounts of acids (citric or phosphoric) and caustic soda are significantly reduced, resulting in the formation of a smaller quantity of soap that can be more easily removed. Consequently, a lower volume of wash water is needed for soap removal from the oil, thereby reducing the amount of wastewater that requires subsequent treatment [11].

iii. Washing and drying

The next stage in the vegetable oil refining process is washing and drying, which serves to remove substances formed or added during the previous step, such as soap, excess caustic soda, and other impurities that were not eliminated earlier. The process involves washing the oil with hot water (approximately 85-90°C), preferably softened, followed by centrifugation and vacuum drying until the moisture content is reduced below 0.1%. Proper preparation of the oil is essential to prevent the formation of emulsions that can hinder soap separation, while thorough drying is required to avoid filter clogging and to ensure the subsequent quality and stability of the refined oil [7].

iv. Bleaching

Bleaching is a key stage in the refining process, which can be carried out under full or partial vacuum at temperatures between 70°C and 110°C, with the aim of improving the quality of vegetable oil. During this step, colored pigments such as chlorophyll and carotenoids are removed, along with other impurities not eliminated in previous stages, including traces of soap, phosphatides, metal ions, and more. As a result, the oil acquires a lighter color.

The decolorization process is conducted with the aid of adsorbent materials, such as bleaching clays, activated carbon, silica-based products, or combinations thereof. Bleaching clays are predominantly utilized in vegetable oils refining due to their high adsorption efficiency and cost-effectiveness, with bentonite being particularly used [6], [7], [12].

v. Dewaxing (Winterization)

Dewaxing primarily aims to remove waxes from oils that are naturally rich in these compounds. Waxes are esters of long-chain primary alcohols and long-chain fatty acids. Certain vegetable oils, such as sunflower, rapeseed, and corn oils, contain waxes

that tend to crystallize at low temperatures, leading to oil turbidity. While waxes do not generally compromise the functional properties of vegetable oils, they can adversely affect the oil's appearance [6], [7], [13].

The dewaxing process involves heating the oil to approximately 55°C to ensure it is fully liquid, followed by gradual cooling to 10-15°C and maintaining this temperature until complete crystallization of the wax occurs. Finally, the cooled oil is filtered and the wax is separated [7].

vi. Deodorization

The final stage in the chemical refining process of vegetable oils is deodorization, which removes unpleasant tastes and odors from the oils. Odoriferous compounds such as aldehydes, ketones, and hydrocarbons formed during oil degradation are eliminated, along with pesticide residues [5], [14].

Depending on the deodorization temperature, compounds such as sterols, tocopherols, and squalene may also be removed. However, the process can also lead to a slight increase in the content of trans fatty acids in the oil due to the isomerization of the carbon-carbon double bonds from the cis to trans configuration. The process involves steam distillation under vacuum at high temperatures (180–240°C) [5], [6], [7].

b. Physical refining oil

Physical refining includes all the stages of the chemical refining process, except for the neutralization step. By omitting this stage, the FFA remain in the oil until the final stage - deodorization. Compared to chemical refining, the deodorization in physical refining is carried out with steam at higher temperatures (200–270°C) under reduced pressure. Because of the elevated temperatures in this final stage, undesirable secondary reactions may occur, leading to the formation of oxidation products and trans C-C double-bond compounds. To minimize these issues, physical refining should be applied primarily to oils with a high content of saturated fatty acids, such as coconut oil and animal fats [3], [6].

In the neutralization stage, a large amount of wastewater is formed that requires treatment, but in the physical refining process it is no longer formed, making it a more environmentally friendly alternative. Oil losses at this stage will also be reduced. In the bleaching process, a larger amount of adsorbent will be required because some of the chlorophylls and pigments were removed in the eliminated stage. The degumming stage requires increased attention to ensure that the acid used is still removed and does not reach the subsequent stages. The process is characterized by low investment costs and a decreased use of chemical reagents when compared to conventional chemical refining methods [3], [15].

c. Advanced Physico-Chemical Methods

i. Membrane Technologies

Membrane technologies (MT) require lower costs and energy consumption compared to traditional processes. Membrane separation occurs based on particle size -

larger particles are separated from smaller ones. Examples of membrane processes include nanofiltration, ultrafiltration, microfiltration, and reverse osmosis. In some fields, membrane technologies have already been implemented at an industrial scale. Since MT does not involve chemical reactions, thermal effects, or biological modifications, their application is particularly suitable for thermolabile substances or in cases where the use of solvents and toxic chemicals must be avoided, such as in the food industry [16], [17].

The four membrane processes mentioned above differ in terms of membrane pore size and, consequently, in the size of the components they separate. The required operating pressure also varies between processes - for membranes with smaller pores (such as in reverse osmosis, up to 1500 psi), higher pressure is needed to force particles through the membrane. In microfiltration, the pore diameter is around 1 micron; in ultrafiltration, surface pore sizes range from 20 to 200 Å; and in reverse osmosis, pore diameters are between 1 and 10 Å.

Currently, these methods have numerous industrial applications -microfiltration and ultrafiltration are widely used in the pharmaceutical and food industries, while reverse osmosis is primarily employed for water purification [16], [18].

Membrane technology has been successfully applied to vegetable oils, primarily replacing the stages that traditionally involved the use of chemical substances, such as degumming and alkali treatment. It has been reported that a single filtration step can remove chlorophylls, pigments, and oxidation products (thus substituting the deacidification and degumming stages); however, free fatty acids were not eliminated [19].

ii. Dry fractionation (Winterization)

Depending on the composition of the oil, various fractions can be obtained by controlled cooling to create a solid and a liquid phase, similar to the winterization process. For example, the solid fraction of cottonseed oil contains high-melting-point saturated triglycerides. This method is also used to obtain palm stearin and palm olein fractions through the fractionation of palm oil [5]. The dry fractionation process has been extensively studied and widely applied, particularly in the case of palm oil, from which two primary fractions are obtained- olein and stearin [20].

iii. Supercritical Fluid Extraction

The use of supercritical carbon dioxide (SC-CO_2) has emerged as an environmentally friendly alternative to conventional solvent extraction of oils and fats. This technique yields products of high purity, which is particularly desirable in the pharmaceutical and cosmetic industries.

Although SC-CO_2 extraction systems initially required high investment costs, these costs have significantly decreased in recent years due to the growing demand for high-purity products and continuous technological development of SC-CO_2 extraction processes [21].

Priyanka et al. evaluated the economic viability of carrot seed oil extraction using SC-CO_2 and reported that for an extraction plant with a capacity of 120 tons per year, the production cost was approximately one-sixth of the selling price, confirming

the profitability of the process. It was also observed that the market price of the obtained oil was about three times higher than its total manufacturing cost [22].

Supercritical fluid extraction has been successfully applied in the food industry for total extraction, deodorization, and fractionation processes -including hop extraction, coffee decaffeination, and cholesterol removal from various animal-derived products such as meat, milk, and eggs. Several studies have been reported up to the pilot-plant scale [23].

4. Health benefits of vegetable oils

Vegetable oils contain not only essential fatty acids, but also a variety of micronutrients such as phytosterols, tocopherols, carotenoids, and phenolic compounds. These bioactive constituents contribute to the functional properties of the oils, including antioxidant activity that helps neutralize free radicals, reduction of blood cholesterol levels, and the prevention of various chronic diseases. The health benefits attributed to vegetable oils are therefore closely linked to the presence and activity of these functional compounds. The components of oils that exhibit antioxidant activity include tocols, phytosterols, phenolics, carotenoids, and fatty acids [1].

The World Health Organization reports that cardiovascular diseases remain the top cause of death globally, claiming around 19.8 million lives in 2022, which represents nearly 32% of total deaths, with heart attacks and strokes responsible for 85% of these fatalities [24].

Recent studies have shown that the consumption of nutritionally rich vegetable oils may help reduce the risk of cardiovascular diseases, an effect attributed to their content of monounsaturated fatty acids, polyunsaturated fatty acids and phytosterols [1], [25].

Chronic inflammation can promote the onset and progression of various conditions, such as autoimmune, cardiovascular and neurodegenerative diseases, type 2 diabetes, as well as gastrointestinal and sleep disorders, thus having a significant impact on overall health [26]. Polyunsaturated fatty acids and phytosterols present in certain vegetable oils exert anti-inflammatory effects [1].

The term cancer refers to a broad group of diseases that can affect any organ or tissue in the body. Globally, one in six people has died from cancer, which is concerning, especially considering that many cases could be treated if diagnosed in time [27].

Following conducted studies, it has been observed that phytosterols, also found in vegetable oils, exhibit anticancer effects by inducing cell apoptosis. Incorporating phytosterols into the diet may help reduce the risk of cancer development [28].

5. Industrial Applications

Vegetable oils and their fractions have numerous applications at the industrial level. For example, palm oil is one of the most widely used vegetable oils, with an estimated production of approximately 78.25 million metric tons for the 2024/2025 season [29].

Palm oil and its derived fractions are extensively used as frying media in both domestic cooking and food manufacturing, including products such as snack chips,

cookies, pastries, doughnuts, and fried potatoes. A notable feature of palm oil is its strong oxidative stability. The olein fraction, specifically, exhibits a long induction period- around 44 hours at 100°C- indicating excellent resistance to thermal oxidation during frying [30].

Mediterranean populations consume olive oil as an integral part of their traditional Mediterranean diet. Olive oil is primarily used in salads. Olive oil can be used for repeated frying, deteriorating much more slowly than other oils commonly used for frying. The natural antioxidants present in this oil, such as tocopherols and squalene, provide it with high thermal stability [31].

Through the fractionation of soybean oil, a solid fraction rich in stearic acid is obtained, which is utilized in the production of margarine and pastry products. Similarly, starting from sunflower oil, fractionation and removal of linoleic acid yield a fraction that can be employed in margarine production [32].

6. Conclusions

The separation of vegetable oils into component classes represents a complex and essential field of study for obtaining products with high nutritional, functional, and technological value. Depending on the applied method, various fractions can be isolated, including free fatty acids, triglycerides, phospholipids, pigments, tocopherols, phytosterols, and other minor bioactive compounds.

Conventional methods, such as chemical refining or thermal fractionation, provide good yields but are often associated with high energy consumption and the generation of chemical waste, which negatively impacts the environment. In contrast, modern techniques such as membrane separation, supercritical fluid extraction, and controlled fractionation (winterization or dry fractionation) - offer sustainable alternatives, enabling selective separation at low temperatures without degrading thermolabile compounds.

However, each method has specific limitations: membrane technologies may exhibit low permeate fluxes and high maintenance costs, while supercritical CO_2 extraction requires significant initial investment. Nevertheless, the advantages of these advanced processes, including the preservation of bioactive components, reduced solvent use, and improved environmental performance - strongly support the transition toward cleaner and more energy-efficient technologies in the vegetable oil industry.

In the future, process optimization and the integration of complementary separation methods could enable the development of sustainable, high-efficiency systems capable of fully exploiting the biochemical potential of vegetable oils and meeting modern demands for environmental responsibility and food quality.

REFERENCES

[1] M. Tian, Y. Bai, H. Tian, and X. Zhao, The Chemical Composition and Health-Promoting Benefits of Vegetable Oils- A Review, *Molecules*, 28, 17, (2023).

[2] P. T. Voon *et al.*, Health Effects of Various Edible Vegetable Oil: An Umbrella Review, *Adv. Nutr.*, 15, 9, (2024).

[3] S. C. Chew and K. L. Nyam, Refining of edible oils, *Lipids and Edible Oils: Properties, Processing and Applications*, Elsevier Inc., (2020), 213–241.

[4] N. J. Oswell, F. D. Gunstone, and R. B. Pegg, Vegetable oils, *Bailey's Industrial Oil and Fat*

Products, (2020).
[5] M. K. Gupta, *Practical Guide to Vegetable Oil Processing*. Elsevier Inc., 2017.
[6] A. Sonawane and S. Waghmode, A Review on Vegetable Oil Refining: Process, Advances and Value Addition to Refining by-Products, *Bioremediation for Global Environmental Conservation*, (2023).
[7] S. Gharby, Refining Vegetable Oils: Chemical and Physical Refining, *Sci. World J.*, 2022, (2022).
[8] J. Ortega-García *et al.*, Refining of high oleic safflower oil: Effect on the sterols and tocopherols content, *Eur. Food Res. Technol.*, 223, 6, (2006), 775–779.
[9] Y. Lv, Z. Ye, S. Luo, Y. Xiong, Y. Liu, and Z. Zhang, Removal strategies for the undesirable components from the crude vegetable oils: A review, *J. Clean. Prod.*, 478, (2024).
[10] Codex standard for named vegetable oils, Retrieved 10 October 2025 from http://www.fao.org/3/y2774e/y2774e04.htm#bm4.1. (2025).
[11] W. F. J. De Greyt, Current and future technologies for the sustainable and cost-efficient production of high quality food oils, *Eur. J. Lipid Sci. Technol.*, 114, 10, (2012), 1126–1139.
[12] S. M. Ghazani and A. G. Marangoni, Minor components in canola oil and effects of refining on these constituents: A review, *J. Am. Oil Chem. Soc.*, 90, (2013), 923–932.
[13] A. J. Dijkstra and G. van Duijn, Vegetable Oils: Oil Production and Processing, *Encyclopedia of Food and Health*, (2016), 373–380.
[14] M. J. Dumont and S. S. Narine, Soapstock and deodorizer distillates from North American vegetable oils: Review on their characterization, extraction and utilization, *Food Res. Int.*, 40, 8, (2007), 957–974.
[15] M. Tasan and M. Demirci, Total and individual tocopherol contents of sunflower oil at different steps of refining, *Eur. Food Res. Technol.*, 220, (2005), 251–254.
[16] E. M. Hernandez, Processing of Fats and Oils Using Membrane Technologies, *Bailey's Ind. Oil Fat Prod.*, (2020).
[17] K. V. Kotsanopoulos and I. S. Arvanitoyannis, Membrane Processing Technology in the Food Industry: Food Processing, Wastewater Treatment and Effects on Physical, Microbiological, Organoleptic, and Nutritional Properties of Foods, *Crit. Rev. Food Sci. Nutr.*, 55, 9, (2015), 1147–1175.
[18] R. W. Baker, *Membrane Technology and Applications:*, 23, 1, (2024).
[19] C. de Morais Coutinho, M. C. Chiu, R. C. Basso, A. P. B. Ribeiro, L. A. G. Gonçalves, and L. A. Viotto, State of art of the application of membrane technology to vegetable oils: A review, *Food Res. Int.*, 42, 5–6, (2009), 536–550.
[20] O. Zaliha, C. L. Chong, C. S. Cheow, A. R. Norizzah, and M. J. Kellens, Crystallization properties of palm oil by dry fractionation, *Food Chem.*, 86, 2, (2004), 245–250.
[21] O. Dhara, K. N. P. Rani, and P. P. Chakrabarti, Supercritical Carbon Dioxide Extraction of Vegetable Oils: Retrospective and Prospects, *Eur. J. Lipid Sci. Technol.*, 124, 8, (2022).
[22] Priyanka and S. Khanam, Supercritical CO2 extraction of carrot seed oil: screening, optimization and economic analysis, *Int. J. Environ. Sci. Technol.*, 17, (2019), 2311–2324.
[23] F. Sahena *et al.*, Application of supercritical CO2 in lipid extraction - A review, *J. Food Eng.*, 95, 2, (2009), 240–253.
[24] https://www.who.int/news-room/fact-sheets/detail/cardiovascular-diseases-(cvds), accessed on October 12, 2025.
[25] I. Djuricic and P. C. Calder, Beneficial outcomes of omega-6 and omega-3 polyunsaturated fatty acids on human health: An update for 2021, *Nutrients*, 13, 7, (2021).
[26] V. P. Chavda, J. Feehan, and V. Apostolopoulos, Inflammation: The Cause of All Diseases, *Cells*, 13, 22, (2024).
[27] https://www.who.int/news-room/fact-sheets/detail/cancer, accessed on October 12, 2025.
[28] N. Shahzad *et al.*, Phytosterols as a natural anticancer agent: Current status and future perspective, *Biomed. Pharmacother.*, 88, (2017), 786–794.
[29] https://www.fas.usda.gov/data/production/commodity/4243000, accessed on October 12, 2025.
[30] S. W. Lin, Palm Oil, *Vegetable Oils in Food Technology: Composition, Properties and Uses*, (2011), 25–58.
[31] D. Boskou Dr., Olive Oil, *Veg. Oils Food Technol. Compos. Prop. Uses*, (2011), 244–271.
[32] D. B. Yayla, Vegetable Oil Fractionation : Technological Methods , Applications , and Future Perspectives, *ZEUGMA Biol. Sci.*, 6, 1, (2025), 1–13.

MONITORING OF THE DIESEL HYDRODESULFURIZATION REACTOR AND PRIMARY STATISTICAL DATA EXPLOITATION

Laura Elisabeta PETRAS[1,2*], Claudia MUNTEAN[3], Oana PARVULESCU[1], Tănase DOBRE[1]

[1]Chemical and Biochemical Engineering Department, University POLITEHNICA of Bucharest, 1-7 Gheorghe Polizu Str., 011061 Bucharest[2]Petromidia Refinery, Navodari Bld 214, Navodari 905700[3]Chemistry and Chemical Engineering Department, Ovidius University124 Mamaia Bld 900527

Abstract

This paper presents the monitoring of an industrial diesel hydrodesulfurization (HDS) reactor and the preliminary statistical analysis of process data. The study focuses on the collection, processing, and interpretation of operational parameters recorded in an industrial unit. The monitoring approach relies on systematic analysis of temperature, pressure, flow rates, and sulfur concentration in the diesel stream. Integration of monitoring software and automated data acquisition ensured reliable operation and continuous performance evaluation. Statistical processing revealed correlations between operating parameters and product quality. The results highlight the importance of real-time monitoring and statistical evaluation as tools for process optimization and predictive control.

Key words: Diesel hydrodesulfurization; process monitoring; statistical analysis; refinery optimization; sulfur removal.

1. Introduction

Diesel hydrodesulfurization (HDS) is a catalytic refining process aimed at removing sulfur-containing compounds from diesel fractions [1-4]. Environmental regulations impose increasingly stringent limits on sulfur levels in fuels, typically below 10 ppm. Continuous monitoring of HDS reactors is crucial to maintain product quality, ensure catalyst performance, and optimize hydrogen consumption.
This paper presents an industrial case study focused on monitoring an HDS reactor processing straight-run diesel and light cycle oil blends. The collected data were statistically analyzed to determine correlations between process parameters and sulfur removal efficiency.

To better interpret and quantify process performance, a mathematical model of the HDS reactor can be used based on monitored operational parameters [4- 6].
The monitored system consists of an industrial HDS reactor operating under steady-state conditions. Key parameters include temperature, total pressure, hydrogen-to-oil ratio, and liquid hourly space velocity (LHSV).
Data acquisition was performed using the refinery Distributed Control System (DCS), which automatically recorded values at fixed time intervals. Between the registered parameters were: i) reactor inlet/outlet temperature (°C), ii) reactor pressure (MPa). iii) hydrogen recycles flow (Nm^3/h), iv) liquid feed flow (t/h), v) product sulfur concentration (ppm).

* Corresponding author: Email address: laurapetras@yahoo.ro

The work is focused on continuous monitoring of an industrial diesel hydrodesulfurization (HDS) reactor under steady-state operation conditions and on statistical analysis of monitored data in order to revealed strong and less strong correlations reactor product sulfur concentration and process factor such as reactor temperature, liquid flow rate through catalytic bed, in reactor feed hydrogen-to-oil ratio, sulphur content and some properties of diesel (density, ASTM distillation curve) at reactor feed. In general and especially in this particular case, the monitoring data serves to update the predictive control model of the installation, to solve some optimization issues, to train artificial intelligence algorithms applicable to the case and also to customize hydrodesulfurization through neural network models [7- 10].

2. Reactor and Process Description

The monitored reactor is part of a diesel hydrotreating unit operating under steady-state conditions. The feedstock is a blend of straight-run diesel and light cycle oil. The process involves hydrogenation and hydrodesulfurization reactions taking place over a $CoMo/Al_2O_3$ catalyst. Operating parameters typically range as follows: temperature: 315–335 °C, pressure: 5.5–6.0 MPa, LHSV: 1.0–1.3 h^{-1}, hydrogen-to-oil ratio: 270–340 Nm^3/m^3. Figure 1 presents the scheme of hydrodesulfurization installation where we have heating section in red, separation section in blue and hydrogen recovery and recirculation in yellow.

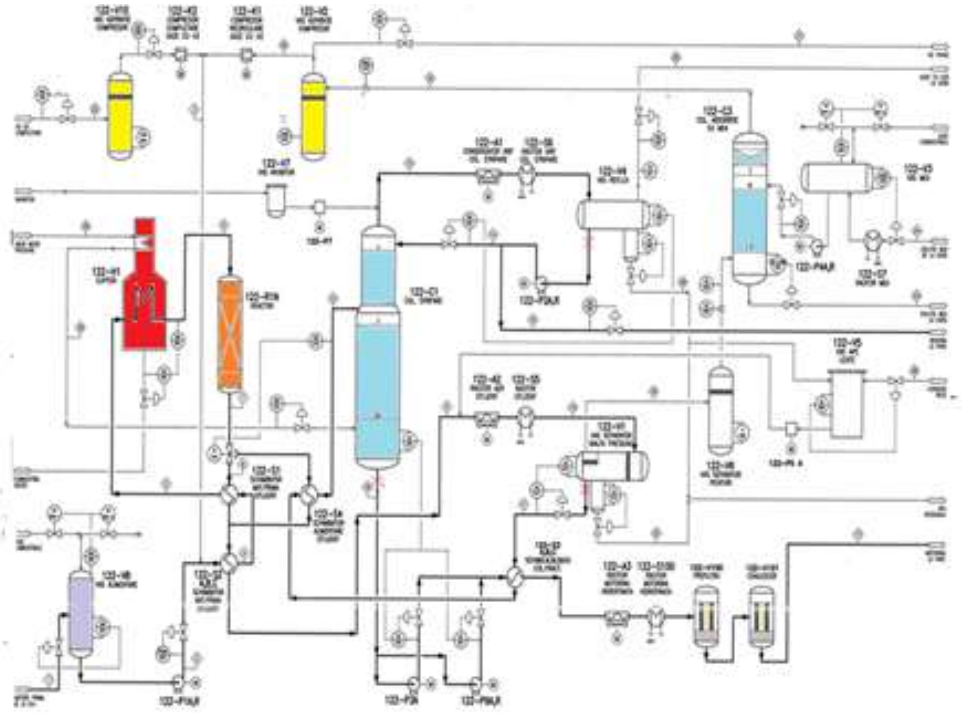

Fig.1.Schematic representation of diesel HDS plant with automation marking in work forprocess monitoring

It identifies that after passing through control valve the feed diesel mixes with hydrogen-rich gas and is gradually heated in heat exchangers reaching 240–300 °C, before entering in plant furnace. The diesel–hydrogen mixture is then sent to reactor, where it flows through the catalyst bed, with temperature and pressure drop closely monitored. The resulting effluent is gradually cooled in heat exchangers and air/water coolers, then separated in the high-pressure separator into gas and liquid phases (hydrotreated diesel and water). The gas separation and desulfurization section removes hydrogen-rich gases from the effluent. These gases are cooled, separated from liquid droplets, and then treated in the DEA absorption column, where hydrogen sulfide is absorbed under controlled temperature and pressure conditions.

2.1 Monitoring System and Data Collection

The refinery's distributed control system (DCS) continuously recorded key process variables including reactor inlet and outlet temperature at selected locations, reactor pressure and reactor gas pressure loss, hydrogen (gas) circulation flow rate, liquid feed flow, hydrodesulfurized diesel sulfur concentration. More others parameters was. Many other parameters were retained in the monitoring process. We thus find data on the formation of the mass fed into the reactor, the density of the liquid reactor input, the ASTM boiling curve of the diesel in reactor feed, the density of the product, the ASTM boiling curve of the product, the nitrogen concentration in the product, etc. This resulted in a large data file whose, a part of table header components, is shown in Figure 1.The data were collected at fixed time intervals and exported as CSV files for statistical analysis.

			Feed rates						Product rates	
			Total	Total	SRGO - Motorina de DA	LCO	LCGO-Motorina usoara de CX	SR Kero - Petrol DA		Naptha Fractie usoara
			Feed rate	Feed rate	Feed 1 rate	Feed 2 rate	Feed 3 rate	Feed 4 rate	TLP rate	Product 1 r
		Client Tags	P122FIC0003/PID1/PV.CV		P122FIC0001/PID1/PV.CV		P122FIC0090/PID1/PV	FIC0202/PID1/PV.CV		P122FIC0025/PID
		Topsoe Tags	FEED-FLOW	FEED-FLOW	FEED_1-FLOW	FEED_2-FLOW	FEED_3-FLOW	FEED_4-FLOW	PROD_TLP-FLOW	PROD_1-FLO
Date	Run Day	Comments	m³/h	BPSD	m³/h	m³/h	m³/h	m³/h	t/h	t/h
12/04/2022	1		20.1		19.8		0.3	0.0		0.0
13/04/2022	2		65.3		65.0		0.3	0.0		0.4
14/04/2022	3		90.9		90.5		0.4	0.0		0.8
15/04/2022	4		84.6		74.8		5.8	4.0		0.9
16/04/2022	5		84.5		64.5		10.0	10.0		1.0

			Heater outlet	Unit inlet	Reactor 1							Thermocouple ring 1 from the top						
					Bed 1							1	2	3	4	5	6	7
					IN							IN	IN	IN	IN	IN	IN	IN
		Client Tags		P122TIC0	Client tag no							P122TI050	P122TI050	P122TI050	P122TI050	P122TI050	P122TI050	P122TI050
		Topsoe Tags	HEATER_OUT-T	R_1-IN-T	R_1_BED_1_IN-T_1							R_1_BED_1_IN-T	R_1_BED_1_IN-T	R_1_BED_1_IN-T	R_1_BED_1_IN-T	R_1_BED_1_IN-T	R_1_BED_1_IN-T	R_1_BED_1_IN-T
Date	Run Day		°C	°C	°C							°C	°C	°C	°C	°C	°C	°C
12/04/2022	1			202.4								203.6	203.6	203.8	203.7	204.0	203.7	204.2
13/04/2022	2			319.5								322.6	323.3	323.7	322.4	322.5	322.6	328.3
14/04/2022	3			325.6								328.8	329.8	329.7	328.6	328.6	328.6	336.6
15/04/2022	4			326.4								331.2	332.4	331.9	330.6	330.8	330.9	339.2

Fig. 2. Image showing the Data Input (top) and some data Temperature from ones bed thermocouples (bottom)

A presentation solution was adopted by dividing the large Excel file into Mathcad in 12–14-column matrix blocks, then reconstructing each matrix as a table. Over 491 operating days with four shutdowns were logged (time, duration, cause, reactor thermal state) and maximum production values for the 130 m³/h designed capacity were noted in

table 1. The he processed diesel rate never fell below 65% of 130 m^3/h reactor input diesel, which design capacity to maintain under 10 ppm sulfur in processed diesel.

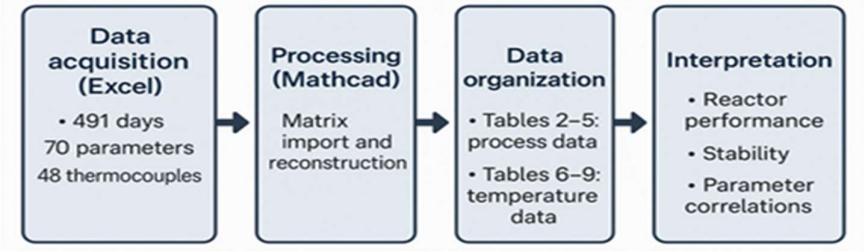

Fig. 3. Short presentation of the organization of monitoring data valorization

Table 1.

Principal details regarding HDS unit shutdowns during the monitoring period

	Position in time	Duration	Cause	Reactor state
	Day 58	2 days	Emergency maintenance	312 ^{0}C
	Day 76	2 days	Recycle gas compressor failure	307 ^{0}C
	Day 272	27 days	Feedstock shortage	302 ^{0}C
Maximum production rates: 127 – 128 m^3/h, days 122, 125, 413 - 465				

Figure 3 shows the sequencing of monitoring data exploitation. Table 2 is an example of breaking the original Excel file into Matchad files, while Figure 4 is intended to show an image of some of the 8 Matchad files, used in this work. They correspond to the working sequence of the installation between days 1 and day 58, when the plant was stopped for emergency maintenance (table1)

Table 2.

Feed and product flow rates for the first 58 days

12/04/2022	1	20.1	19.8	0.3	0.0	0.0	119.7	111.2	32.3	1676.2
13/04/2022	2	65.3	65.0	0.3	0.0	0.4	95.2	95.0	18.9	2711.2
14/04/2022	3	90.9	90.5	0.4	0.0	0.8	81.3	86.9	10.0	2635.0
15/04/2022	4	84.6	74.8	5.8	4.0	0.9	74.5	83.8	5.1	2655.8
16/04/2022	5	84.5	64.5	10.0	10.0	1.0	70.2	77.5	6.8	2798.6
17/04/2022	6	84.2	64.2	10.0	10.0	1.1	70.2	78.2	6.0	2895.7
18/04/2022	7	85.4	62.5	10.0	12.9	1.1	70.3	78.0	6.4	3120.6
19/04/2022	8	85.9	57.9	10.0	17.9	1.3	72.0	78.0	8.7	3585.0
20/04/2022	9	85.9	55.9	10.0	20.0	1.4	71.9	77.8	9.2	3818.7
21/04/2022	10	86.8	56.8	10.0	20.0	1.3	71.8	78.1	8.3	3831.7
22/04/2022	11	86.7	56.8	10.0	20.0	1.3	71.0	77.3	8.2	3703.5
23/04/2022	12	86.4	56.4	10.0	20.0	1.3	69.0	76.8	6.4	3833.8
24/04/2022	13	85.4	55.4	10.0	20.0	1.3	69.2	76.7	7.1	3610.2
25/04/2022	14	103.8	81.3	14.2	8.4	1.1	86.0	83.8	20.1	3841.1
26/04/2022	15	121.9	98.6	15.6	7.7	1.3	101.6	78.9	42.4	2874.0

C_1 – day, C_2 - current day number C_3 –Total feed flow m^3/h, C_4 - DAV diesel flow m^3/h, C_5 – CX diesel flow m^3/h, C_6 – DA Kerosene flow m^3/h, C_7 – Nafta product flow t/h, C_8 – Hydrorefined diesel t/h, C_9 – Pass-through diesel 1 t/h C_{10} – Pass-through diesel 2 t/h. C_{11} – New gas flow Nm3/h

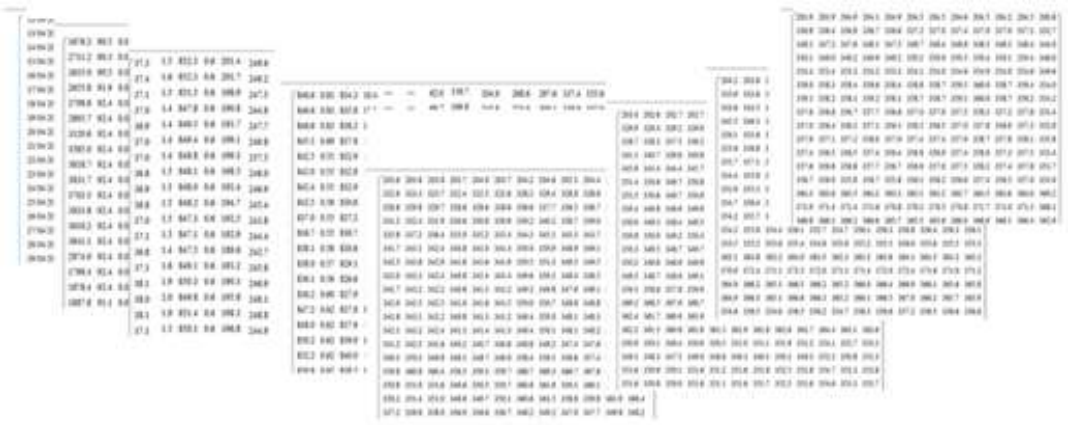

Fig. 4. Presentation image of Mathcad files (Table 2-9) separated from Excel file

Tables 2–9 compile the essential monitoring data recorded up to the first shutdown, covering both process performance and catalyst behavior. Tables 2–5 summarize daily variations in feed and product flow rates, gas phase composition, operating pressure, and sulfur and nitrogen contents in the diesel streams, while Tables 6–9 focus on the detailed temperature distribution across the four radial levels of the catalyst bed. Together, these datasets provide a comprehensive view of reactor operation, process stability, and parameter interdependence during steady-state industrial HDS performance.

2.2 Statistical Processing

Collected data were processed using statistical software (e.g., Excel, Minitab, or MATLAB and MathCad). The following monitored data processing were performed: i)descriptive statistics (mean, standard deviation, range), ii) graphical dependences respect to influence of factors process on sulfur content of processed diesel, iii) correlation analysis through covariance and correlation coefficient calculations, iv)an attempt at regression analysis regarding the dependence of the sulfur content on some process factors.

3. Capitalization of data from diesel HDS reactor monitoring files

Obviously, the first step in exploiting the data from the monitoring files is to establish as clearly as possible which are the response (dependent) variables, and which are the independent, most important ones. We reiterate, with reference to the data presented in tables 2–9, that the main dependent variables are the sulfur concentration and nitrogen concentration in the hydrofined diesel fuel, the density of the hydrofined diesel fuel and the ASTM curve of the hydrofined diesel fuel.

The first solution to exploit the monitoring data is their use in modelling to identify parameters contained in accepted models.

A simpler solution to exploit these data is the graphical representation of the monitored parameters dynamics in relation to what is called the accepted value (minimum and maximum) of each of these.

.

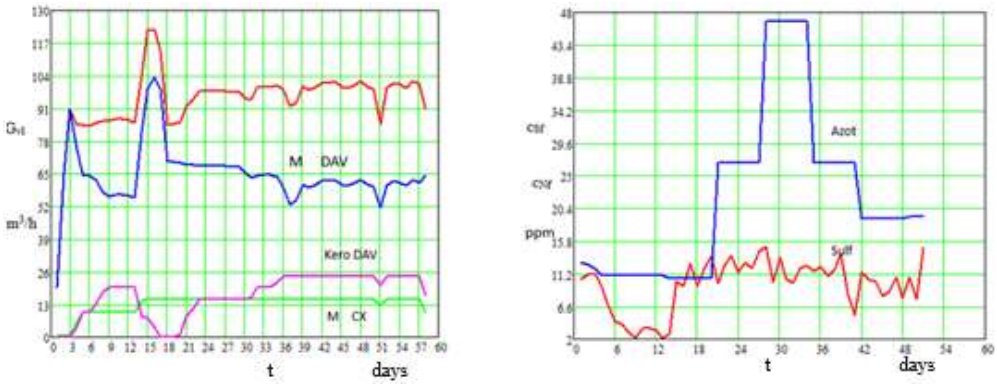

Fig. 5. Dynamics of diesel fuel supply (right) and sulfur and nitrogen concentration in hydrorefined diesel for the working sequence until the first shutdown

This solution is illustrated in Figure 5, where on the left side the dynamics of the total diesel flow, together with its components (DAV diesel, CX diesel, DAV kerosene), are shown. On the right side, the dynamics of sulfur and nitrogen in hydrorefined diesel are presented as an especially important aspect. In the first case, the red values represent the average values of each flow rate, while, in the second case, the red line for sulfur corresponds to 10 ppm threshold, and for nitrogen to 20 ppm threshold.

Given that the HDS facility is designed and operated for stationary conditions, another solution for valorizing the monitoring data is their detailed statistical analysis [11], using in this regard: i) means, dispersions and confidence intervals for each data column from the four sequences of the monitoring files;ii) grouping and dispersion analysis to identify the influence of independent variables on those considered dependent; iii) correlation analysis, in order to identify strong links between the response variables and the other variables; iv) generalized regression analysis on each of the 4 sequences (table 1) of monitoring data, together with the comparative analysis of the results; v) use of the EVOP (Evolutionary Operation) method in order to assess whether one or another of the 4 operating sequences, specified in table 1, is ordered, according to the most relevant response (sulfur concentration in the processed diesel fuel), progressively or not. This problem of detailed statistical analysis of monitoring data from the HDS plant will probably be the subject of future work.

In the following, some links between variables considered dependent and others considered independent are presented through correlation analysis. We thus can observe, in pairs, the links between some variables of the reactor operation, in particular between the sulfur concentration in the processed diesel fuel and other monitoring variables. The simplest way to appreciate the correlation (relationship) between a dependent variable y (e.g.: c_{Sf} – sulfur concentration in processed diesel fuel) and an independent variable x (e.g.: c_{S0} – sulfur concentration in fed diesel fuel) is to plot y against x [11]. This type of observation could be illustrated by a very large number of plots, using the y and x

variables from the Data Input and Thermocouple files (figure 2). Relevant examples are illustrated in Figures 6–8, whose selections are intentional.

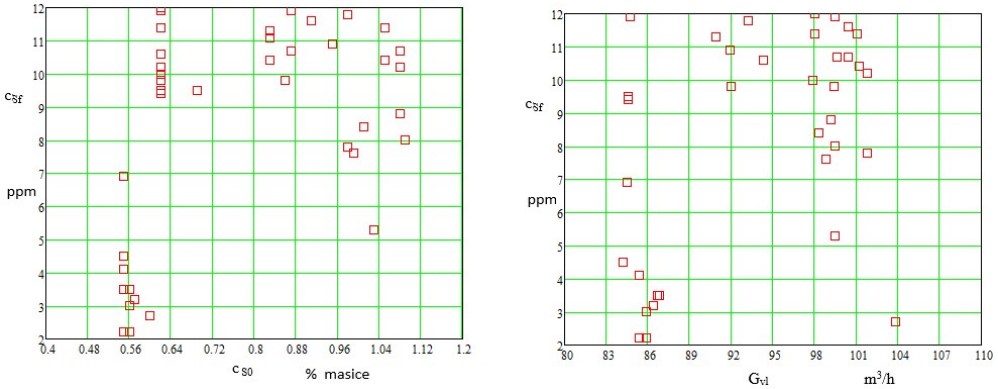

Fig. 6. Dependence of sulfur concentration in processed diesel fuel (c_{Sf}) on sulfur concentration in fed diesel fuel (c_{S0}) and on fed diesel fuel flow rate (G_{vl})

Thus: i) Figure 6 (left) shows that c_{Sf} is dependent (correlated) on c_{S0}, the average increase being evident, but there are also points indicating the intervention of other factors (e.g. the group of points for $c_{S0} \approx 0.63\%$).ii) Figure 5 (right) reveals a similar influence to the previous one, when instead of c_{S0} the diesel fuel feed rate is considered, iii) Figure 7 shows that the temperature, regardless of the measurement point in the reactor, correlates with c_{Sf} with an almost linear decrease up to 352–354 °C, after which other factors intervention completely change the correlation, iv) Figure 8 (right) shows that the relationship between the concentration of nitrogen compounds in the product and temperature (at any level in the catalytic layer) is non-existent up to 352–354 °C, after which it becomes complex, explainable only by the influence of several factors: for example, at 356 °C both values of 11 ppm nitrogen compounds and 23 ppm can be observed (figure 6 left), v) If the diesel flow rate through the reactor is increased, it would be logical that the gas flow rate should also increase, and figure 7 (right) supports this aspect, despite the complexity of the intervention of other factors, one of which is the hydrogen content in the gas.

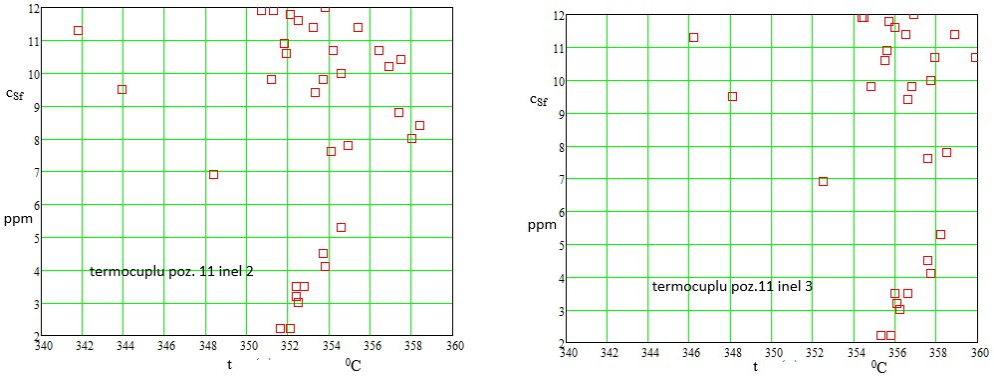

Fig. 7. Dependence of sulfur concentration in processed diesel fuel (c_{Sf}) on the temperature (t) at position of reactor ring 2 (left) and ring 3 (right) respectively

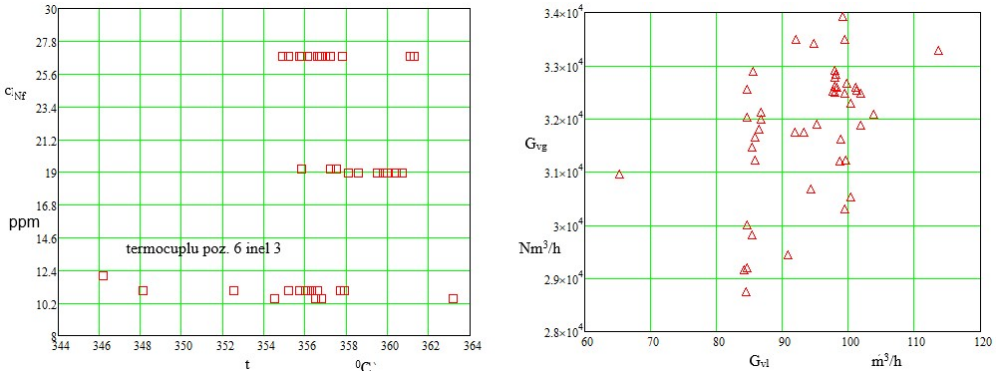

Fig. 8. Dependence of processed diesel fuel nitrogen concentration (c_{Nf}) on temperature (t) at reactor 3 (left) and of the gas flow rate (G_{vl}) through the reactor

As a brief introduction to correlation analysis, we show that for a process with a dependent variable and an independent variable, the statistical analysis of the process provides a chain with values y_i, i = 1, n and another with values x_i, i=1, n. where n is the number of processed experiments or in particular a number of data monitored per parameter. Correlation analysis shows that the process variables y (example c_{Sf} - sulfur concentration in processed diesel fuel) and x (example c_{S0} - sulfur concentration in fed diesel fuel) are correlated if the indicator *cov(x,y),* given here by relation (1), presents a significant value [11]. In relation (1) x_m and y_m are the mean values for the data series x_i and y_i respectively. Calculating with relation (1) the covariance between y and x for a set of values and then for a new set of repeated values, then the two values can by or will be different. This inconvenience is eliminated by replacing the covariance with the correlation coefficient of the variables y and x, expressed with the relation (2), where σ_x and σ_y are the standard deviations for the series of the variable x and y respectively.

$$cov(y,x) = \frac{\sum_{i=1}^{n}(x_i - x_m)(y_i - y_m)}{n-1} \quad (1)$$

$$r_{yx} = \frac{\sum_{i=1}^{n}(x_i - x_m)(y_i - y_m)}{\sqrt{\sum_{i=1}^{n}(x_i - x_m)^2 (y_i - y_m)^2}} = \frac{cov(y,x)}{\sigma_x \sigma_y} \quad (2)$$

The computed values of the correlation coefficient are between –1 and +1, sor_{yx}:R→[-1,1]. The following observations [11] can be made for correlation coefficient: 1) If the value of the correlation coefficient approaches zero, then we can accept the variables x and y as independent, so the variations of the dependent variable do not affect the values of the independent variable; 2) When the correlation coefficient takes a positive value, the independent and dependent variables increase simultaneously. The opposite case corresponds to a negative value of the correlation coefficient; 3).The extreme values for which the correlation coefficient r_{yx} tends to 1 or r_{yx} tends to - 1 shows that there is a linear relationship (correlation) between the dependent and independent variables.

Table 3 shows the result of calculations for some of the most expected correlations, related to the data in Tables 2-9, which refers to first monitored work

sequence of the diesel hydrodesulfurization plant (table1). The table notes whether the correlation is of little importance (SI), important (I) or extremely important (VI).

Table 3

Computed values for some important y vs. x correlations in monitoring of the diesel hydrodesulfurization reactor

	Variable y	Variable x	cov(y,x)	σ_x	σ_y	r_{yx}	Obs.
1	Sulph. conc. PD c_{Sf}	Sulph/ con. FDc_{S0}	0.181	0.192	3,592	0.262	I
2	Sulph. conc. PD c_{Sf}	Liq. flow rateG_{vl}	8.633	9.601	3.592	0.255	II
3	Sulph. conc. PD c_{Sf}	Gas flow rateG_{vg}	1224	194.5	3.592	0.177	S I
4	Sulph. conc. PD c_{Sf}	Reactor pressure$p$	0.501	0.400	3.592	0.409	V I
5	Sulph. conc. PD c_{Sf}	Pressure lossΔp	0.305	0.141	3.592	0.602	VI
6	Sulph. conc. PD c_{Sf}	Ring 1 temp, $t_{mpc1}{}^0$C	-1.336	5.807	3.592	-0.46	VI
7	Sulph. conc. PD c_{Sf}	Ring 2 temp, $t_{mpc2}{}^0$C	-0.633	5.314	3.592	-0.24	I
8	Sulph. conc. PD c_{Sf}	Ring 3 temp, $t_{mpc3}{}^0$C	-0,773	4.956	3,592	-0.31	I
9	Sulph. conc. PD c_{Sf}	Ring 4 temp, $t_{mpc4}{}^0$C	-0.573	4.586	3.592	-0.24	I
10	Sulph. conc. PD c_{Sf}	Liq. Dens, ρ_D kg/m^3	6.199	4.702	3.592	0.404	VI
12	Gas flow rate G_{vg}	Liq.flowrate G_{vl}	4891	9.601	1224	0.416	VI
13	Pressure lossΔp	Liq. Flow rateG_{vl}	0.723	9.601	0.141	0.728	VI
14	Pressure lossΔp	Gas flow rateG_{vg}	3688	1224	0.141	0.425	VI

Data from table 3 show that all correlation coefficients referring to the dependence of the sulphur concentration in the processed diesel fuel on any of the 10 variables considered to influence, show that they are important. We thus find that:1) r_{cSfcS0} has the value 0.262 which says that c_{Sf} increases, as expected, with c_{S0}, in a significant manner,2) as expected the increase in the diesel fuel flow rate leads to an increase in the sulphur content in the processed diesel fuel, fact shown by the positive value of the correlation coefficient, which is r_{cSfGvl} = 0.255, almost equal to r_{cSfcS0},3) the positive value of the coefficient r_{cSfGvg} surprises even if it is below 0.2, which would indicate a weak correlation between the sulphur concentration in the processed diesel fuel and the gas flow rate through the reactor; restoring this index by taking into account the hydrogen flow rate instead of the gas flow rate leads to $r_{cSfGvH2}$ = - 0.11 which shows a weak influence, because the hydrogen is in excess, but in the expected direction; 4) it surprises the strong positive correlation of the sulphur concentration in the diesel fuel produced by the pressure, r_{cSfp}=0.409, which would seem to urge to reduce the hydrogenation pressure, but this is practically impossible because the temperature necessary for the catalyst to function could no longer be ensured; 5) apparently also surprising is the very strong, positive correlation of the sulphur concentration in the diesel fuel produced by the pressure drop, $r_{cSf\Delta p}$=0.409 but in fact it can be considered that the pressure loss is responsible for reduction of hydrogen partial pressure in the gas and therefore of its concentration in the liquid, so that the hydrogenation of sulphur compounds decreases in intensity,6) the 4 values of the correlation coefficient $r_{cSftmpci}$ (i=1.4), which indicates the relationship between the sulphur concentration and the temperature of thermocouple 6 in rings 1-4 of the reactor, all have negative values, as expected (temperature increases, sulphur concentration in the product decreases) and indicates, by generalization, that temperature is an important factor, even very important in process control; 7) if the process in the hydrodesulfurization reactor were analysed from a hydrodynamic point of view, it should be clear that for the equicurrent flow of the

phases, as is the case of the hydrodesulfurization reactor, we must have the pressure drop strongly influenced by the flow rate of each of the two phases. This is what is observed in lines 13 and 14 of table 3.

4. Conclusions

The industrial case study refers to a diesel hydrodesulfurization (HDS) reactor operating within a modern refinery hydrotreating unit. The unit processes blended diesel fractions consisting primarily of straight-run diesel and light cycle oil. The main objectives of this reactor are to remove sulfur compounds to meet ultra-low sulfur diesel specifications and to stabilize the product through hydrogenation of olefins and partial saturation of aromatics.

The HDS reactor operates in a trickle-bed configuration, under controlled and monitored conditions, having fixed bed of Co-Mo/Al_2O_3 pellets catalyst.The typical operating ranges are characterized by temperature -315–335 °C, pressure-3.3–4.2 MPa, liquid hourly space velocity - 1.0–1.3 $h^{-1}$and hydrogen-to-oil ratio- 270–340 Nm^3/m^3_{lq}.

The presentation of the role of monitoring in the predictive control of the diesel hydrorefining plant focuses on the fact that the mathematical model within the control must be continuously adapted through monitoring.

The process diagram reported to the considered refinery plant, and some details regarding the hydrodesulfurization reactor are presented in such way as to sustain the process variables considered in the monitoring.

The data contained in the Data Input and Thermocouple files are explained in terms of their selection and importance in monitoring of HDS.

The dynamics of some parameters and the correlation between some pairs, considered important, are graphically presented and commented accordingly.

Special attention is paid to the statistical analysis of the monitoring data, specifically insisting on its characterization through correlation analysis, which brings numerous conclusions, some particularly interesting.

Acknowledgement: Monitoring data was obtained through the refinery Petromidia SA support

REFERENCES

[1] Jimenez F., Nunez M., Kafarov V. (2005). Study and modeling of simultaneous hydrodesulfurization, hydrodenitrogenation and hydrodearomatization on vacuum oil hydrotreatment. In: *European Symposium on Computer-Aided Processes*, Elsevier Science, 2005

[2] Babich I. V., Moulijn J. A., Science and technology of novel processes for deep desulfurization of oil refinery streams: A review.*Fuel*, 82, 607–631, 2003

[3] Chowdhury R., Pedernera E., Reimert R., Trickle-bed reactor model for desulfurization and dearomatization of diesel. *AIChE J.,* 48, 126–135, 2004

[4] Petras L. E., Dobre T., Serbănescu N., Pop F. D., Pârvulescu O.C., Monitored and Predicted Data for a Diesel Fuel Hydrotreating Reactor, *Materials* 18, 2481, 2025

[5] Baloochy B., Shokri S., Marvasar A. M., Design and implementation of simulator for hydrotreating reactor in RTO development,*Int. J. Chemical Engineering and Applications*, 1(4), 287–293, 2010

[6] Novaes L. R., Resende N. S., Salim V. M., Secchi A. R., Modeling, simulation and kinetic parameter estimation for diesel hydrotreating.*Fuel*, 209, 184–193, 2017
[7] Wang S., Liu Q., Zhang Y., AI-based predictive control for hydroprocessing units, *Chemical Engineering Research and Design*, 148, 22–35, 2019
[8] Iplik E., Aslanidou I., Kyprianidis K., A Feedforward Model Predictive Controller for Optimal Hydrocracker Operation, Processes 10, 2583, 2022
[9] Borja P.B., AliFanaei M., Esfandyari M., Naddaf A., DJafarid D., BaghmishehGh., Machine learning-assisted methods for predictionand optimization of oxidative desulfurization of gas condensate via an oxidation system, *Journal of Sulfur Chemistry*, 45, 1, 84–100, 2024
[10]Wang W., Qikai Zhang Q.,Lianhui Ding L., Ying Zheng Y., Simulation of hydrodesulfurization using artificial neural network, *The Canadian Journal of Chemical Engineering*, 88, 5, 801-807, 2010
[11] Dobre T., Sanchez J.M., Chemical Engineering Modelling Simulation and Similitude, Chapter 5 - Statistical Modelling, *Wiley VCH*, 2007

STRUCTURE EQUATIONS OF TERMAL ROCKS AI MODELS

Ioana PURGHEL[1], Maria STOICESCU[2]*, Claudiu DOLETE[1]

[1]Ph.D. School, Petroleum-Gas University
[2]Geological and Oil Engineering, Petroleum-Gas University

Abstract
Geothermal energy, sourced from the Earth's internal heat, is a key renewable resource. This study focuses on the geothermal potential of the Ploiești subsoil, where a consistent thermal gradient is observed. At a depth of 100 meters, temperatures are constant year-round, ranging from 13.2°C to 13.8°C depending on the rock composition. The reliability of this low-enthalpy geothermal field makes it suitable for industrial use. To explore this potential, we have developed a numerical model to simulate the thermal behavior of the area's rock formations.

Key words: Thermal rocks, ANNs model, Environment Simulation

1. Introduction

Unlike solar or wind power, **geothermal energy** is not dependent on the sun but is a direct manifestation of the Earth's internal dynamics.

This energy originates from two primary sources:

- **Primordial Heat:**
  This is the residual thermal energy from our planet's violent formation 4.5 billion years ago. The collision of celestial bodies and the differentiation of the core, mantle, and crust generated immense heat, which is still stored at the Earth's center, where temperatures exceed 5000°C [1].
- **Radiogenic Heat:**
  This is heat continuously generated by the natural radioactive decay of isotopes within the Earth's crust and mantle, such as uranium (^{238}U, 235U), thorium (^{232}Th), and potassium (^{40}K).

This process acts as a natural nuclear "engine," ensuring the resource's sustainability and accounting for roughly 50% of the total heat reaching the surface [2, 3].

Together, these two sources generate a constant heat flux of approximately 44.2 terawatts (4.42×10^{13} watts) radiating from the planet's interior to its surface [4].

The Earth's ability to continuously produce its own heat gives geothermal energy a major advantage: **sustainability on a geological timescale** [5].

While fossil fuels are finite and other renewables are intermittent, geothermal is a constant and enduring resource.

The hydrogeology of the Ploiești municipality is defined by its position over two regionally important groundwater bodies, the **ROIL18 (Telajen Alluvial Cone)** and the **ROAG12 (Eastern Valahe Depression)**.

* Corresponding author: stoicescu.maria@yahoo.com

This location has significant potential for groundwater resources, demonstrated by excellent filtration coefficients (50−150 m/day) and transmissivities (500–2000 m^2/day) [6].

Local studies have distinguished three main aquifer horizons.

- The shallowest is a **phreatic aquifer** in Quaternary deposits at depths down to 8-10 meters, which is vulnerable to surface pollution and has a low flow rate.
- Deeper, between 42 and 52 meters, lies another **aquifer** within the cracked Oligocene-Miocene rock formations.
- The third and deepest is a **pressurized aquifer layer**, found at 78-92 meters, which is confined within permeable sands of Middle Pleistocene age.

2. Materials and Methods

Following this analysis, we can conclude the following aspects of the thermal groundwater in the UPG Ploiești area:

- The average water temperature is 8.92 ºC,
- The average basement temperature is 16.8 ºC,
- The average loss of basement temperature (due to water injection) is 6.33 ºC,
- The average loss of water temperature (due to use in the heat pump) is 4.11 ºC,

In current practice, the following relationship is used to calculate the thermal power of the extracted water:

$$P = Q_m \, c \, \Delta t \tag{1}$$

Where:

- Q_m is the mass flow rate of water (kg/s),
- c is the specific heat capacity of water (4188 J/kg ºC),
- Δt represents the temperature difference of the water at the outlet compared to the inlet ºC.

At a flow rate of 3 mc/h the variation of the extracted power (kW) as a function of the temperature difference is shown in figure 1.

Also, for the first time in the literature, we simulated the value of geothermal energy extracted by a well and then used the data to generate, train and evaluate four different Artificial Intelligence (AI) models.

This simulation started from the creation of a numerical model that would provide us with data on the variation of geothermal power with respect to the depth of the well and the type of rock through which the water flows (figure 2).

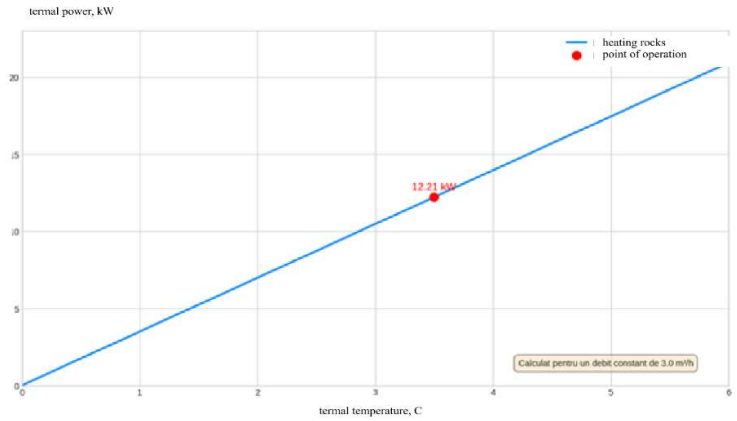

Fig. 1. Variation of thermal energy extracted from a water well as a function of the temperature difference given off

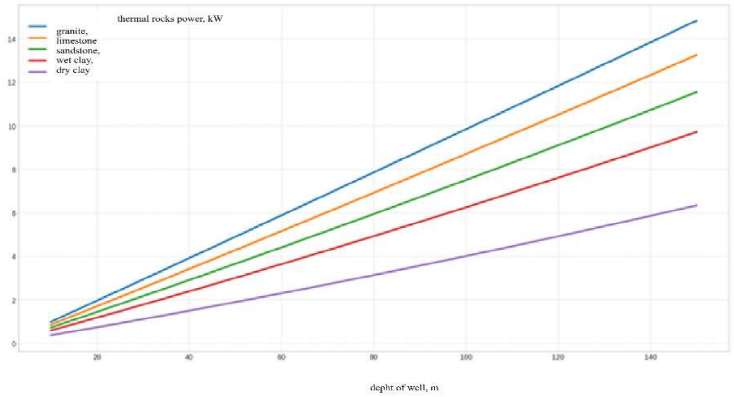

Fig. 2. Geothermal power depending on depth and rock type

3. Results and discussions

I generated a dataset with 500 records.

	MSE	R^2
Linear Regression	0.975736	0.945059
Ridge Regression	0.982796	0.944662
Random Forest	0.080075	0.995491
Neural Network (MLP)	0.267770	0.984923

The model equations is describted to four models.

Linear Regression
Power_kW = -1.8696 + (0.0748 * Depth) + (0.2419 * Flow) – (1.9598 * RockType_Dry Clay) + (1.0953 * RockType_Limestone) + (3.0403 * RockType_Granite) + (2.0691 * RockType_Sandstone) (5.5)
Random Forest

Feature Importances:
- Depth: 0.7169
- Flow: 0.0099
- Dry_Clay_RockType: 0.1791
- Limestone_RockType: 0.0114
- Granite_RockType: 0.0522
- Sandstone_RockType: 0.0305

Neural Network (MLP)
Neural Network Structure:
- Architecture (hidden layers): (100, 50)
- Activation function: relu
- Solver (optimization algorithm): adam
- Number of iterations until convergence: 331

Ridge Regression
Power_kW = -1.8163 + (0.0748 * Depth) + (0.2418 * Flow) – (1.9844 * Dry_Clay_RockType) + (1.0332 * Limestone_RockType) + (2.9529 * Granite_RockType) + (1.9943 * Sandstone_RockType) (5.6)

Groundwater Temperature Estimation

While specific public studies on groundwater temperature in Ploiești are unavailable, a reliable estimate can be made. At depths exceeding 20-30 meters, ground and water temperatures typically stabilize, closely matching the local average annual air temperature. For Ploiești, this average is approximately 11−12°C. Therefore, it's reasonable to assume that water in medium-depth aquifers (50-150 m) maintains a constant temperature in this range, making it an ideal thermal source for geothermal heat pump applications.

Major Aquifers and Water Availability

The Ploiești area has abundant groundwater resources.

The primary catchment fronts supplying the city with drinking water are located at Crângul lui Bot, Ploiești Nord-Vest, and Ploiești Nord-Est.

The scale of these deep aquifers confirms the presence of large, sustainable volumes of underground water suitable for geothermal projects.

Important Consideration: Contamination Risk

A critical factor for any geothermal project is water quality.

Some historical studies indicate that shallow groundwater in the southern and southeastern areas of the municipality may be contaminated with petroleum products.

This potential contamination is an important consideration, and a thorough water quality analysis is mandatory before designing or implementing an open-loop geothermal system.

4. Conclusion

A reliable estimate for groundwater temperature in Ploiești places it at 11−12 ºC in medium-depth aquifers (50-150m), as this reflects the local average annual air temperature where ground temperatures stabilize.

This constant temperature is ideal for geothermal heat pump systems.

The region's rich groundwater resources are confirmed by major deep aquifers at Crângul lui Bot, Ploiești Nord-Vest, and Ploiești Nord-Est.

However, a crucial caveat exists: potential petroleum contamination has been noted in shallow groundwater in the southern and southeastern parts of the city. This risk necessitates a mandatory water quality analysis before proceeding with any open-loop geothermal system design.

5. Data Availability

The data presented in this article are real and collected from the area of interest.

The data can be used by anyone in accordance with applicable international regulations. Data is available in the article and can be provided upon request.

6. Conflicts of Interest

No data or information is presented that could endanger companies or commercial or public companies. There are no conflicts regarding the exposed data. The data taken from the soil samples analyzed and presented in the article are part of oil fields abandoned and handed over to the public domain.

The authors did not benefit from public, private or other resources.

REFERENCES

[1] Allan, M. L. and Kavanaugh, S. P., –Thermal conductivity of cementitious grouts and impact on heat exchanger length design for ground source heat pumps, International Journal of HVAC&R Research, Vol. 5, (2), 1999.

[2] Allan, M. L. and Philippacopoulus, A. J., –Thermalyl Conductive Cementitious Grouts for Geothermal Heat Pumps, FY 1998 Progress Report, BNL 66103, 1998.

[3] Bini, R., Manciana, E., - Organic Rankine Cycle Turbogenerators for Combined Heat and Power Production from Biomass. In: Proceedings of the 3rd Munich Discussion Meeting 1996, ZAE Bayern (ed.), Munich, Germany, 1996.

[4] Claesson, J. And P. Eskilson – Conductive Heat Extraction to a Deep Borehole, Thermal Analysis and Dimensioning Rules. Energy 13/6, 2024

[5] Feidt, M. - Thermodynamique et Optimisation Energetique de Systemes et Procedes, Technique et Documentation (Lavoisier), Paris, 2024

[6] Incropera, F.P., David P. DeWitt - Fundamentals of Heat and Mass Transfer, Editura John Wiley & Sons, New York, 1990.

[7] Sanner, B. - Shallow Geothermal Energy Liebig University, Giessen, Germany.

ANALYSIS OF VOLATILE COMPOUNDS EMISION TO OIL STORAGES

Maria STOICESCU[1]*, Sorin STEFLEA[2], Iolanda POPA[3], Vasile LAVRIC[4]

[1]Oil and Gas Engineering Faculty, Petroleum-Gas University
[2]Ph.D. School, Petroleum-Gas University
[3]Ph.D. School, Politehnica University
[4]Național Science and Technology Politehnica University

Abstract

This paper presents the method of calculating the losses of petroleum products during storage and transportation for different products generally handled in an oil terminal. An important element in determining the losses is also the environmental conditions in the location area (wind, sun, seismicity, etc.).There are several methods for determining the emissions of tanks with fixed or removable lids, the easiest being their determination by calculating the vapor balance. The basic model used in this study is a calculation model developed according to API standards, from which a proprietary methodology was developed and presented for estimating losses during the transport of various products. The study took into account both environmental factors (wind, temperature, tank paint color) and basic properties of the products such as density. The mathematical models that best correlated the data proved to be polynomial equations of degree 2 to degree 5. The simulations performed are among the first performed in this field, the determination of parameters with major influence being of major interest both for finding solutions to reduce losses on the service flow but also being opportune to develop mathematical models that correlate several parameters to facilitate the evaluation of these fugitive emissions.

Key words: volatile compounds emission, emission modelling,

.

1. Introduction

The evolution of fugitive emissions monitoring has been influenced by technological advances, the gradual awareness of the impact on the environment And the regulations implemented for the petroleum industry. Their monitoring has evolved in recent decades, and the main stages were:
- 1950: American Petroleum Institute (A.P.I.) publishes a technical bulletin containing the first research on the evaporation losses of petroleum products with [1];
- 1951: in Russia, scientific studies are published on fugitive emissions as a technological problem;
- 1961: in Romania, the Research and Design Institute for the Petroleum Industry starts a study with the aim of quantifying the amount of petroleum product that can be contaminated through the mixing plugs and that can be lost through evaporation during

* Corresponding author: maria.stoicescu@yahoo.com

storage and transport, so that this amount (establishing technological losses) is not taxed as a final product by the tax administration [2];
- 1970: the price of crude oil is increasing, and research in the field is intensified by taking over the determination of technological consumption by research institutes and regulating them through working standards [3];
- 1988: the first study was carried out that formed the basis for issuing the Order regarding the approval of maximum coefficients of technological consumption, specific to the activities of storage, handling, distribution and transport of petroleum products [4];
- 1990: the Research and Design Institute (I.C.P.P.G. Cîmpina) promoted the techniques implemented by the American Petroleum Institute (API) for determining crude oil losses during its transport and storage;
- 1992: the United Nations Conference on Development and Environment takes place in Rio de Janeiro, where the concept of sustainable development and the "Framework Convention on Climate Change" are introduced. The Convention imposed the settlement of greenhouse gas emissions by the participating countries that signed the declaration, a payment that represents penalties regarding the quantities of combustion gases emitted into the atmosphere by industrial consumers.
In order to quantify fugitive emissions at a global level, several standards and directives have been developed, all of which have the role of establishing their calculation method and so that they can be determined theoretically and uniformly. Currently, the standards used by operators in the field are those published by the American Petroleum Institute, among which we mention:
- Evaporative Loss From External Floating-Roof Tanks, API STANDARD 2517, 1989 [5];
- Lining of Aboveground Petroleum Storage Tank Bottoms, API RECOMMENDED PRACTICE 652,1997 [6];
- Design and Construction of Large, Welded, Low-Pressure Storage Tanks, API STANDARD 620, 2002 [7];
- Tank Inspection, Repair, Alteration, and Reconstruction, API STANDARD 653, 2003 [8];
- Manual of Petroleum Standards, Chapter 19.1, Evaporative Loss from Fixed-Roof Tanks, 2010 [9];
- Welded Tanks for Oil Storage, API STANDARD 650, 2012 [10];
- Inspection Practices for Atmospheric and Low-Pressure Storage Tanks API STANDARD 575, 2014 [11].
A defining aspect in fugitive emissions monitoring is the determination of the effect of volatile organic compounds on the environment and the living world.
Studies have shown that in the case of children in paint factories, in areas where formaldehyde is present, respiratory problems can increase by 20%, predominantly

among children [13], asthmatic symptoms appear when the value of 100 micrograms/m^3 of formaldehyde vapors or volatile organic compounds is exceeded [14].
Some studies recommend that in cases of volatile organic compounds being released into the atmosphere, in order not to affect the life and safety of children, the volumetric quantities should not exceed the threshold of 1000 ppm/mc.
In the case of volatile organic compounds that may occur following the vaporization of crude oil or petroleum products, an increase in the intensity of skin diseases was observed in the first period of exposure to this type of pollutant, but after a period of time (1-10 weeks) this type of disease decreased in intensity (the body provides antibodies to this type of exposure) [15].
Particular attention in the petroleum field is also paid to environmental problems arising from accidental spills into soil or water [16], and in order to reduce the amount of gases resulting from the evaporation of stored petroleum products, several chemical materials have been studied to ensure reduced contact with the atmosphere, with high efficiency being established for polyurethane substances and potassium oleate ($C_{17}H_{33}COOK$) [12].

Another global issue is the effect of emissions on the ozone layer. The first materials that presented the effects of volatile organic compounds on the ozone layer were developed in 1993 [18] and 1994 [13], subsequent research indicated the effect of chemical photosynthesis of the tropospheric for 83 chemicals present in emissions of volatile organic compounds (VOCs) [11].
At the opposite pole, chemicals that help form ozone have also been determined, namely isoprene, 2-methyl-2-butene and acrolein [11].

2. Materials and Methods

In 2004, Order 33 of the Ministry of Economy and Trade legislated the maximum technological consumption coefficients, specific to the activities of storage, handling, distribution and transport of petroleum products within the National Oil Company Petrom - S.A. Bucharest and the Commercial Company Petrotrans - S.A. Ploiești [4].
This order established the technological consumption coefficients for petroleum products, in order to determine the quantities of products that are not subject to excise duty. Gasoline is of particular interest due to its high vapor pressure, the data collected and made available to operators in the petroleum industry include several variables: the type of gasoline stored, the geographical areas, the period of the year in which they are stored, the type of tank used for storage, the filling heights. It should be noted that all data obtained for maximum filling heights take into account the useful capacities of the reservoirs. The annual periods established were summer (between April 1 and September 30) and winter (between October 1 and March 31).

In general, crude oil losses can be classified, depending on the system where they may occur, into:
a. Underground losses resulting from:
- communication between productive layers due to errors in well cementing (leaks from the column or behind the column);

- errors that may occur during drilling (the well getting out of control, drilling a non-productive layer and communicating with the productive layer);
- errors when putting wells into operation (cracking a layer more than what is necessary for the flow of crude oil, cracking a layer that will subsequently communicate with a cavern, cracking a salt layer).

b. Surface losses that may occur in the system:
- reception facilities for pumping and transportation by pipelines, railcars and trucks;
- crude oil extraction equipment (extraction, transportation, processing and storage in oil fields).

Losses of crude oil, petroleum products and condensate that may occur in the transportation and storage system are classified according to the nature of the causes that cause them into real losses and apparent losses.

Real losses are losses that may occur due to objective causes, namely:
- losses due to the phenomenon of evaporation of stored petroleum products or even during transport;
- losses that occur when cleaning tanks as a result of eliminating sludge deposited on the bottom of tanks and on their walls (in the corrosive interstices of the tank shell);
- losses that occur when cleaning paraffin deposits (when crude oil is also eliminated);
- losses that occur during successive transport through pipelines (in the mixing plug);
- losses of petroleum product in emulsion (water in crude oil or crude oil in water) or entrained by water (after separation from crude oil or condensate), which leaks from storage tanks or transport tanks;
- losses that may occur when filling or emptying road and rail tankers;
- leaks in the extraction, treatment, transportation, storage and processing systems of crude oil, petroleum products and gasoline.

Apparent losses of petroleum products occur due to subjective causes, such as:
- measurement errors: erroneous reading of the product level, erroneous determination by calculation or in the laboratory of the density, erroneous reading of the temperature;
- non-compliant calibration of the tanks,
- insufficient heating of the CF tanks (remaining petroleum product on the walls of the wagon after unloading).

In fuel and lubricant depots, of the total losses that occur, about 75% are losses through evaporation, the rest being due to other causes (leaks, damage, etc.). Losses through evaporation are the most important sources of losses, from a quantitative and qualitative point of view and depend directly on the following factors:

a. vapor pressure of the liquid product;
b. diameter of the tank,
c. height of the product stock in the tank (the free space remaining between the liquid and the tank roof),
d. variation of the product temperature in the tank;
e. construction type of the tank;
f. technical condition of the storage tank;
g. frequency of filling and emptying of the tank.

The cause of losses represents the factor that contributes to the occurrence of the phenomenon of losses in the places mentioned as sources [38]. The main causes of losses in storage tanks are:
- storage in storage tanks with a fixed lid and without the possibility of recovering petroleum product vapors;
- long storage time of the product;
- high temperature of the stored liquid;
- multiple and simultaneous filling and emptying operations of storage tanks;
- oversizing of storage tanks compared to the small quantities of product transported or stored;
- lack of automation of transport and storage facilities as well as of the efficient control means necessary for measuring the liquid level in the tank, the temperature of the stored product, determining its density and impurities;
- riveting of the tank shells;
- lack of the possibility of completely emptying the tank (to reduce "dead" or non-evacuable stocks);
- product discharge through the overflow discharge system;
- lack of external protection of the tanks (coat of paint with the appropriate color), depending on the microclimate in the area;
- lack of internal protection of the tanks to reduce the action of corrosive factors, leakage of water and oil-in-water emulsions from storage tanks with product entrainment;
- discharge of sludge when cleaning tanks that have an appreciable product content, damages to the storage system followed by product leakage;
- common keyboard with beneficiaries or other types of petroleum products at the reception tanks, both upon receipt and delivery;
- subjective assessment of the moment of appearance of the product in the water leakage from the tank;
- improper treatment of the petroleum product leading to the increase of emulsion and sediment in the clean petroleum product, above the allowed limit;
- keeping the sampling systems open (in contact with the outside air).

The causes that generate losses in pipelines and tankers and/or CF are the following:
a. pipelines (including pumping stations)
- leaks in the component installations (valves, safety valves, measurement and control equipment);
- successive pumping of petroleum products or different stocks of crude oil;
- dewaxing of pipelines;
- routine repairs and replacements of pipeline sections;
- caused or technological damage;

b. tankers and/or CF boilers:
- evaporation of products during the product loading-unloading operation and during transport (through breathing);
- leaks in the loading or unloading system;
- leaks in the manlock of tankers or CF boilers;
- level measurement errors;

- insufficient heating of tankers upon unloading (remaining product);
- washing of tankers and failure to recover entrained petroleum product;
- failures of loading and unloading systems;
- operating errors in the case of shared keyboards for petroleum products or with other beneficiaries.

3. Results and discussions

This subchapter includes the evaluation of the differences between the quantities of gasoline standardized and calculated according to the standards in force, which could be lost through evaporation during storage, this analysis is necessary to perform calculations in order to correctly determine this value of petroleum product losses. At the same time, the data available in the specialized literature for the different types of tanks were evaluated, the trend being analyzed
For the calculations, it was considered that the type of tank was with a fixed lid, the product height 0.25 m.

Table 1 presents the results obtained when varying the tank capacity, the values taken into account being between 30 and 100 m^3.
As can be seen (figure 1,2,3,4,5) the standardized quantity is greater than the calculated quantity, the values obtained, however, increase with the tank capacity.

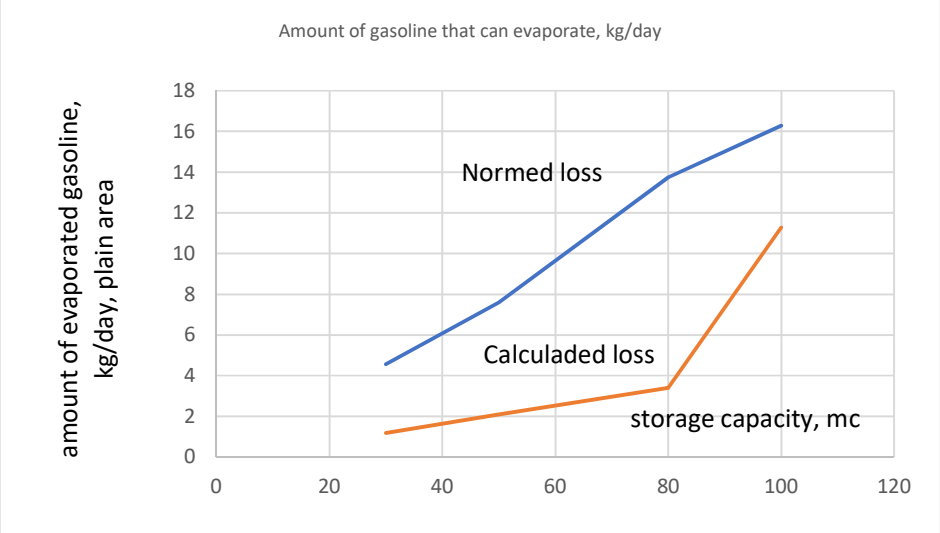

Fig. 1. Differences between the normalized and calculated values for gasoline storage, tank with fixed lid and product height of 0.25 m

Table 1.

Differences between the standard and calculated values for gasoline storage, tank with fixed lid and product height of 0.25 m

tank capacity, mc	Normed loss, kg/day	Loss calculated kg/zi	diferences, kg/zi
30	4.56	1.18	3.38
50	7.6	2.1	5.5
80	13.74	3.4	10.34
100	16.29	11.28	5.01

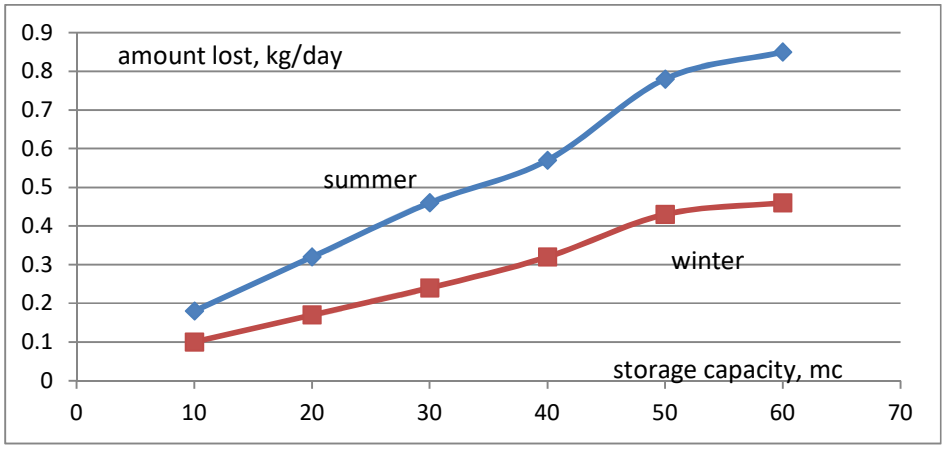

Fig. 2. Losses of petroleum products (gasoline) during storage in buried tanks

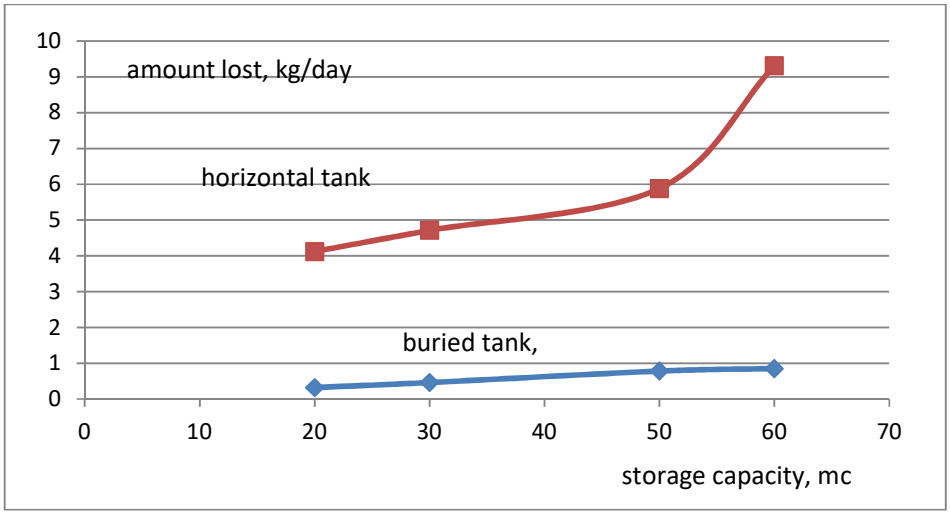

Fig. 3. Losses of petroleum products (gasoline) during storage in buried and horizontal tanks during the summer period

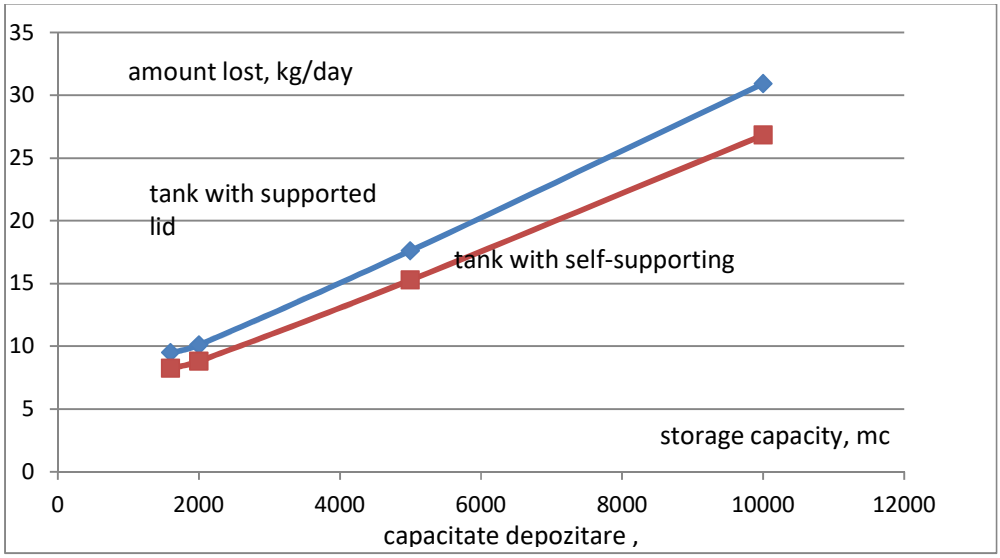

Fig. 4. Losses of petroleum products (gasoline) during storage in membrane tanks (pillar-supported and self-supporting) during the summer period

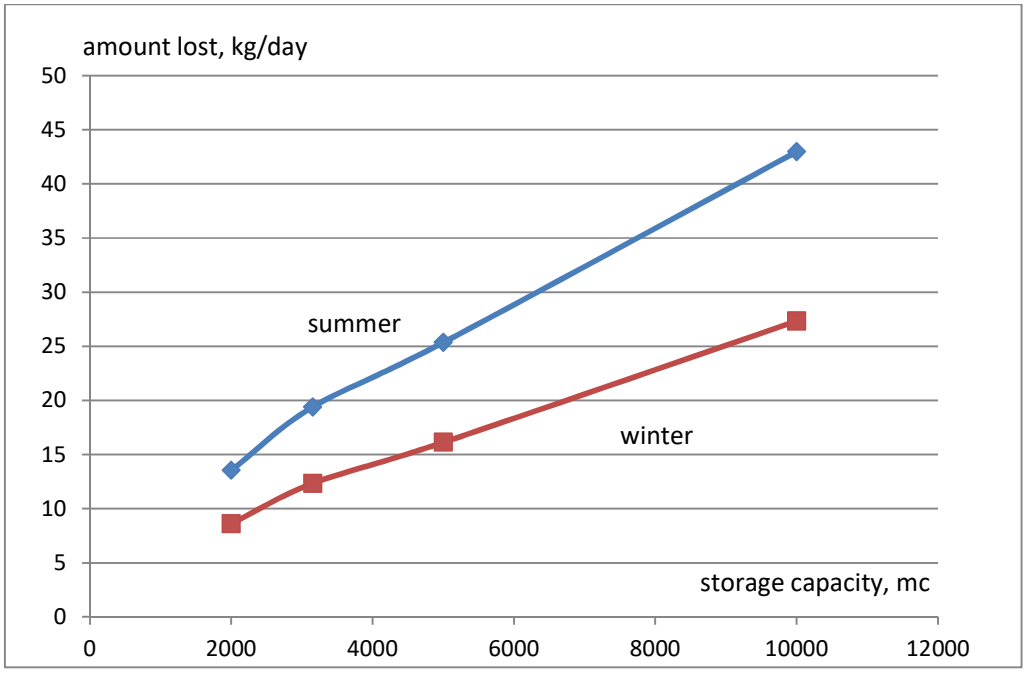

Fig. 5. Losses of petroleum products (gasoline) during storage in floating-lid tanks during summer and winter

Determination of the composition of gases emitted into the atmosphere when filling tanks

In order to observe the composition of gases that are discharged during the filling process of a fixed-lid tank, the composition of gases was measured with a VOC determination device.

Thus, the temperature of the crude oil in the tank at the time of the measurements was 50°C, 37 °C, 70 °C and 12 °C.

The crude oil considered is processed by the operator OMV PETROM, its density being 820 kg/m3.

Table 2.

Composition of gases emitted into the atmosphere (% volume)

Analysis	CO_2	Air	Metane	Etane	Propane	Izobutane	n-butane	Pentane	Hexane
A-12 °C	0,40	71,40	19,50	1,09	2,47	0,68	2,10	1,37	0,99
B-37 °C	0,60	71,40	6,92	1,54	5,99	2,66	4,65	4,32	1,92
C-50°C	1,20	46,60	10,64	1,88	11,67	4,81	10,12	8,92	4,16
D-70 °C	1,20	46,60	4,72	0,66	11,96	4,61	14,38	11,14	4,73

4. Conclusion

Analyzing the legislation in force and also the studies carried out in order to establish technological consumptions for gasoline storage, the following conclusions can be drawn:

a. In order to eliminate any suspicions regarding the maximum quantity of petroleum products that can be passed as technological consumptions (i.e. can be untaxed), the tax authorities propose that these losses be analyzed and studied by specialized companies and institutions with experience in the field of transportation and storage of petroleum products,

b. Losses of petroleum products in buried tanks are greater in summer than in winter and in buried ones they are lower,

c. The smallest losses are in membrane tanks.

5. Data Availability

The data presented in this article are real and collected from the area of interest.

The data can be used by anyone in accordance with applicable international regulations. Data is available in the article and can be provided upon request.

6. Conflicts of Interest

No data or information is presented that could endanger companies or commercial or public companies. There are no conflicts regarding the exposed data. The data taken from the soil samples analyzed and presented in the article are part of oil fields abandoned and handed over to the public domain.

The authors did not benefit from public, private or other resources.

REFERENCES

[1] *Evaporation Loss From Tank Cars, Tank Trucks And Marine Vessels*, Bulletin No. 2514,American Petroleum Institute, Washington, DC, 1959,
[1] Titkov V.I., *Rezervoare pentru păstrarea produselor petroliere sub presiune*, I.D.T., 1951,
[3] *Atmospheric Hydrocarbon Emissions From Marine Vessel Transfer Operations*, Publication 2514A, American Petroleum Institute, Washington, DC, 1981,
[4] *Ordinului privind aprobarea coeficienţilor maximi de consumuri tehnologice, specifici activităţilor de depozitare, manipulare, distribuţie şi transport al produselor petroliere*, 1978 reactualizat, 2004,
[5] *Evaporative Loss From External Floating-Roof Tanks*, API, 1989,
[6] *Lining of Aboveground Petroleum Storage Tank Bottoms*, API RECOMMENDED PRACTICE 652,1997,
[7] *Design and Construction of Large, Welded, Low-Pressure Storage Tanks*, API STANDARD 620, 2002,
[8] *Tank Inspection, Repair, Alteration, and Reconstruction*, API STANDARD 653, 2003,
[9] *Manual of Petroleum Standards, Chapter 19.1, Evaporative Loss from Fixed-Roof Tanks*, API, 2010,
[10] *Welded Tanks for Oil Storage*, API STANDARD 650, 2012,
[11] *Inspection Practices for Atmospheric and Low-Pressure Storage Tanks*, API STANDARD 575, 2014,
[12] A J Venn, M Cooper, M Antoniak, C Laughlin, J Britton, S A Lewis, "*Effects of volatile organic compounds, damp, and other environmental exposures in the home on wheezing illness in children*", Thorax 2003;58:955–960, 2003,
[13] Omar Mohammed Said Ismaila, Reda S. Abdel Hameeda, "*Environmental effects of volatile organic compounds on ozone layer*", Advances in Applied Science Research, 4(1):264-268, 2013,
[14] RA.Brost, PB.Chatfield, J.Greenberg, PL.Haagenson, B.Heikes,S Madronich, et al. "*Three-dimensional model study of transport from continents to the remote*", *Atlantic ocean,* 2009**,**
[15] J. Altenstedt. and K. Pleijel. "*An alternative approach to photochemical ozone creation potentials applied under European conditions*", *Swedish Environmental Research Institute, Göteborg, SUEDE,* 2000,
[16] Cleen Air Act, https://en.wikipedia.org/wiki/Clean_Air_Act_(United_States),

CO_2 CAPTURE AND CLIMATE POLICY DYNAMICS

Eliza-Gabriela BRETTFELD[1,2], Tănase DOBRE[2*]

[1] INCDCP-ICECHIM Bucharest, 202 Spl. Independentei, 6th District, Romania
[2] UNST Politehnica Bucharest, Faculty of Chemical Engineering and Biotechnology

Abstract

Between 2022 and 2025, global CO_2 dynamics reflected a paradox of technological advancement amid geopolitical regression. Major conflicts — Ukraine, Israel–Gaza, Sudan, Yemen — triggered unprecedented military emissions and redirected European funding from climate research to defense. Despite this setback, scientific innovation advanced through lithium–CO_2 batteries, accelerated mineralization, and redox-active materials. The European Union faced temporary setbacks caused by coal and gas plant restarts, delaying the net-zero trajectory by approximately six to eight months. Nonetheless, large-scale investments in renewables and CCUS restored the long-term pathway toward 2050 climate neutrality [1, 2]. This review synthesizes the intertwined political, economic, and technological shifts that defined the 2022–2025 period, framing carbon management as both an environmental necessity and a geopolitical strategy.

Key words: Carbon capture, utilization and storage (CCUS); Energy geopolitics; Net-zero transition

1. Introduction and Global Context (2022–2025)

Between 2022 and 2025, amid the escalation of major armed conflicts - the war in Ukraine, the Israel–Gaza confrontation, and the wars in Sudan and Yemen - global developments related to carbon dioxide (CO_2) have been marked by a profound paradox between scientific progress and political-financial regression.

At the global level, atmospheric CO_2 concentrations continued to rise sharply, surpassing 420 ppm in 2025, more than 50% above pre-industrial levels. Simultaneously, the prioritization of defense budgets and successive energy crises led to a decrease in European funding for climate research, including a €2.1 billion reduction of the Horizon Europe budget.

This context has amplified the contradiction between the acceleration of CO_2-related technological innovation and the slowdown in political action and financial support for climate mitigation.

2. Impact of Armed Conflicts on Climate Research

The Russian invasion of Ukraine generated approximately 230 $MtCO_2e$ emissions during the first three years of conflict [3], transforming the war into the largest

* Corresponding author: Email address: mihaila.eliza.gabriela@gmail.com, tghdobre@gmail.com

single national source of pollution - equivalent to the combined annual emissions of Austria, Hungary, and the Czech Republic.

According to European Commission analyses (2025), military operations, fuel combustion, the destruction of energy infrastructure, and large-scale fires have contaminated the air and soils of Ukraine and the Black Sea basin [4].

Socially, a marked decline in public concern for environmental protection and in support for "green" parties was observed across Europe [5], driven by rising energy prices and growing geopolitical anxiety.

3. Reconfiguration of Climate Funding and CO_2 Research

Despite the contraction of European budgets, the European Union maintained its goal of capturing at least 50 million tonnes of CO_2 annually by 2030, as defined in the EU Carbon Management Industrial Strategy (2024) [6].

Future European Commission programs (2025–2034) [7] foresee expanded funding for carbon dioxide removal (CDR) technologies - including biochar, direct air capture (DAC), and ocean sequestration - within the broader framework of climate-neutral industrial policy.

However, the temporary shift of resources toward security and defense has left many research initiatives underfunded, slowing pilot-scale deployment of capture and storage facilities and delaying the integration of CO_2 valorization pathways into the circular economy.

4. Restart of Coal and Gas Power Plants in Europe

The restart of fossil-fuel power plants, especially coal-fired units, represented one of the most significant energy and climate consequences of the war in Ukraine and of sanctions imposed on the Russian Federation between 2022 and 2025 [8-9].

The 2022 embargo on Russian gas and coal triggered a structural energy crisis that forced the EU to rely temporarily on domestic fossil sources to prevent electrical system collapse.

In summer 2022, Germany authorized the reopening of 27 coal-fired plants, including Heyden-4 (Petershagen) and Mehrum (Hanover), to compensate for the loss of Russian gas. Other countries such as Austria, Italy, the Netherlands, and France reactivated previously closed or stand-by facilities - for instance, the Saint-Avold plant in France was reconnected to the grid for the 2022–2023 winter [10-12]. These decisions added 100–200 TWh to the European energy mix, equivalent to 25–50% of France's annual nuclear output.

The Netherlands lifted its coal-production cap in June 2022, while Germany increased lignite utilization - the most carbon-intensive coal type. By 2023, nearly one-third of European mining regions (Germany, Poland, Czechia) postponed their green transition plans until after 2030.

5. Regional Distribution of Fossil Fuel Restarts

Between 2022 and 2025, coal and fossil-fuel restarts across Europe were heterogeneous, ranging from short-term emergency measures to medium-term structural reopenings in regions economically dependent on fossil resources.

Data from Global Coal Plant Tracker and Ember show that about 13.5 GW of coal capacity were temporarily reactivated - roughly 12% of the EU's total coal fleet [13-14].

5.a. Temporary Restarts (2022–2024)

The vast majority of reopened power plants - particularly in Germany, France, the Netherlands, and Czechia - operated temporarily during the energy crises of the 2022–2023 and 2023–2024 winters.

- **Germany** reactivated 15 coal-fired units, including Heyden 4 and Mehrum, under a "special reserve" regime until March 2024 [15].
- **France** reopened the Émile Huchet 6 plant (595 MW), previously closed, solely to avoid seasonal shortages [14].
- **Austria and Greece**, which had planned full coal phase-outs by 2023 and 2025, postponed their deadlines until after 2028 [16].
- **The Netherlands** temporarily lifted its 35% output cap on coal plants, allowing full-capacity operation to substitute Russian gas [14].

These reopenings were officially defined as emergency coal reserves, intended to ensure short-term electricity system stability without additional structural investments.

5.b. Long-Term Restarts and Dependent Regions

In Central and Eastern Europe, several regions maintained operational capacities beyond the announced closure timelines:

- Upper Silesia (**Poland**) and the Ostrava–Karviná Basin (**Czechia**) extended coal-mine operations and plant lifespans through 2024–2025, citing energy-security concerns [14].
- **Romania** partially resumed operations at Rovinari and Paroșeni units under force-majeure provisions, while simultaneously accelerating investments in gas- and renewables-based generation [14].
- **Italy**, although planning a full coal phase-out by 2026, continues to operate Fiumesanto and Sulcis "Grazia Deledda" plants in Sardinia until completion of the Tyrrhenian Link interconnector, expected in 2028 [17].
- In the broader Eastern Europe region (including the Balkans and Ukraine), several non-EU countries such as **Serbia** and **Bosnia-Herzegovina** continue to operate lignite plants, facing fewer climate-policy constraints [17].

5. c. Geographical Distribution of Restarts

According to Eurostat and Ember reports (2024–2025), the highest number of fossil-fuel capacity restarts occurred in:

- **Germany** – approximately 6 GW of temporarily reintroduced plants [18];
- **Poland** – around 3 GW (extensions and partial reopenings) [18-19];
- **Czechia, Romania, the Netherlands** and **France** – between 500 MW and 1.5 GW each [14];
- **Greece** – a partial lignite-based revival, with the Ptolemaida V plant maintained beyond 2030 [14, 20].

In Eastern Europe, the war-induced energy crisis intensified disparities between Member States with diversified renewable portfolios and those reliant on fossil-based baseloads. Romania and Bulgaria, for instance, accelerated investments in natural-gas transition projects and photovoltaic capacity under REPowerEU [21], while maintaining partial coal operations under force majeure clauses. This dual approach reflected a pragmatic energy-security paradigm rather than a structural deviation from the Green Deal trajectory.

In total, nine EU Member States resorted to partial restarts, most located in central and eastern industrial regions with existing production infrastructure and active mining capacity.

6. Impact on National and EU Net-Zero Timelines

The restart of fossil-fuel power plants after the 2022 invasion of Ukraine had measurable effects on national net-zero deadlines across Europe. Facing geopolitical and economic pressure, several EU Member States announced delays, adjustments, or renegotiations of their 2040–2050 climate plans [22-24].

The volatility of the EU Emissions Trading System (EU ETS) between 2022 and 2025 mirrored the geopolitical turbulence. Carbon prices fluctuated between €65 and €105 per tonne, influenced by industrial slowdown, speculative trading, and temporary exemptions for energy-intensive sectors. Despite these oscillations, the ETS remained a key driver for low-carbon innovation, particularly in carbon capture, utilization, and storage (CCUS) projects [25-28].

7. Climatic and Economic Impact

The European Commission acknowledges that coal dependency temporarily increased, accounting for approximately 13% of the EU's energy mix in 2023, compared with 9% in 2021. According to Global Energy Monitor, this "strategic setback" prevented a decline in European emissions, stabilizing values at around 2.6 $GtCO_2$ annually between 2022 and 2024 [29]. However, the Boom and Bust Coal 2025 report notes that, from 2024 onward, the trend is once again downward, as these reactivations were

designed as emergency measures rather than a structural reversal of Europe's energy transition [30].

Economists from IDDRI describe the resumption of coal extraction as a "necessary evil" to avoid full dependency on Asian liquefied gas imports, though it came with significant ecological costs, estimated at an additional 220 $MtCO_2$ in 2023. From 2025, the European Union reaffirmed its commitment to phasing out coal by 2030 for most Member States, maintaining extended deadlines only for Poland (2049) and Bulgaria (2038) [31-32].

8. Corrective Strategies (2024–2025)

Through the REPowerEU and Fit for 55 programs, the Commission increased investments in solar and wind energy by more than €65 billion in 2024, partially offsetting the emission growth of previous years [33-36]. At the same time, the development of green hydrogen and carbon capture, utilization, and storage (CCUS) infrastructure accelerated, aiming to rapidly transition former coal-mining regions toward climate-neutral economies.

This temporary restart of fossil-fuel power plants represents a turning point in European energy policy: a strategic step backward to maintain system stability, followed by an unprecedented acceleration of investments in renewable energy, energy efficiency, and CO_2 sequestration technologies.

9. Scientific Advances in CO_2 Capture and Utilization

Despite adverse geopolitical and economic conditions, scientific research on CO_2 capture and utilization has progressed in several innovative directions:

• CO_2-breathing batteries - The University of Surrey (2025) developed lithium–CO_2 batteries that capture and mineralize CO_2 during discharge [37].

• Accelerated mineralization - Stanford researchers (2025) discovered a rapid process converting common minerals into stable carbonates [38].

• Compact CCS and clean hydrogen - The 8 Rivers company introduced the $8RH_2$ process, capturing 99.5% of CO_2 from hydrogen production [39-40].

• Hybrid materials and novel sorbents - Functionalized graphene and redox-active MOFs achieved high-selectivity CO_2 adsorption with reduced cost [41].

Emerging research increasingly explores the integration of CO_2 capture and conversion across materials, energy, and biotechnological systems. Hybrid electrochemical platforms coupling CO_2 absorption with energy storage - such as lithium–CO_2 cells and redox-active MOFs - represent the frontier of multifunctional decarbonization technologies. Their combined deployment could bridge gaps between storage, utilization, and permanent sequestration, offering a circular-carbon framework adaptable to both industrial and agricultural environments.

10. Outlook and Conclusions

NASA and IPCC assessments suggest that, without a massive acceleration in emission reduction and CO_2 removal, the global carbon budget consistent with 1.5 °C warming will be exhausted by 2031.

CO_2 research between 2025 and 2030 will focus on scaling DAC technologies below \$100/tCO_2, expanding European CO_2 transport and storage networks, integrating capture into agriculture and industry, and re-targeting EU funding post-2027 toward sustainable carbon management.

Nevertheless, the expansion of carbon-capture technologies raises socio-ethical questions regarding environmental justice, resource allocation, and public acceptance, especially in regions where industrial decarbonization intersects with employment restructuring.

The 2022–2025 period was defined by a strategic contradiction: while wars increased emissions and eroded public support for climate action, technological advances in CO_2 capture and conversion achieved remarkable industrial progress.

The convergence of policy, innovation, and geopolitical resilience will determine whether the next decade transforms CO_2 management from a scientific endeavor into a cornerstone of sustainable industrial civilization.

Aknowledgement: *The research leading to these results has received funding from project PN.23.06.02.01 InteGral, Nucleu Program, funded by the Romanian Ministry of Education and Research, National Agency for Research.*

REFERENCES

[1] NASA, „Carbon Dioxide Earth Indicator", *NASA Science*, Washington DC, September 25 2025.
[2] Viloria E., Avornic R., Delerce S., Loopesko L., „Funding CDR Research, Development & Innovation for a Net Zero Competitive EU", *Carbon Gap*, February 2025
[3] Joint Research Centre (JRC). *War worsens climate and environmental challenges in Ukraine*, 11 April 2025. The Joint Research Centre: EU Science Hub, Brussels
[4] Igini M., *Warfare now largest source of Ukraine's annual carbon emissions, report warns on third anniversary of Russia's invasion*, Earth.Org, 24 February 2025.
[5] D'Ecclesiis E. A. R., Levi E., Patriarca F., *The impact of Ukraine's war outbreak on green preferences in Europe*, **Ambio**, 54(6), 1095–1102, 2025, doi: 10.1007/s13280-025-02173-1.
[6] Viloria E., Avornic R., Delerce S., Loopesko L., *Funding CDR research, development & innovation for a net zero competitive EU*, Carbon Gap, February 2025.
[7] Dena – Deutsche Energie-Agentur GmbH, *State of CCU/S in Europe 2024/2025 (Factsheet EnTrans)*, EnTrans / Dena, 2025.
[8] European Commission, *Sanctions on energy – EU sanctions against Russia following the invasion of Ukraine*, European Commission: EU Solidarity with Ukraine, 18 July 2025.
[9] EU NEIGHBOURS east, *It's time to turn off the tap: new EU sanctions to target Russian energy exports*, EU NEIGHBOURS east, 19 September 2025.
[10] European Commission, *EU coal regions in transition – Clean Energy Transition initiative*, Directorate-General for Energy, Brussels, 2025.
[11] Egerer J., Kunz F., Schill W.-P., *The coal phase-out in Germany and Central Western Europe: Policy lessons for secure and affordable transition pathways*, **Energy Economics**, Vol. 136, Article 107133 (2025).

[12] Global Times, *Europe restarts coal power amid Russia-Ukraine conflict, sparking debate over energy security and climate goals*, **Global Times**, 22 June 2022.
[13] Global Energy Monitor, *Global Coal Plant Tracker*, Global Energy Monitor, San Francisco (CA), 2025.
[14] Bociaga R., *Will coal become the new normal for Europe?*, FairPlanet, 14 November 2022.
[15] CBC News, *Germany restarts coal plants to offset Russian gas cuts, raising climate concerns*, **CBC News – Science**, 21 June 2022.
[16] Friedrich-Ebert-Stiftung (FES), *The Future of Coal in Europe – Managing a Just Transition*, **Just Climate – FES Dialogue Platform**, Berlin, 2025.
[17] EURACOAL, *Other EU & Energy Community – Country Profiles of Coal Use*, EURACOAL Info Library, Brussels, 2025.
[18] Ember, *European Electricity Review 2024*, London, 2024.
[19] Eurostat – European Commission, *Shedding light on energy in Europe – 2025 edition*, Brussels, 2025.
[20] Friedrich-Ebert-Stiftung (FES), *The Future of Coal in Europe: Is This the Exit from the Exit?*, Just Climate – FES Dialogue Platform, Berlin, 12 October 2022.
[21] European Commission, *REPowerEU – reliable, affordable and clean energy for Europe*, Brussels, 2025.
[22] Reuters, *EU countries delay deal on new climate goal, diplomats say*, **Reuters – Sustainability / COP**, 12 September 2025.
[23] European Parliamentary Research Service (EPRS), *The EU's 2040 climate target: Towards a 90% emission reduction by 2040*, **Briefing 772867**, European Parliament, Brussels, 2025.
[24] Reuters, *EU set to miss UN climate deadline amid internal divisions*, **Reuters – Sustainability / COP**, 18 September 2025.
[25] Ember, *European Electricity Review 2025: Five Years of Progress*, London, January 2025.
[26] European Commission, *EU Action to Address the Energy Crisis*, Brussels, 2025.
[27] Euronews Italia, *Where Europe Stands on Replacing Fossil Energy with Renewables*, 2 July 2025.
[28] ASU-ENE (US Blog), *Addressing the EU Energy Crisis: Challenges and Strategic Responses in 2025 and Beyond*, US Blog, June/2025.
[29] Eurostat – European Commission, *Shedding light on energy in Europe – 2025 edition*, Brussels, 2025. (
[30] Global Energy Monitor (GEM), *Boom and Bust Coal 2025 – Tracking the Global Coal Plant Pipeline*, San Francisco (CA), April 2025.
[31] *Despite climate commitments, the EU is going back to coal*, **Le Monde – Economy**, 2 September 2022
[32] Perdana S., Vielle M., Schenckery M., *European economic impacts of cutting energy imports from Russia: A computable general equilibrium analysis*, **Energy Research & Social Science**, Vol. 86, Article 102571 (2022). doi:10.1016/j.erss.2022.102571.
[33] European Commission, *EU Action to Address the Energy Crisis*, Brussels, 2025.
[34] Euronews Italia, *Where Europe Stands on Replacing Fossil Energy with Renewables*, 2 July 2025.
[35] ASU-ENE, *Addressing the EU Energy Crisis: Challenges and Strategic Responses in 2025 and Beyond*, US Blog, June 2025.
[36] European Commission, *EU Coal Regions in Transition – Clean Energy Transition Initiative*, Directorate-General for Energy, Brussels, 2025.
[37] Ecole Polytechnique Fédérale de Lausanne (EPFL), *Scalable graphene membranes: A leap for carbon capture*, **ScienceDaily**, 15 April 2025.
[38] Stanford University, *New process gets common rocks to trap carbon rapidly, cheaply*, **ScienceDaily**, 19 February 2025.
[39] AZoCleantech, *Graphene-based materials for CO_2 capture and conversion: future prospects*, AZoCleantech Online, 2025.
[40] CarbonHerald, *Scientists explore graphene potential for CO_2 removal from atmosphere*, 16 August 2024.
[41] Society of Petroleum Engineers (SPE), *4 Cutting-Edge CCS Technologies Reshaping the Future of Carbon Capture*, **The Way Ahead – SPE Journal**, 2025.